CGER'S SUPERCOMPUTER MONOGRAPH REPORT Vol.31

Development of Process-based NICE Model and Simulation of Ecosystem Dynamics in the Catchment of East Asia (Part VIII)

Tadanobu Nakayama

Center for Global Environmental Research

National Institute for Environmental Studies, Japan

CGER'S SUPERCOMPUTER MONOGRAPH REPORT Vol.31

Development of Process-based NICE Model and Simulation of Ecosystem Dynamics in the Catchment of East Asia (Part VIII)

Tadanobu Nakayama

Center for Global Environmental Research

National Institute for Environmental Studies, Japan

CGER'S SUPERCOMPUTER MONOGRAPH REPORT Vol.31

Development of Process-based NICE Model and Simulation of Ecosystem Dynamics in the Catchment of East Asia (Part VIII)
....**Tadanobu Nakayama**

Foreword

The Center for Global Environmental Research (CGER) at the National Institute for Environmental Studies (NIES) was established in October 1990, with the main objectives of contributing to the scientific understanding of global environmental change and identifying solutions to critical environmental problems. CGER conducts environmental research from an interdisciplinary, multi-agency, and international perspective, and provides an intellectual infrastructure for research activities in the form of databases and a supercomputer system. CGER also ensures that data from its long-term monitoring of the global environment is made available to the public.

CGER installed its first supercomputer system (NEC SX-3) in March 1992, and the system was upgraded to an NEC SX-4 in 1997, an NEC SX-6 in 2002, an NEC SX-8R in 2007, an NEC SX-9 in 2013, and an NEC SX-ACE in June 2015. The current system consists of an NEC SX-Aurora TSUBASA/type A511-64 and 22PB file storage to provide more computational resources and data capacity. The NIES supercomputer system is available for researchers at research institutions and universities in Japan, including NIES. The Supercomputer Steering Committee is comprised of Japan's leading scientists in climate modeling, carbon cycle, atmospheric chemistry, marine environment, and other fields related to global environmental research, and one of its functions is to evaluate research proposals that require the use of the NIES supercomputer system. To promote the dissemination of results, we publish Annual Reports and occasional Monograph Reports. Annual Reports deliver the results of all research projects that used the NIES supercomputer system each year, whereas Monograph Reports present the integrated outcomes of a particular research project.

This Monograph Report (Part VIII) presents the results of the development process of the National Integrated Catchment-based Ecohydrology (NICE) model after the 11th (Part I), 14th (Part II), 18th (Part III), 20th (Part IV), 26th publications (Part V), 29th publications (Part VI), and 30th publications (Part VII). This volume reviews the NICE processes developed since Part VII was published, and how the model has been further refined from Part VII to improve the accuracy of plastic cycles in various basins from regional to global scales. In order to solve this problem, NICE coupled with plastic debris model was further extended to incorporate resuspension, bedload transport, estuarine dynamics, heteroaggregation, and biofouling for quantifying the plastic dynamics on terrestrial-aquatic-estuarine continuum. The model also improved the accuracy of plastic cycle in urban regions. This methodology is useful for developing solutions and efficient measures to reduce the plastic load on a global scale. In future, we intend to continue our support for environmental research by using supercomputer resources and disseminating practical information based on our results.

December 2025

Hiroshi Tanimoto
Director
Center for Global Environmental Research
Earth System Division
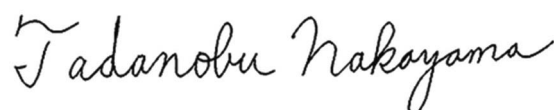National Institute for Environmental Studies

Preface

This volume of the CGER's SUPERCOMPUTER MONOGRAPH REPORT series is the 31st publication on research outcomes achieved by the users of supercomputer facilities at the Center for Global Environmental Research (CGER) at the National Institute for Environmental Studies (NIES).

An advanced process-based model, known as the National Integrated Catchment-based Eco-hydrology (NICE) model, has been developed to evaluate ecosystem dynamics in catchments. NICE is a 3-D, grid-based eco-hydrology model that simulates the complex interactions between forest canopy, surface water, unsaturated zones, aquifers, lakes, and rivers. It also iteratively simulates nonlinear interactions between hydrogeomorphic and vegetation dynamics. The model can also be coupled with complex subsystems to simulate systems such as irrigation, urban water usage, stream junctions, and dams/canals; develop integrated human and natural systems; and analyze the impact of anthropogenic activity on eco-hydrologic change. Water resources are vital for human activity, but their overuse has caused serious environmental degradation, economic stagnation, and immense burdens on the surrounding environment. This is particularly evident in Asia, where finding a solution to environmental pollution is crucial.

This monograph (Part VIII) succeeds the 11th (Part I), 14th (Part II), 18th (Part III), 20th (Part IV), 26th publications (Part V), 29th publications (Part VI), and 30th publications (Part VII). This volume reviews the NICE processes developed since Part VII was published, and describes how the model has been further refined from Part VII to improve the accuracy of plastic cycles in various basins from regional to global scales. In order to solve this problem, NICE coupled with plastic debris model was further extended to incorporate resuspension, bedload transport, estuarine dynamics, heteroaggregation, and biofouling for quantifying the plastic dynamics on terrestrial-aquatic-estuarine continuum. The model also improved the accuracy of plastic cycle in urban regions. Establishment of complete model for the whole picture of plastic dynamics on basin scale becomes a big step forward. The results are also important for predicting and estimating the change of plastic dynamics under climate change. These results help to devise solutions and measures for reduction of plastic input to the ocean.

NICE is now being expanded to incorporate multimedia models including interaction between suspended matter, nutrient, carbon, plastic, and other media. Plastic pollution is considered to be one of today's main environmental problems, and such pollutants in streams, rivers, and oceans pose potential risks to human health and the environment. From this viewpoint, the results help develop solutions and efficient measures to reduce the plastic load on a global scale. This will be reported in the next monograph (Part IX). I hope that this publication will help integrate knowledge and provide the understanding needed to reach sustainability by 2030 in the UN Sustainable Development Goals, which supports climate action, clean water, sustainable cities, life below water, and life on land.

December 2025

Tadanobu Nakayama
Prime Senior Researcher
Regional Environment Conservation Division
National Institute for Environmental Studies

Contents

Chapter 3
Evaluation of Plastic Flux and Fate in Terrestrial-Aquatic-Estuarine Continuum Using an Advanced Process-Based Model..**37**

Chapter 4
Improvement in the Simulation of Plastic Dynamics and Their Relation to Biogeochemical Cycles in Global Rivers by Considering the Effect of the Interaction Processes of Biofouling and Heteroaggregation **61**

List of Figures

(Some of the figures in Chapter 1 are reprinted from Nakayama, T. [2023a] Evaluation of global biogeochemical cycle in lotic and lentic waters by developing an advanced eco-hydrologic and biogeochemical coupling model. Ecohydrology, 17(4), e2555, doi:10.1002/eco.2555, and Nakayama, T. [2025c] Improvement to simulate plastic dynamics and their relation to biogeochemical cycles in global rivers by considering effect of interaction processes of biofouling and heteroaggregation. Global and Planetary Change, 253, 104917, doi:10.1016/j.gloplacha.2025.104917)

Chapter 3

Chapter 4

transport, (c) TSS (total suspended solid) flux, and (d) TOC flux. The continents shaded in grey show the major river basins (153 basins, 325 river channels) considered in this study. In panel a, the value was obtained by calculating the ratio of the microplastic concentration without interaction processes to that with interaction processes in the water. In panel b, the circle size means the magnitude of fluxes, and each pie chart shows the proportions of pristine, heteroaggregated, biofouled, and biofouled & heteroaggregated microplastics.......78

Chapter 5

(The figures in Chapter 5 are reprinted from Nakayama, T. [2025b] Improvement in understanding of plastic cycle in Japanese urban regions. Hydrological Processes, 39(6), e70168, doi:10.1002/hyp.70168)

Chapter 6

List of Tables

(The tables in Chapter 2 are reprinted from Nakayama, T. [2025a] Impact of settling and resuspension on plastic dynamics during extreme flow and their seasonality in global major rivers. Hydrological Processes, 39(2), e70072, doi:10.1002/hyp.70072)

(The tables in Chapter 3 are reprinted from Nakayama, T. [2024b] Evaluation of flux and fate of plastic in terrestrial-aquatic-estuarine continuum by using an advanced process-based model. Ecohydrology, 17(6), e2678, doi:10.1002/eco.2678)

(The tables in Chapter 4 are reprinted from Nakayama, T. [2025c] Improvement to simulate plastic dynamics and their relation to biogeochemical cycles in global rivers by considering effect of interaction processes of biofouling and heteroaggregation. Global and Planetary Change, 253, 104917, doi:10.1016/j.gloplacha.2025.104917)

(The tables in Chapter 5 are reprinted from Nakayama, T. [2025b] Improvement in understanding of plastic cycle in Japanese urban regions. Hydrological Processes, 39(6), e70168, doi:10.1002/hyp.70168)

- 1 -

Chapter 1

General Introduction

1.1 Background

Plastic pollution is a major environmental problem, and pollutants in streams, rivers, and oceans pose potential risks to human health and the environment (Siegfried et al., 2017). Plastic accumulation on riverbanks, deltas, coastlines, and ocean surfaces is rapidly increasing, and approximately 60% of all manufactured plastics have been discarded in landfills or the natural environment (Meijer et al., 2021). Plastic waste can be roughly categorized as macroplastics (≥5 mm) or microplastics (<5 mm), with the latter being further divided into primary and secondary microplastics according to their origin (Siegfried et al., 2017). Once plastic is released into the environment, it is gradually degraded by physical, chemical, and biological processes, leading to its further subdivision into many forms that cannot be removed and therefore remain indefinitely in the environment (Zhang et al., 2021).

Previous studies on the origin and fate of plastic waste in freshwater systems have suggested that land-derived plastics are one of the main sources of marine plastic pollution (Thompson et al., 2004) because of direct emissions from coastal areas (Jambeck et al., 2015) or transport via rivers (Lebreton et al., 2017; Schmidt et al., 2017). Over the last decade, significant progress has been made in modeling the fate and transport of plastics. Kooi et al. (2018) classified plastic debris models for freshwater systems into four categories: emission-based mass balance, global, multimedia, and spatio-temporally explicit models. Because most of the above plastic debris models are analogous to sediment models for inland waters, whether these models are reasonably adaptable for modeling the dynamics of plastics with various sizes, densities, shapes, polymer types, and contact angles remains to be clarified (Nizzetto et al., 2016; Waldschlager and Schüttrumpf, 2019).

Regarding the waste plastic trade, Japan is among the top exporting countries after Europe and America, although countries such as China have historically imported this waste plastic (Nakayama and Osako, 2024). China imported approximately 45% of all cumulative plastic waste imports between 1988 and 2016 (Brooks et al., 2018; Dominish et al., 2020; EIA, 2021). This situation changed greatly after the establishment of the "Basel Convention" (United Nations, 2019) because some importing countries introduced import regulations mainly for environmental protection. Developing a framework for reversing global water resource degradation, especially plastic pollution, is important for achieving Sustainable Development Goals (SDGs) (UNESCO, 2022). The G20 Osaka Summit in 2019 endorsed the "Osaka Blue Ocean Vision" (Ministry of Foreign Affairs of Japan, 2019). A quantitative assessment of the fate and transport of plastics is necessary to realize this vision because countries worldwide have decided on concrete future measures for addressing plastics based on scientific results.

The author developed a process-based model that couples eco-hydrology with the biogeochemical cycle (National Integrated Catchment-based Eco-hydrology (NICE)-BioGeochemical Cycle (BGC)) (Nakayama, 2017a,b), which also incorporates complex terrestrial-aquatic linkages in the hydrological–biogeochemical cycle. Recently, the author coupled this process-based NICE-BGC with a plastic debris (engineered materials) model and evaluated the spatiotemporal variations in plastic debris at a regional scale based on the entirety of Japan (Nakayama and Osako, 2023a) and a global scale based on the world's major rivers (Nakayama and Osako, 2023b). The successful application of the NICE model to existing research has enabled the detection of spatiotemporal hotspots in plastic fluxes by quantifying the impact of plastic waste on terrestrial and aquatic ecosystems. The results will also help improve the plastic cycle and develop better solutions and efficient measures to reduce plastic loads globally.

1.2 Description of a Process-Based NICE Model to Quantify Plastic Dynamics

The NICE model, which includes surface-unsaturated–saturated water processes and assimilates land-surface processes, has been developed to describe phenology variations based on satellite data (Nakayama, 2008a–c, 2009, 2010, 2011a–d, 2012a–d, 2013, 2014a,b, 2015, 2016, 2017a–c, 2018, 2019, 2020, 2022, 2023a,b; 2024a–c; 2025a–d; Nakayama and Fujita, 2010; Nakayama and Hashimoto, 2011; Nakayama and Maksyutov, 2018; Nakayama and Osako, 2023a,b, 2024; Nakayama and Pelletier, 2018; Nakayama and Shankman, 2013a,b; Nakayama and Watanabe, 2004, 2005, 2006a,b, 2008a–c; Nakayama et al., 2006, 2007, 2010, 2012, 2021a,b, 2023) (Fig. 1.1). NICE has been applied to various basins/catchments at local and regional scales, such as the Tokyo Metropolitan Area in Japan, Kushiro Wetland (the largest wetland in Japan), and Lake Kasumigaura catchment (a highly eutrophic lake in Japan), and to continental and global scales, such as the Changjiang and Yellow Rivers in China, Ob River in West Siberia, Mekong River in Southeast Asia, and Mongolia. The results of these studies are described in the papers cited above and have been summarized in previous *CGER Supercomputer Monograph Report Series* Vols. 11 (Part I) (Nakayama and Watanabe, 2006b), 14 (Part II) (Nakayama, 2008c), 18 (Part III) (Nakayama, 2012d), 20 (Part IV) (Nakayama, 2014b), 26 (Part V) (Nakayama, 2019), 29 (Part VI) (Nakayama, 2023b), and 30 (Part VII) (Nakayama, 2024c) (Fig. 1.2).

NICE consists of complex sub-models: surface hydrology model, land-surface model including urban and crop processes, groundwater model, regional atmospheric model, mass-transport models of sediment, nutrients, carbon, and plastics, and vegetation succession model. The model can iteratively simulate nonlinear interactions between hydrologic, geomorphic, and ecological processes and includes novel feedback mechanisms through downscaling from regional to local simulations at a fine resolution. NICE applies a rectangular coordinate system based on the Albers or Universal Transverse Mercator (UTM) projection (Nakayama, 2014a,b, 2015). In addition, the model was extended to incorporate coordinate transformation from a rectangular coordinate to a longitude-latitude coordinate system, which applies to a continental/global scale and higher latitude regions, by implementing a map factor and a non-uniform grid (Nakayama and Maksyutov, 2018). It also incorporates surface–groundwater interactions, assimilating land-surface processes to describe satellite data-derived leaf area index (LAI) variations and the fraction of photosynthetically active radiation (FPAR). The NICE surface hydrology model consists of a kinematic wave theory-based hillslope hydrology model and a distributed stream network model based on both kinematic and dynamic wave theories. NICE also solves partial differential equations describing the three-dimensional groundwater flow for unconfined and confined aquifers. The integration of sub-models considers water and heat fluxes from the ground to the surface, including the hydraulic potential gradient between the deepest unsaturated flow layer and groundwater level, effective precipitation calculated from actual precipitation, infiltration into the upper soil moisture store, evapotranspiration, and seepage between river water and groundwater.

Recently, to fill the current eco-hydrology gap, the author further developed a new model in which the original NICE was coupled with various biogeochemical cycle models (NICE-BGC) (Nakayama, 2016, 2017a, 2017b) (Fig. 1.3). Each sub-model can efficiently perform iterative simulations by combining online and offline modes (online: data input/output through I/O memory; offline: data input/output through file), which means that the newly developed model incorporates the connectivity of the biogeochemical cycle accompanied by the hydrologic cycle between surface water and groundwater, hillslopes, and river networks and

other intermediate regions (Nakayama, 2016). In addition, the author modified the NICE-BGC model to include the effect of reservoirs (Nakayama and Pelletier, 2018) and two key parameters (soil organic carbon and carbon emissions from the intermediate soil pool) to improve the accuracy of long-term simulations (Nakayama, 2020) and extend the model to global estuaries (Nakayama, 2022). The model was further extended to couple with LAKE2K via a stratified water quality model to evaluate the global biogeochemical cycle in lotic and lentic waters (Nakayama, 2023a). Based on these previous developments, NICE has been applied to analyze water, heat, sediment, nutrient, and carbon cycles in various basins at regional, continental, and global scales.

Based on the above matters and the information contained in section 1.1, the plastic debris model and its relationship with water and material cycles are important. Therefore, an accurate model for quantifying the fate and transport of plastics is required to evaluate the spatiotemporal dynamics of macro- and microplastics in each basin. Based on this background, NICE-BGC was recently extended to couple with the plastic debris model for freshwater systems and applied to all first-class (class A) river basins in Japan (109 river basins) and the world's major rivers (325 rivers) (Nakayama and Osako, 2023a, 2023b). The model was also applied to evaluate the impact of the waste plastic trade on changes in riverine plastic transport in Asian regions by including the effect of the waste plastic trade on MPW as an extension of previous studies (Nakayama and Osako, 2024). Further, the model was extended to couple with LAKE2K in a stratified water quality model to evaluate the global plastic dynamics in both lotic and lentic waters (Nakayama, 2024a). Thus, NICE is a useful tool for predicting and resolving future problems related to plastic pollution in various basins. In addition, future advances in the uncertainty model will greatly contribute to elucidating the transport and retention of macro- and microplastics in rivers, together with further field surveys and laboratory experiments about plastic degradation through photodegradation, temperature, physical abrasion, biodegradation, and weathering.
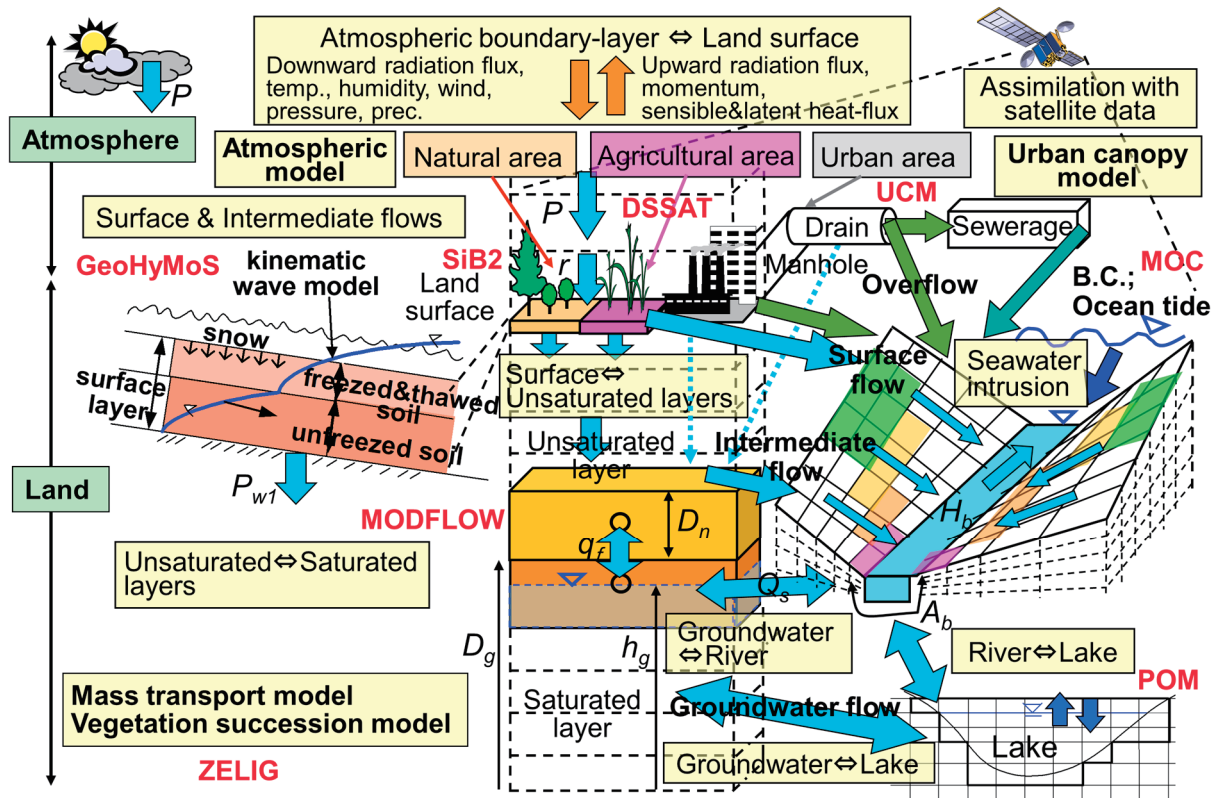
Figure 1.1 Process-based National Integrated Catchment-based Eco-hydrology (NICE) model.
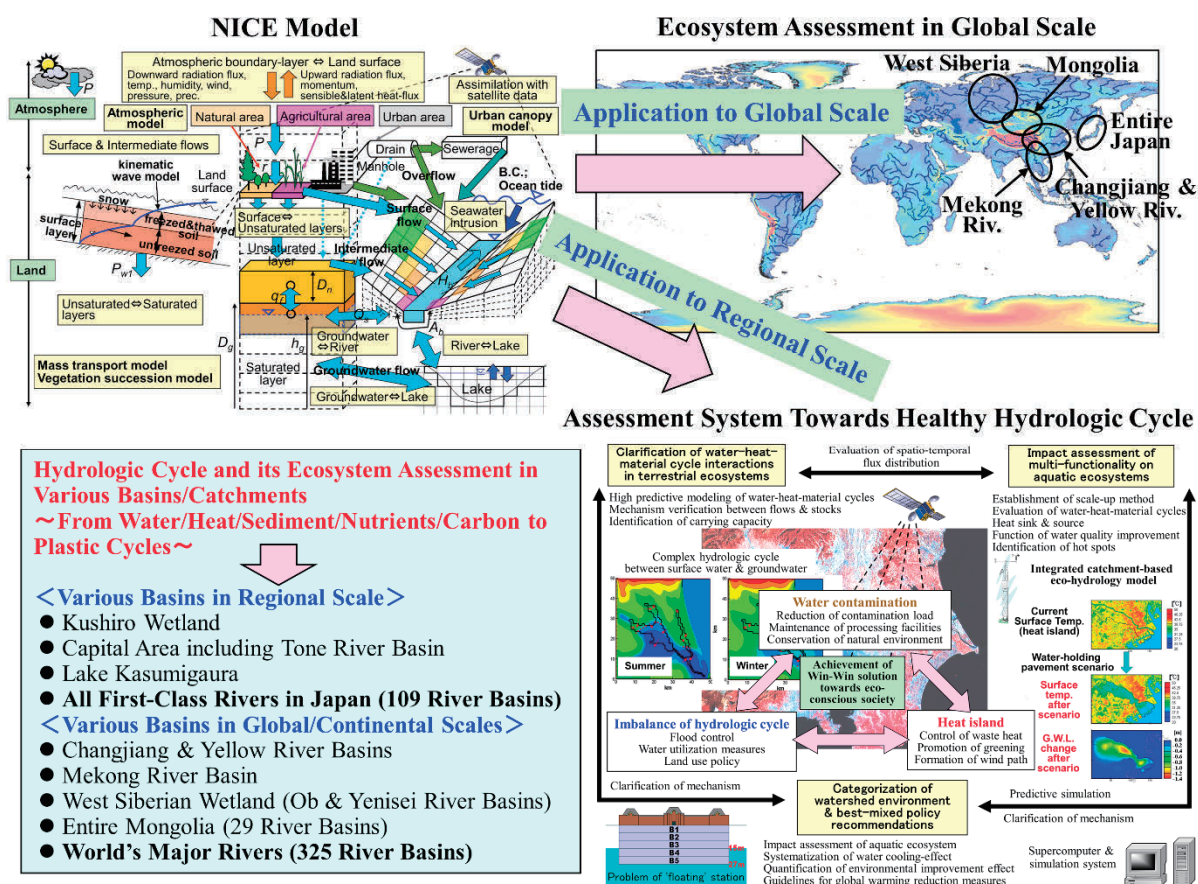
Figure 1.2 NICE simulation for quantifying the hydrologic cycle and its ecosystem assessment in various basins/catchments from regional to global scales. Previous model applications to regional, continental, and global scales (Part I–VI) and plastic dynamics (Part VII–VIII).
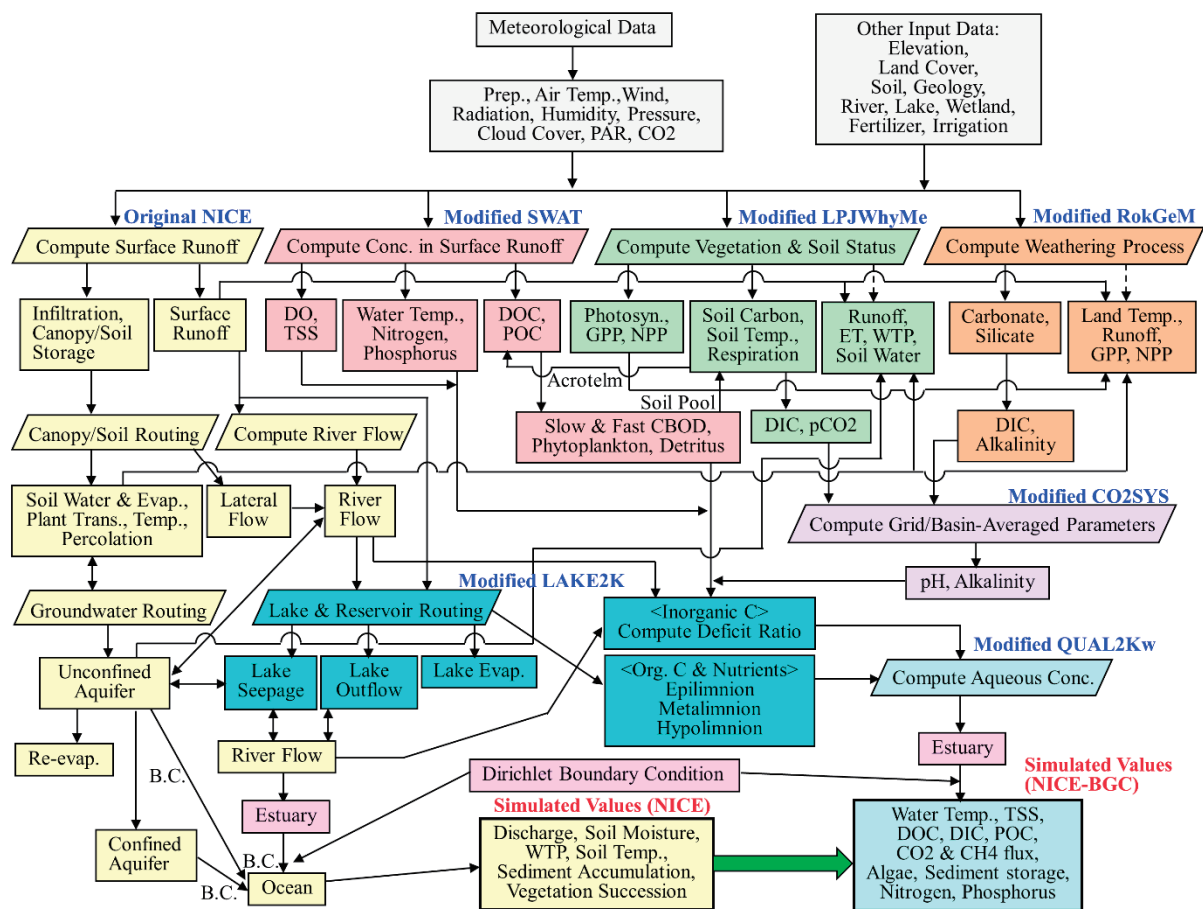
Figure 1.3 Flow diagram of the original NICE regarding water resources and recent developments of the eco-hydrological and biogeochemical coupling model (NICE-BGC).

1.3 Objective and Methods toward Efficiently Reducing Plastic Input to Oceans

To study ecosystem dynamics in catchments in East Asia, a method that combines a grid-based numerical model, a ground–truth observation network, satellite data, and statistical analysis has been developed. The current monograph (Part VIII) follows the *CGER Supercomputer Monograph Report Series* regarding the NICE model (Fig. 1.2).

(i) 11th publication (Part I), 2006: Governing Equation of NICE (Nakayama and Watanabe, 2006b)

(ii) 14th publication (Part II), 2008: For Nature Restoration and Urban Regeneration (Nakayama, 2008c)

(iii) 18th publication (Part III), 2012: Application of NICE to Urban Areas in Japan and China (Nakayama, 2012d)

(iv) 20th publication (Part IV), 2014: Continental-scale in Changjiang and Yellow River Basins (Nakayama, 2014b)

(v) 26th publication (Part V), 2019: Evaluation of the Missing Role of Inland Water in Global Biogeochemical Cycle (Nakayama, 2019).

(vi) 29th publication (Part VI), 2023: Evaluation of Anthropogenic Activity on Hydrologic Alteration in Arid and Semi-Arid Regions of Mongolia (Nakayama, 2023b).

(vii) 30th publication (Part VII), 2024: Evaluation of Flux and Fate of Plastics by Coupling NICE with Plastic Debris Model (Nakayama, 2024c).

In this monograph (Part VIII), NICE coupled with a plastic debris model was further extended to incorporate resuspension, bedload transport, estuarine dynamics, heteroaggregation, and biofouling to quantify the plastic dynamics on the terrestrial-aquatic-estuarine continuum to further improve the accuracy of the plastic model obtained in Part VII (Fig. 1.4). To fill the gap in current plastic debris models in different categories (Kooi et al., 2018), a comprehensive investigation was conducted by surveying existing research on plastic cycles. The model also improved the accuracy of the plastic cycle in urban regions and clarified that the plastic cycle, particularly the microplastic cycle, in rivers flowing through urban areas has been significantly altered. The establishment of a complete model to capture the total plastic dynamics at the basin scale represents a great step forward. This methodology is powerful for predicting and estimating changes in plastic dynamics under climate change. The results will also help devise solutions and measures for reducing plastic input to the ocean. Details on this process are described in the following chapters.
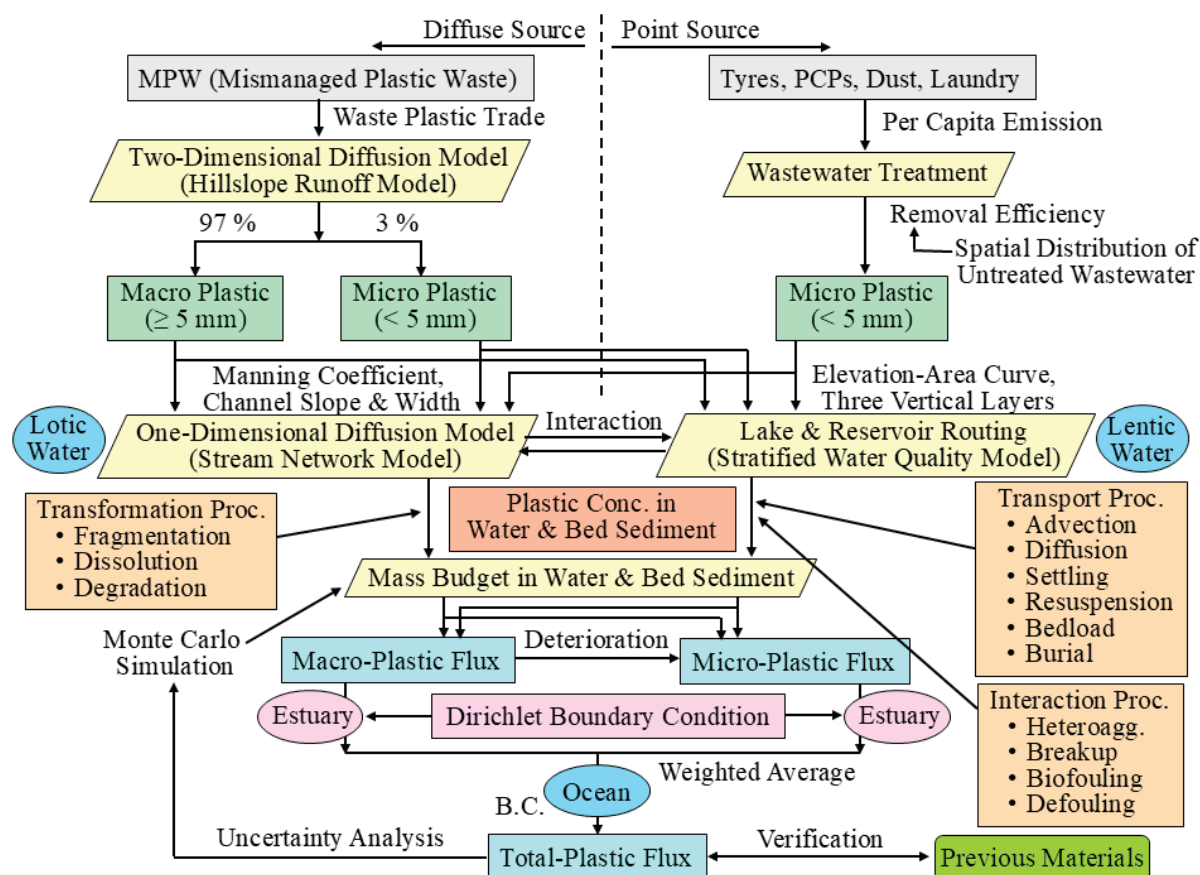
Figure 1.4 Flow diagram of the latest version of the plastic debris model on the terrestrial-aquatic-estuarine continuum by extending the NICE model.

References

Brooks, A.L., Wang, S., Jambeck, J.R. (2018) The Chinese import ban and its impact on global plastic waste trade. Scientific Advances, 4(6), eaat0131. doi:10.1126/sciadv.aat0131

Dominish, E., Retamal, M., Wakefield-Rann, R., Florin, N. (2020) Environmentally responsible trade in waste plastics Report 1: Investigating the links between trade and marine plastic pollution. Institute for Sustainable Futures, University of Technology Sydney. https://www.dcceew.gov.au/sites/default/files/documents/ert-waste-plastics-report-1.pdf

Environmental Investigation Agency (EIA). (2021) The Truth Behind Trash: The scale and impact of the international trade in plastic waste. https://eia-international.org/wp-content/uploads/EIA-The-Truth-Behind-Trash-FINAL.pdf

Jambeck, J.R., Geyer, R., Wilcox, C., et al. (2015) Plastic waste inputs from land into the ocean. Science, 347, 768–771. doi:10.1126/science.1260352

Kooi, M., Besseling, E., Kroeze, C., et al. (2018) Modelling the fate and transport of plastic decries in freshwaters: review and guidance. In: Wagner, M., Lambert, S. [Eds] Freshwater Microplastics. The Handbook of Environmental Chemistry 58, Springer, pp.125–152

Lebreton, L, van der Zwet, J., Damsteeg, J.-W., et al. (2017) River plastic emissions to the world's oceans. Nature Communications, 8, 15611. doi:10.1038/ncomms15611

Meijer, L.J.J., van Emmerik, T., van der Ent, R., et al. (2021) More than 1000 rivers account for 80% of global riverine plastic emissions into the ocean. Science Advances, 7, eaaz5803. doi:10.1126/sciadv.aaz5803

Ministry of Foreign Affairs of Japan. (2019) G20 Osaka Leader's Declaration. https://www.mofa.go.jp/policy/economy/g20_summit/osaka19/en/documents/final_g20_osaka_leaders_declaration.html

Nakayama, T., Watanabe, M. (2004) Simulation of drying phenomena associated with vegetation change caused by invasion of alder (Alnus japonica) in Kushiro mire. Water Resources Research, 40, W08402. doi:10.1029/2004WR003174

Nakayama, T., Watanabe, M. (2005) Re-evaluation of groundwater dynamics about water and nutrient budgets in Lake Kasumigaura, Annual Journal of Hydroscience and Hydraulic Engineering, 49, 1231–1236 (Abst. in English)

Nakayama, T., Watanabe, M. (2006a) Simulation of spring snowmelt runoff by considering micro-topography and phase changes in soil layer. Hydrology and Earth System Sciences Discussions, 3, 2101–2144

Nakayama, T., Watanabe, M. (2006b) Development of process-based NICE model and simulation of ecosystem dynamics in the catchment of East Asia (Part I). CGER's supercomputer monograph report, 11, NIES, 100 p. http://www.cger.nies.go.jp/publications/report/i063/I063e

Nakayama, T., Yang, Y., Watanabe, M., Zhang, X. (2006) Simulation of groundwater dynamics in the North China Plain by coupled hydrology and agricultural models. Hydrological Processes, 20, 3441–3466. doi:10.1002/hyp.6142

Nakayama, T., Watanabe, M., Tanji, K., Morioka, T. (2007) Effect of underground urban structures on eutrophic coastal environment. Science of the Total Environment, 373, 270–288. doi:10.1016/j.scitotenv.2006.11.033

Nakayama, T. (2008a) Factors controlling vegetation succession in Kushiro mire. Ecological Modelling, 215, 225–236.. doi:10.1016/j.ecolmodel.2008.02.017

Nakayama, T. (2008b) Shrinkage of shrub forest and recovery of mire ecosystem by river restoration in northern Japan. Forest Ecology and Management, 256, 1927–1938. doi:10.1016/j.foreco.2008.07.017

Nakayama, T. (2008c) Development of process-based NICE model and simulation of ecosystem dynamics in the catchment of East Asia (Part II). CGER's supercomputer monograph report, 14. NIES, 91 p. http://www.cger.nies.go.jp/publications/report/i083/i083_e

Nakayama, T., Watanabe, M. (2008a) Missing role of groundwater in water and nutrient cycles in the shallow eutrophic Lake Kasumigaura, Japan. Hydrological Processes, 22, 1150–1172. doi:10.1002/hyp.6684

Nakayama, T., Watanabe, M. (2008b) Role of flood storage ability of lakes in the Changjiang River catchment. Global and Planetary Change, 63, 9–22. doi:10.1016/j.gloplacha.2008.04.002

Nakayama, T., Watanabe, M. (2008c) Modelling the hydrologic cycle in a shallow eutrophic lake. SIL Proceedings, 1922–2010, 30, 345–348

Nakayama, T. (2009) (Chapter 1) Simulation of ecosystem degradation and its application for effective policy-making in regional scale. In: Mattia N. Gallo, Ferrari, Marco H. (Eds) River Pollution Research Progress. Nova Science Pub., Inc., New York, pp. 1–89

Nakayama, T. (2010) Simulation of hydrologic and geomorphic changes affecting a shrinking mire. River Research and Applications, 26, 305–321. doi:10.1002/rra.1253

Nakayama, T., Fujita, T. (2010) Cooling effect of water-holding pavements made of new materials on water and heat budgets in urban areas. Landscape and Urban Planning, 96, 57–67. doi:10.1016/j.landurbplan.2010.02.003

Nakayama, T., Sun, Y., Geng, Y. (2010) Simulation of water resource and its relation to urban activity in Dalian City, Northern China. Global and Planetary Change, 73, 172–185. doi:10.1016/j.gloplacha.2010.06.001

Nakayama, T. (2011a) Simulation of complicated and diverse water system accompanied by human intervention in the North China Plain. Hydrological Processes, 25, 2679–2693. doi:10.1002/hyp.8009

Nakayama, T. (2011b) Simulation of the effect of irrigation on the hydrologic cycle in the highly cultivated Yellow River Basin. Agricultural and Forest Meteorology, 151, 314–327. doi:10.1016/j.agrformet.2010.11.006

Nakayama, T. (2011c) Feedback mechanism and complexity in ecosystem-development of integrated assessment system towards eco-conscious society-, Chemical Engineering of Japan, 75, 789–791 (in Japanese)

Nakayama, T. (2011d) Construction of integrated assessment system for win-win solution of hydrothermal degradations in urban area towards eco-conscious society, Chemical Information and Computer Sciences, 29, 63–65 (in Japanese)

Nakayama, T., Hashimoto, S. (2011) Analysis of the ability of water resources to reduce the urban heat island in the Tokyo megalopolis. Environmental Pollution, 159, 2164–2173. doi:10.1016/j.envpol.2010.11.016

Nakayama, T. (2012a) Visualization of the missing role of hydrothermal interactions in a Japanese megalopolis for a win-win solution. Water Science and Technology, 66, 409–414. doi:10.2166/wst.2012.205

Nakayama, T. (2012b) Feedback and regime shift of mire ecosystem in northern Japan. Hydrological Processes, 26, 2455–2469. doi:10.1002/hyp.9347

Nakayama, T. (2012c) Impact of anthropogenic activity on eco-hydrological process in continental scales. Procedia Environmental Sciences, 13, 87–94. doi:10.1016/j.proenv.2012.01.008

Nakayama, T. (2012d) Development of process-based NICE model and simulation of ecosystem dynamics in the catchment of East Asia (Part III). CGER's supercomputer monograph report, 18. NIES, 98 p. http://www.cger.nies.go.jp/publications/report/i103/en/

Nakayama, T., Hashimoto, S., Hamano, H. (2012) Multiscaled analysis of hydrothermal dynamics in Japanese megalopolis by using integrated approach. Hydrological Processes, 26, 2431–2444. doi:10.1002/hyp.9290

Nakayama, T. (2013) For improvement in understanding eco-hydrological processes in mire. Ecohydrology and Hydrobiology, 13, 62–72. doi:10.1016/j.ecohyd.2013.03.004

Nakayama, T., Shankman, D. (2013a) Impact of the Three-Gorges Dam and water transfer project on Changjiang floods. Global and Planetary Change, 100, 38–50. doi:10.1016/j.gloplacha.2012.10.004

Nakayama, T., Shankman, D. (2013b) Evaluation of uneven water resource and relation between anthropogenic water withdrawal and ecosystem degradation in Changjiang and Yellow River Basins. Hydrological Processes, 27(23), 3350–3362. doi:10.1002/hyp.9835

Nakayama, T. (2014a) (Chapter 16) Hydrology–ecology interactions. In: Saeid Eslamian (Ed.) Handbook of Engineering Hydrology, 1: Fundamentals and Applications. Taylor & Francis, pp. 329–344

Nakayama, T. (2014b) Development of process-based NICE model and simulation of ecosystem dynamics in the catchment of East Asia (Part IV). CGER's supercomputer monograph report, 20. NIES, 102 p. http://www.cger.nies.go.jp/publications/report/i114/en/

Nakayama, T. (2014) (Chapter 33) Integrated assessment system using process-based eco-hydrology model for adaptation strategy and effective water resources management. In: Venkat Lakshmi (Ed.) Remote Sensing of the Terrestrial Water Cycle (Geophysical Monograph Series 206), pp. 521–535. doi:10.1002/9781118872086.ch33

Nakayama, T. (2016) New perspective for eco-hydrology model to constrain missing role of inland waters on boundless biogeochemical cycle in terrestrial-aquatic continuum. Ecohydrology and Hydrobiology, 16, 138–148. doi:10.1016/j.ecohyd.2016.07.002

Nakayama, T. (2017a) Development of an advanced eco-hydrologic and biogeochemical coupling model aimed at clarifying the missing role of inland water in the global biogeochemical cycle. Journal of Geophysical Research: Biogeosciences, 122, 966–988. doi:10.1002/2016JG003743

Nakayama, T. (2017b) Scaled-dependence and seasonal variations of carbon cycle through development of an advanced eco-hydrologic and biogeochemical coupling model. Ecological Modelling, 356, 151–161. doi:10.1016/j.ecolmodel.2017.04.014

Nakayama, T. (2017c) Biogeochemical contrast between different latitudes and the effect of human activity on spatiotemporal carbon cycle change in Asian river systems. Biogeosciences Discussions. doi:10.5194/bg-2017–447

Nakayama, T. (2018) Interaction between surface water and groundwater and its effect on ecosystem and biogeochemical cycle. Journal of Groundwater Hydrology, 60, 143–156. doi:10.5917/jagh.60.143 (in Japanese)

Nakayama, T., Maksyutov, S. (2018) Application of process-based eco-hydrological model to broader northern Eurasia wetlands through coordinate transformation. Ecohydrology and Hydrobiology, 18, 269–277. doi:10.1016/j.ecohyd.2017.11.002

Nakayama, T., Pelletier, G.J. (2018) Impact of global major reservoirs on carbon cycle changes by using an advanced eco-hydrologic and biogeochemical coupling model. Ecological Modelling, 387, 172–186. doi:10.1016/j.ecolmodel.2018.09.007

Nakayama, T. (2019) Development of process-based NICE model and simulation of ecosystem dynamics in the catchment of East Asia (Part V). CGER's supercomputer monograph report, 26. NIES, 122 p. http://www.cger.nies.go.jp/publications/report/i148/en/

Nakayama, T. (2020) Inter-annual simulation of global carbon cycle variations in a terrestrial-aquatic continuum. Hydrological Processes, 34, 662–678. doi:10.1002/hyp.13616

Nakayama, T., Wang, Q., Okadera, T. (2021a) Evaluation of spatio-temporal variations in water availability using a process-based eco-hydrology model in arid and semi-arid regions of Mongolia. Ecological Modelling, 440, 109404. doi:10.1016/j.ecolmodel.2020.109404

Nakayama, T., Wang, Q., Okadera, T. (2021b) Sensitivity analysis and parameter estimation of anthropogenic water uses for quantifying relation between groundwater overuse and water stress in Mongolia. Ecohydrology and Hydrobiology, 21, 490–500. doi:10.1016/j.ecohyd.2021.07.006

Nakayama, T. (2022) Impact of anthropogenic disturbances on carbon cycle changes in terrestrial-aquatic-estuarine continuum by using an advanced process-based model. Hydrological Processes, 36, e14471. doi:10.1002/hyp.14471

Nakayama, T. (2023a) Evaluation of global biogeochemical cycle in lotic and lentic waters by developing an advanced eco-hydrologic and biogeochemical coupling model. Ecohydrology, 17(4), e2555. doi:10.1002/eco.2555

Nakayama, T. (2023b) Development of process-based NICE model and simulation of ecosystem dynamics in the catchment of East Asia (Part VI). CGER's supercomputer monograph report, 29. NIES, 95 p. http://www.cger.nies.go.jp/publications/report/i164/en/

Nakayama, T., Okadera, T., Wang, Q. (2023) Impact of various anthropogenic disturbances on water availability in the entire Mongolian basins towards effective utilization of water resources. Ecohydrology and Hydrobiology, 23(4). doi:10.1016/j.ecohyd.2023.04.006

Nakayama, T., Osako, M. (2023a) Development of a process-based eco-hydrology model for evaluating the spatio-temporal dynamics of macro- and micro-plastics for the whole of Japan. Ecological Modelling, 476, 110243. doi:10.1016/j.ecolmodel.2022.110243

Nakayama, T., Osako, M. (2023b) The flux and fate of plastic in the world's major rivers: Modelling spatial and temporal variability. Global and Planetary Change, 221, 104037. doi:10.1016/j.gloplacha.2023.104037

Nakayama, T. (2024a) Impact of global major reservoirs and lakes on plastic dynamics by using a process-based eco-hydrology model. Lakes and Reservoirs: Research and Management, 29, e12463. doi:10.1111/lre.12463

Nakayama, T. (2024b) Evaluation of flux and fate of plastic in terrestrial-aquatic-estuarine continuum by using an advanced process-based model. Ecohydrology, 17(6), e2678. doi:10.1002/eco.2678

Nakayama, T. (2024c) Development of process-based NICE model and simulation of ecosystem dynamics in the catchment of East Asia (Part VII). CGER's Supercomputer Monograph Report, 30, NIES, 111 p. http://www.cger.nies.go.jp/publications/report/i169/en/

Nakayama, T., Osako, M. (2024) Plastic trade-off: Impact of export and import of waste plastic on plastic dynamics in Asian region. Ecological Modelling, 489, 110624. doi:10.1016/j.ecolmodel.2024.110624

Nakayama, T. (2025a) Impact of settling and resuspension on plastic dynamics during extreme flow and their seasonality in global major rivers. Hydrological Processes, 39(2), e70072. doi:10.1002/hyp.70072

Nakayama, T. (2025b) Improvement in understanding of plastic cycle in Japanese urban regions. Hydrological Processes, 39(6), e70168. doi:10.1002/hyp.70168

Nakayama, T. (2025c) Improvement to simulate plastic dynamics and their relation to biogeochemical cycles in global rivers by considering effect of interaction processes of biofouling and heteroaggregation. Global and Planetary Change, 253, 104917. doi:10.1016/j.gloplacha.2025.104917

Nakayama, T. (2025d) Grazing impacts on Mongolian grasslands assessed by an eco-hydrology model. Environmental Science Pollution Research 32, 13626–13637. doi:10.1007/s11356-025-36083-2

Nizzetto, L., Bussi, G., Futter, M.N., et al. (2016) A theoretical assessment of microplastic transport in river catchments and their retention by soils and river sediments. Environmental Science: Processes & Impacts, 18, 1050–1059. doi:10.1039/c6em00206d

Schmidt, C., Krauth, T., Wagner, S. (2017) Export of plastic debris by rivers into the sea. Environmental Science & Technology, 51, 12246–12253. doi:10.1021/acs.est.7b02368

Siegfried, M., Koelmans, A.A., Besseling, E., Kroeze, C. (2017) Export of microplastics from land to sea. A modelling approach. Water Research, 127, 249–257. doi:10.1016/j.watres.2017.10.011

Thompson, R.C., Olsen, Y., Mitchell, R.P., et al. (2004) Lost at sea: Where is all the Plastic? Science, 304, 838. doi: 10.1126/science.1094559

UNESCO. (2022) IHP-IX: Strategic Plan of the Intergovernmental Hydrological Programme: Science for a Water Secure World in a Changing Environment, ninth phase 2022–2029. https://unesdoc.unesco.org/ark:/48223/pf0000381318.locale=en

United Nations. (2019) Basel Convention: Controlling transboundary movements of hazardous wastes and their disposal. http://www.basel.int/Implementation/MarinePlasticLitterandMicroplastics/Overview/tabid/6068/Default.aspx

Waldschläger, K., Schüttrumpf, H. (2019) Erosion behavior of different microplastic particles in comparison to natural sediments. Environmental Science & Technology, 53, 13219–13227. doi:10.1021/acs.est.9b05394

Zhang, K., Hamidian, A.H., Tubic, A., et al. (2021) Understanding plastic degradation and microplastic formation in the environment: A review. Environmental Pollution, 274, 116554. doi:10.1016/j.envpol.2021.116554

- 15 -

Chapter 2

Settling and Resuspension Impacts on Plastic Dynamics during Extreme Flow and Their Seasonality in Global Major Rivers

Abstract

In recent decades, environmental contamination by plastics has received considerable attention from scientists, policymakers, and the public. Although some models have successfully simulated the transport and fate of plastic debris in freshwater systems, a complete model is currently being developed to clarify the dynamic characteristics of the plastic budget on a continental scale. Recently, two process-based eco-hydrology models, the National Integrated Catchment-based Eco-hydrology (NICE) and NICE-BioGeochemical Cycle (NICE-BGC), were linked to a plastic debris model that accounts for both the transport and fate of plastic debris (advection, dispersion, diffusion, settling, dissolution, and biochemical degradation by light and temperature), and this new model was applied on a regional scale and for global major rivers. This study incorporates resuspension and bedload transport by extending the author's previous investigations. The simulation results showed that large-sized microplastics are distributed to a greater extent in riverbeds than in river water. Although small-sized microplastics are suspended in the water and large-sized microplastics settle in the riverbed under normal flow, floods completely disturb this equilibrium and resuspend large microplastics in the water. Because the percentage of the exported microplastic load stored in the riverbed during flood periods is relatively high in some major global rivers, the amount of plastic deposited in riverbeds may be smaller than that in lakes and dams. The riverine plastic transport to the ocean revised in the present study was 1.218 ± 0.393 Tg/yr, with macroplastic flux 0.793 ± 0.305 Tg/yr and microplastic flux 0.426 ± 0.248 Tg/yr, which is within the range of previous values, i.e., 0.41–4.0 Tg/yr. These results aid in the development of solutions and measures for reducing plastic input to the ocean and help quantify the magnitude of plastic transport under climate change.

Keywords: Eco-hydrology model; extreme flow; plastic mobilization; riverine plastic transport

2.1 Introduction

Plastic pollution is a main environmental problem, and pollutants in streams, rivers, and oceans pose potential risks to human health and the environment (Siegfried et al., 2017). Once plastic is released into the environment, it is gradually degraded by physical, chemical, and biological processes, leading to its further subdivision into an enormous number of forms that are impossible to remove and remain indefinitely in the environment. Plastic can be roughly categorized as macroplastic (≥5 mm) or microplastic (<5 mm), and the latter is further divided into primary and secondary microplastics according to origin (Siegfried et al., 2017). Previous studies on the origin and fate of plastic waste in freshwater systems suggested that land-derived plastics are among the main sources of marine plastic pollution (Thompson et al., 2004). Studies (Jambeck et al., 2015; Lebreton et al., 2017; Schmidt et al., 2017) have estimated the distribution of global riverine plastic emissions into the ocean using empirical indicators representative of waste generation (mismanaged plastic waste, MPW) inside a river basin. Recently, Meijer et al. (2021) applied a probabilistic approach to devise a more accurate form of analysis to account for the spatial distribution of plastic waste generation (Lebreton and Andrady, 2019) and the climatological/geographical differences within river basins. Other studies (Siegfried et al., 2017; van Wijnen et al., 2019; Strokal et al., 2021) have adapted a process-oriented model at both the continental and global scales by extending an existing non-dynamic nutrient export model.

However, these global plastic transport models have ignored the impact of flood events on plastic mobilization and suggested its high interannual variability, whereby plastic transport increases up to a factor of five to ten during floods (van Emmerik et al., 2019; Roebroek et al., 2021). Other studies have shown that 90% of the plastic load transported out of urban catchments during high-flow periods occurs only 20% of the time (Wagner et al., 2019), and that flooding contributes 40% of the annual plastic mass flux over 14.5% of the year (Treilles et al. 2022). Macroplastic debris consisting of low-density polymers, such as polyethylene (PE), polypropylene (PP), and polystyrene (PS), is predominantly transported under normal water flow, whereas a relatively large fraction of plastic litter retained in the bottom sediment is efficiently flushed from riverbeds during flooding (Nizzetto et al., 2016; Hurley et al., 2018; Schwarz et al., 2019). This is also related to the fact that large microplastics are distributed more efficiently in bed sediments than in the water column because the aggregation of microplastics mixed with organic minerals is one of the mechanisms responsible for microplastic sedimentation (Kooi et al., 2018; Koutnik et al., 2021; Liu et al., 2021). In terms of temporal plastic dynamics, research has focused on the flow threshold above which rivers move from a sink to a source of microplastics (Ockelfold et al., 2020) and the characteristics of deposition and remobilization between rising and falling limbs (Drummond et al., 2022). This is also related to the inflection point that marks the transition between transport modes during normal and flood conditions caused by floodplain inundation, additional inputs from flooded tributaries, and higher plastic concentrations in the aquatic environment (van Emmerik et al., 2023). Because extreme events such as floods and droughts are expected to increase further with climate change, the impact of flood events on plastic mobilization and its high variability must be evaluated using a process-oriented model.

The development of a framework to reverse global water resource degradation, especially plastic pollution, is vital for achieving Sustainable Development Goals (SDGs) (UNESCO, 2022). The G20 Osaka Summit in 2019 shared the "Osaka Blue Ocean Vision" (Ministry of Foreign Affairs of Japan, 2019), which is positioned alongside the Conference of the Parties (COP) as part of global warming countermeasures. Quantitative assessment of the fate and

transport of plastics will be necessary to realize this vision because countries around the world have decided on concrete future measures for dealing with plastics based on scientific results. Previous studies have revealed that the summer monsoon in Asia makes a dominant contribution to plastic pollution, with more than 74% of waste delivered between May and October from a limited number of large rivers (Lebreton et al., 2017; Best, 2018; Nakayama and Osako, 2023b).

The author previously developed a process-based model that couples eco-hydrology with the biogeochemical cycle (National Integrated Catchment-based Eco-hydrology (NICE)-BioGeochemical Cycle(BGC)) (Nakayama, 2017a, 2017b), incorporating complex terrestrial-aquatic linkages in the hydrological–biogeochemical cycle. Recently, this process-based NICE-BGC was extended by coupling it with a plastic debris (engineered materials) model and applied to the evaluation of spatiotemporal variations of plastic debris on a regional scale for all of Japan (Nakayama and Osako, 2023a) and on a global scale for the world's major rivers (Nakayama and Osako, 2023b) (Fig. 2.1). Based on this background, three basic issues were addressed: (i) How does the movement of plastic particles between water and riverbed sediment affect plastic mobilization and transport? (ii) To what extent do extreme flow and seasonality affect plastic dynamics? (iii) What is the impact of plastic mobilization on the plastic balance? To clarify these issues, resuspension and bedload transport were incorporated based on previous studies (Nakayama and Osako, 2023a, 2023b). This new model simulates seasonal variations in plastic flux to quantify the impact of flood events on plastic mobilization and the high intra-annual variability caused by settling, resuspension, and bedload transport during 2014–2015. The present study represents an important step not only for the qualification of the various processes, but also for the identification of the driver hierarchy in a range of river catchments.
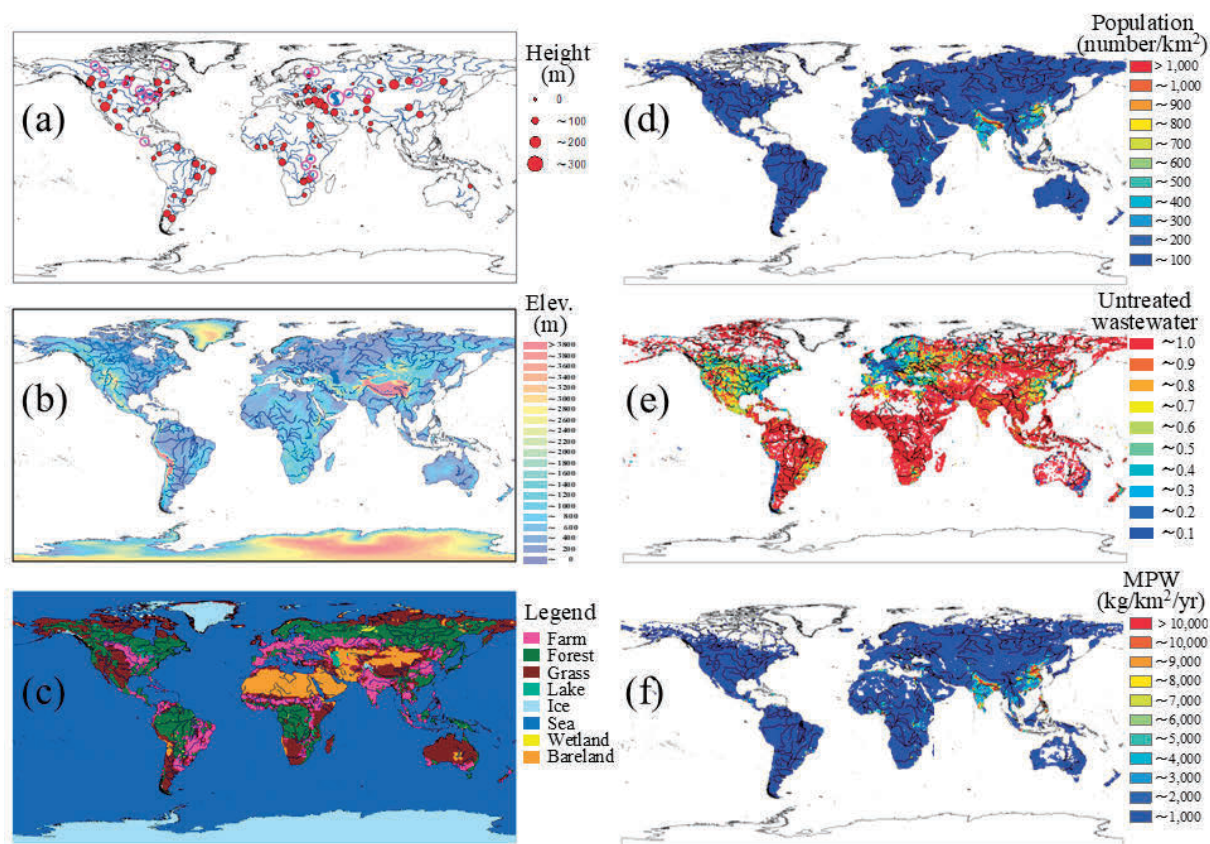
Figure 2.1 Location of study area in the global scale; (a) world's major rivers (153 basins, 325 river channels) with 82 major reservoirs (red circle) and 19 lakes (blue mesh) included in these basins; (b) elevation, (c) land cover, (d) population density, (e) untreated wastewater calculated from wastewater treatment and wastewater production, and (f) mismanaged plastic waste (MPW), respectively. In the figure, line shows the world's major rivers in HYDRO1K.

2.2 Methods

2.2.1 Model Description of Mass Transport Process in NICE-BGC

The NICE series of process-based catchment models have been developed for application to natural, agricultural, and urban regions in various catchments and basins (Nakayama, 2008a–c, 2009, 2010, 2011a–d, 2012a–d, 2013, 2014a,b, 2015, 2016, 2017a–c, 2018, 2019, 2020, 2022, 2023a,b; Nakayama and Fujita, 2010; Nakayama and Hashimoto, 2011; Nakayama and Maksyutov, 2018; Nakayama and Osako, 2023a,b, 2024; Nakayama and Pelletier, 2018; Nakayama and Shankman, 2013a,b; Nakayama and Watanabe, 2004, 2005, 2006a,b, 2008a–c; Nakayama et al., 2006, 2007, 2010, 2012, 2021a,b, 2023) (Fig. 1.1). The NICE model consists of complex sub-models: a surface hydrology model; a land-surface model including urban and crop processes; a groundwater model; a regional atmospheric model; a mass transport model of sediment, nutrients, carbon, and plastics; and a vegetation succession model.

2.2.2 Modeling Fate and Transport of Plastics by Incorporating Resuspension and Bedload Transport

The advanced process-based model that couples the NICE model with various biogeochemical cycle models (NICE-BGC) (Nakayama, 2017a, 2017b, 2022) incorporates the connectivity of the biogeochemical cycle, accompanied by the hydrological cycle between surface water and groundwater, hillslopes, river networks, and other intermediate regions. Recently, this model was extended by combining it with a plastic debris (engineered materials) model and used to evaluate spatiotemporal variations of plastic debris on a regional scale for all of Japan (Nakayama and Osako, 2023a) and on a global scale for the world's major rivers (Nakayama and Osako, 2023b) (Fig. 2.1). The new model also included advection, dispersion, diffusion, settling, dissolution and deterioration due to light and temperature, but assumed no interaction with suspended matter (heteroaggregation) (Praetorius et al., 2012), resuspension (Waldschläger and Schüttrumpf, 2019), biofouling (Kooi et al., 2017, 2018), or wind effects.

In the present study, resuspension, bedload transport and settling were incorporated based on previous studies (Nakayama and Osako, 2023a, 2023b; Nakayama, 2024) (Fig. 2.2). The resuspension rate predicted by the original model assumed that the riverbed would be under equilibrium conditions with a uniform particle size distribution, making it difficult to apply directly to plastic. Determining the heterogeneous distribution of settled and deposited plastic on riverbeds is difficult, although some studies have evaluated the erosion behavior of microplastic particles in comparison to sediments (Waldschläger and Schüttrumpf, 2019). The new model now includes the mass budget in the water and the bed sediment of any given reach, which is consistent with previous studies (Nizzetto et al., 2016; Koutnik et al., 2021);

$$\frac{dM_{sed,i}}{dt} = m_{dep,i} - m_{res,i} \tag{2.1}$$

$$V\frac{dC_{w,i}}{dt} = QC_{w,i}{}^{up} - QC_{w,i} + m_{eff,i} + \sum_u Am_{out,i} + LW(m_{res,i} - m_{dep,i}) \tag{2.2}$$

where subscript i refers to each plastic size; M_{sed} (kg/m^2) is the mass of microplastic of a specific size class present in the sediment; m_{dep} (kg/m^2/s) is the mass of microplastic deposited from the water column on the sediment; m_{res} (kg/m^2/s) is the mass of microplastic entrained (resuspended) from the streambed sediment; C_w (kg/m^3) is the concentration of microplastic suspended in the water in a control volume of length L (m) and width W (m); $C_w{}^{up}$ (kg/m^3) is the concentration of suspended microplastic from upstream; Q (m^3/s) is the river discharge; m_{eff} (kg/m^2/s) represents the microplastics discharged from point source effluents such as wastewater treatment plants; A (m^2) is the surface of each land use unit (u) contributing to delivery of microplastics to the river; and m_{out} (kg/m^2/s) is the mass of microplastic delivered to the river by overall runoff during rainfall,. Thus, the model can simulate the concentration of plastics in both the water and bed sediment and evaluate the hydrograph for plastic transport under various shear stresses during storm events, as proposed by Kumar et al. (2021). Because the new model in equations (2.1) and (2.2) did not assume that the riverbed was in equilibrium as in previous studies (Nakayama and Osako, 2023a, 2023b; Nakayama, 2024), the simulation could separately assess the hydrological effects (during the rising limb, falling limb, and normal flow) and plastic material impacts (size and density) (Fig. 2.2).
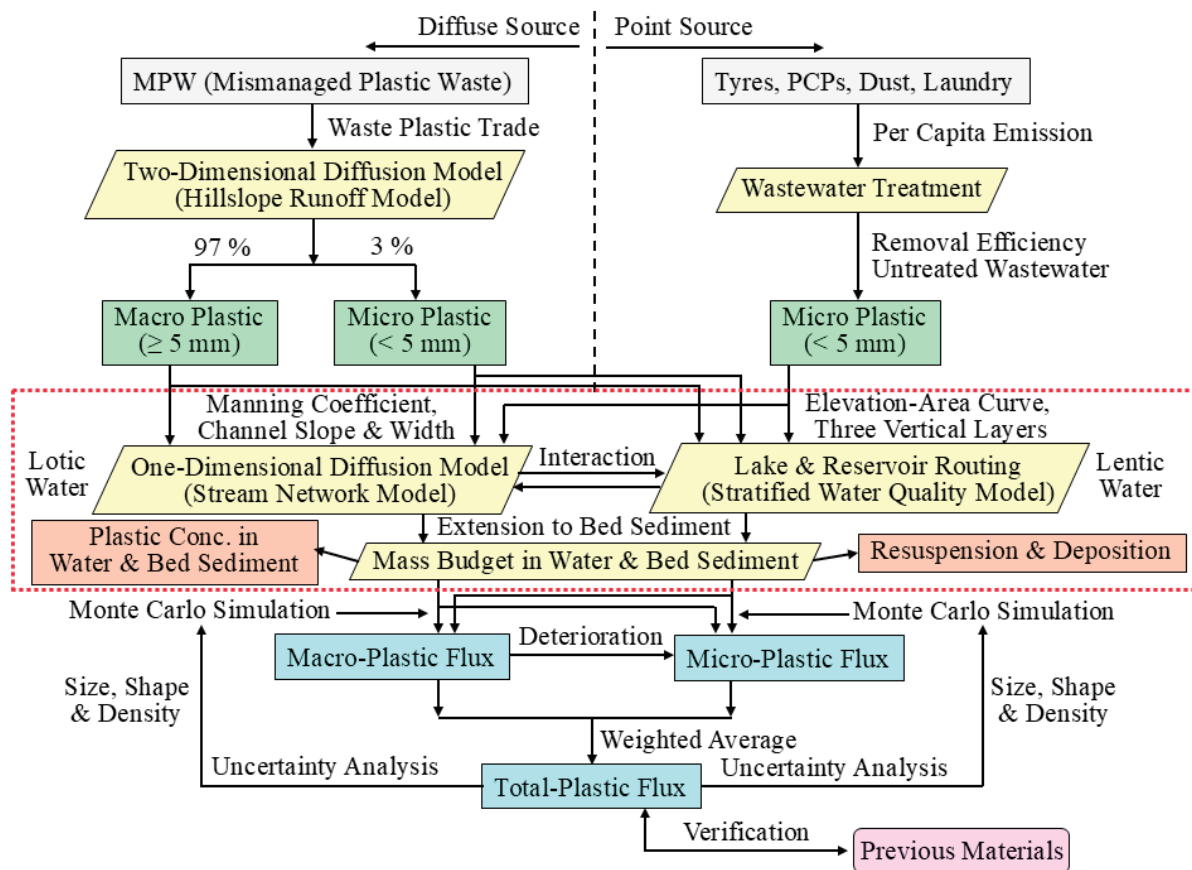
Figure 2.2 Flow diagram showing the transport of macro- and microplastics over land and in inland waters obtained by extending the NICE-BGC model. Red dotted frames indicate the newly developed processes in the model to include resuspension and bedload transport in addition to settling by extension of the author's previous studies.

Recently (Nakayama, 2023), the author coupled NICE-BGC with LAKE2K, a stratified water quality model (Chapra and Martin, 2012). LAKE2K simulates a lake as a one-dimensional system consisting of three vertical layers (epilimnion, metalimnion, and hypolimnion). Therefore, this coupled model makes it possible to simulate hydrological and biogeochemical cycles in global lentic water reservoirs and lakes. It is possible to simulate the effects of reservoirs and lakes on organic carbon (DOC and POC) and nutrient fluxes without assuming a deficit ratio (Nakayama and Pelletier, 2018). In this study, the coupled model was extended to simulate the plastic dynamics in both lotic and lentic waters based on previous studies (Nakayama and Osako, 2023a, 2023b; Nakayama, 2024). After simulating plastic transport on a hillslope, the estimated rate of conversion of macroplastics to microplastics (3%/yr) was applied based on the method of van Wijnen et al. (2019) and the extension of the conversion rate employed by Jambeck et al. (2015) (Fig. 2.2). This model was applied to the world's major rivers (153 basins and 325 river channels), including 82 reservoirs and 19 lakes (Fig. 2.1).

2.3 Input Data and Boundary Conditions for Simulation

2.3.1 Model Input Data

The input data at hybrid spatial resolution were prepared and arranged to calculate a spatially averaged 1° × 1° grid using the Spatial Analyst Tools in ArcGIS v10.3 software for the global simulation (Fig. 2.1). Elevation, land cover, soil texture, vegetation type, river networks, lakes and wetlands, reservoirs and dams, geological structures, crop type, irrigation type, irrigation water use, fertilizer use, and manure use were categorized based on global datasets. Although data on plastics are scarce, global plastic debris were simulated using gridded population data at 1 km resolution from 2015 global data (NASA, 2018); wastewater production, collection, treatment, and reuse data at 5 arcmin (approximately 10 km) resolution (Jones et al., 2021), and MPW at 1 km resolution (Lebreton and Andrady, 2019) as a diffuse source (Table 2.1). To reasonably create grid data from point, polyline, and polygon data for different sources with different spatial resolutions, an overlay analysis was conducted using GIS tools (intersect, union, and identity) (ESRI, 2019).

Table 2.1 List of input data sets for the NICE and NICE-BGC simulations.

Data set	Original resolution	Year	Source and reference
Climatology	1.0° 1.0°	1998-2015 1998-2015	ERA-interim; ECMWF (2019) CRU TS3.24; CRU (2017)
Elevation	1.0km	around 1996 around 2018	GTOPO30; U.S. Geological Survey (1996a) SRTM; U.S. Geological Survey (2018)
Land cover	1.0km	around 2000	GLC2000; European Commission (2015)
Soil texture	1.0km	around 1970-2000	HWSD; European Commission (2012)
Vegetation type	0.25°	around 2000	GLDAS Vegetation Class; NASA (2013)
River networks	1.0km	around 1996	HYDRO1K; U.S. Geological Survey (1996b)
Lakes and wetlands	0.5 min	around 1990-2000	GLWD; Lehner and Döll (2004)
Reservoirs and Dams	point	around 2010	GRanD; Lehner et al. (2011)
Geological structures	0.5°	around 1970-2000	GLiM; Hartmann and Moosdorf (2012)
Crop type	5 min	around 2000	MIRCA2000; Portmann et al. (2010)
Irrigation type	5 min	2000-2008	GMIA; FAO (2016)
Irrigation water use	5 min	1998-2002	GCWM; Siebert and Döll (2010)
Fertilizer use	5 min	around 2000	Earth Stat; Mueller et al. (2012)
Manure use	5 min	1998-2014	Zhang et al. (2017)
Atmospheric N deposition	0.5°	1998-2015	ISIMIP2a; Tian et al. (2018)
Population	1.0km	2015	NASA (2018)
Wastewater production and treatment	5 min	2015	Jones et al. (2021)
Mismanaged plastic waste	1.0 km	2015	Lebreton and Andrady (2019)

The per capita emissions of microplastics in each economic region determined in a previous study were also used (van Wijnen et al., 2019). Generally, microplastics at point sources

originate from four sources: personal care products (PCPs) (0.0007–0.0055 kg/cap. /yr), laundry fibers (0.007–0.11 kg/cap. /yr), car tire wear (0.0072–0.18 kg/cap. /yr), and fragmentation of macroplastics (8.5–27 kg/cap. /yr) for each region (Nakayama and Osako, 2023a, 2023b). We estimated the potential fluxes of microplastics by multiplying the per capita emissions and their population distribution for each catchment flow into wastewater treatment plants (WWTPs) in the NICE-BGC simulation (Fig. 2.2). We also applied "untreated wastewater" and converted it to estimate the efficiency of microplastic removal, with the former calculated by subtracting the ratio of wastewater treatment and wastewater production at 5 arcmin resolution (Jones et al., 2021). This revealed that the efficiency of microplastic removal in WWTPs in developed countries was much higher than that in developing countries (Fig. 2.1c) because almost all treatments were secondary and tertiary (Nakayama and Osako, 2023a). It was also assumed that the microplastic concentration on hillslopes would be constant (Wagner et al., 2019), and the time series proportional to hillslope runoff was calculated at each time step. The details are described in the author's previous studies (Nakayama and Osako, 2023a, 2023b).

2.3.2 Running the Simulation and Verification

The simulation was conducted at a $1° \times 1°$ resolution in the horizontal direction and in the same layers in the vertical direction (Nakayama and Osako, 2023b) (Fig. 2.1). The NICE-BGC simulation for terrestrial ecosystems was conducted at the same spatial resolution with a time step of $\Delta t = 1$ d for two years during 2014–2015 by iteratively inputting values simulated by NICE after calculating the daily averaged data from 1-hourly data (Fig. 2.2). The author used previous data on per capita emissions of microplastics into rivers (PCPs, dust, laundry fibers, and tires) and the removal efficiency of WWTPs as a point source. The model also simulated the outflow of macroplastics originating from MPW (Lebreton and Andrady, 2019) as a diffuse source. Then, a NICE-BGC simulation for aquatic ecosystems was conducted by inputting the simulated results for land to a stream network model with a time step of $\Delta t = 0.70$ min to ensure model stability. The hydrological cycle and plastic transport in rivers were simulated and verified using previous datasets and materials on a continental scale (Nakayama and Osako, 2023b). Because most of the previous data were expressed as the number of plastics (items), these data were converted to plastic weight, assuming that the mass per particle would be 0.0000294 (g), which is the value averaged from Schmidt et al. (2017) and Zhao et al. (2019). For simplicity, sediment density was assumed to be equal to 2,650 kg/m³, and the sediment depth was assumed to equal 10 cm to calculate plastic deposition in the riverbed.

To simulate the plastic flux, the weighted average value was calculated by multiplying each probability by each flux and their summation. This was based on the assumption that both micro- and macroplastics are pure and totally inert polymers with a continuous probability distribution of size, shape, and density (Kooi and Koelmans, 2019), in the same way as the author's previous study (Nakayama and Osako, 2023b). Uncertainty and sensitivity analyses were conducted by ranking the model parameters according to their contribution to prediction uncertainty using Monte Carlo model simulations. The details are described in the author's previous studies (Nakayama and Osako, 2023b; Nakayama, 2024). The results yielded quantitative measures of model performance in terms of reproducing seasonality and intraannual variability in the hydrologic cycle and plastic transport.

2.4 Results and Discussion

2.4.1 Evaluation of Plastic Concentrations in Water and Riverbeds for the World's Major Rivers

The author previously showed that both macro- and microplastic fluxes into the ocean simulated by the models were reasonably consistent with previous data for global major rivers and closely related to population density (Nakayama and Osako, 2023b). In the present study, the author compiled as many previous data as possible and calculated the average values and standard deviations of plastic concentration in the water (Table 2.2) (Eerkes-Medrano et al., 2015; Lebreton et al., 2017; Schmidt et al., 2017; van Wijnen et al., 2019; Xiong et al., 2019; Han et al., 2020; Li et al., 2020; Mai et al., 2020; Waldschläger et al., 2020; Haberstroh et al., 2021; Singh et al., 2021; Weiss et al., 2021; Zhao et al., 2022; Huang et al., 2023; Qian et al., 2023) and plastic deposition in riverbeds (Table 2.3) (Pojar et al., 2021; Singh et al., 2021; Tsering et al., 2021; Yang et al., 2021; Zhao et al., 2022; Gao et al., 2023; Qian et al., 2023). The new model also compared the plastic concentration in water and plastic deposition in riverbeds with previous findings for global major rivers (Fig. 2.3). The result shows that when the simulated concentration of plastic in water has a density lower than that of water, the value is overestimated related to the observations (density = 988.0 kg/m^3 for floating condition) and that the case with a relatively low density better reproduces the observations (density = 1000.1 kg/m^3 for a density slightly greater than the water) (Fig. 2.3a-b). This is supported by previous research, indicating that PP and PE are the dominant polymers in freshwater (Burns and Boxall, 2018). In addition, most observations were performed in the downstream sections of these rivers near estuaries, where PP is the most prevalent in water, whereas PE is more prevalent in sediments (Koutnik et al., 2021). In contrast, the simulated deposition in the riverbed varies considerably from the observed value, and further improvements in accuracy are required, including in the evaluation of the existing deposition volume (Fig. 2.3c).

Table 2.2 Summary of micro- and macroplastic concentrations in the waters of different rivers.

River	Micro-plastic (mg/m³)	Macro-plastic (mg/m³)	Total plastic (mg/m³)	Reference
Danube	9.8	1.1	10.9	Lebreton et al. (2017)
Danube	2	0.2	2.2	Lebreton et al. (2017)
Danube	31.8	38	69.8	Lebreton et al. (2017)
Danube	9.8	1.1	10.9	Mai et al.(2020)
Danube	2	0.2	2.2	Mai et al.(2020)
Danube	4.1			van Wijnen et al. (2019)
Danube			10.9	Schmidt et al. (2017)
Danube			2.2	Schmidt et al. (2017)
Danube	0.748			Weiss et al.(2021)
Average	**8.61**	**8.12**	**15.59**	
SD	**10.88**	**16.71**	**24.30**	
Yangtze	0.153	7.5	7.65	Mai et al.(2020)
Yangtze	12			van Wijnen et al. (2019)
Yangtze (11 sites)	158			Weiss et al.(2021)
Yangtze			805.2 **	Haberstroh et al. (2021)
Yangtze	82.32±45.28 *			Xiong et al. (2019)
Yangtze	57.17±33.65 *			Zhao et al. (2022)
Yangtze	157.29±142.59 *			Qian et al. (2023)
Yangtze	37.338 *			Qian et al. (2023)
Yangtze downstream	54.56934 *			Huang et al. (2023)
Average	**69.86**	**7.50**	**406.43**	
SD	**60.03**		**563.95**	
Yangtze Estuary	204			Weiss et al.(2021)
Yangtze Estuary	0.193			Weiss et al.(2021)
Yangtze Estuary	71.8			Weiss et al.(2021)
Yangtze Estuary	0.121637±0.072368 *			Waldschlager et al.(2020)
Yangtze Estuary	1.9845 *			Li et al. (2020)
Yangtze Estuary	157.29±142.59 *			Xiong et al. (2019)
Yangtze Estuary	30.85236 *			Huang et al. (2023)
Average	**66.61**			
SD	**83.08**			
Yellow River (wet)	14141.4±2969.4 *			Zhao et al. (2022); Han et al. (2020)
Yellow River (dry)	29620.5±11304.3 *			Zhao et al. (2022); Han et al. (2020)
Yellow River	26048.4±14876.4 *			Qian et al. (2023)
Yellow River (wet)	73818.4±87355.3 *			Qian et al. (2023)
Yellow River (dry)	12715.5±7171.88 *			Qian et al. (2023)
Average	**31268.84**			
SD	**24889.81**			
Ganga River	0.2415±0.0985 *			Singh et al. (2021)
Average	**0.24**			
SD	**0.10**			
Mekong			220.95 **	Haberstroh et al. (2021)
Average			**220.95**	
SD				
Hudson River	0.731			Weiss et al.(2021)
Hudson River	28.812 *			Han et al. (2020)
Average	**14.77**			
SD	**19.86**			
St. Lawrence River	0.404515±0.402339 *			Eerkes-Medrano et al.(2015)
Average	**0.40**			
SD	**0.40**			
Global River (n=414)	**0.018669 ***			Koutnik et al. (2021)
Global Stormwater (n=14)	**1.63023 ***			Koutnik et al. (2021)
Global Lake (n=235)	**0.07056 ***			Koutnik et al. (2021)
Global Estuary (n=130)	**0.0044982 ***			Koutnik et al. (2021)

* Calculated values by assuming that mass per particle is equal to 0.0000294 (g).

** Calculated value by assuming that floating plastic is equal to total plastic.

Table 2.3 Summary of the abundance and characteristics of microplastics in freshwater sediment. In the table, "TGD" means the Three Gorges Dam.

River	Abundance (items/kg)	Abundance (g/m^2) *	Shape	Size	Chemical component	Reference
Danube	350±250				Fiber	Pojar et al. (2021)
	165					Pojar et al. (2021)
Average	**257.50**	**2.01**				
SD	**176.78**	**1.38**				
Yangtze	182.5±157.5					Qian et al. (2023)
Yangtze	286.2					Qian et al. (2023)
Yangtze Estuary	180±160		93% fiber	31.19% < 100um	Rayon, PES, AC, PET, PS	Yang et al. (2021)
				62.15% 500 - 1000um		Yang et al. (2021)
Average	**216.23**	**1.68**				
SD	**91.66**	**0.71**				
TGD	162.5±137.5		33.9 - 100% fiber	500 - 1000 um 1.7% to 77.8%	PS(39%), PP(29%), PE(21%)	Yang et al. (2021)
TGD	472±392		70% fragment	1 - 5 mm 71.4%	PP(80%)	Yang et al. (2021)
TGD	162.5±137.5		Fiber	0.5 - 5 mm		Zhao et al. (2022)
Average	**265.67**	**2.07**				
SD	**146.94**	**1.14**				
Yellow River	3766.67±1625.63					Qian et al. (2023)
Average	**3766.67**	**29.35**				
SD	**1625.63**	**12.67**				
Ganga River	254.565±155.295				PET(39%), PE(30%), PP(19%)	Yang et al. (2021)
Ganga River	26.5±9.5					Singh et al (2021)
Ganga River	259±151			63 - 5000 um		Tsering et al. (2021)
Average	**180.02**	**1.40**				
SD	**82.96**	**0.65**				
Brahmaputra River	2008±1477			20 - 150 um		Tsering et al. (2021)
	130±110			150 - 5000 um		Tsering et al. (2021)
Average	**1069.00**	**8.33**				
SD	**966.61**	**7.53**				
Indus River	1138.5±613.5			20 -150 um		Tsering et al. (2021)
	200±140			150 - 5000 um		Tsering et al. (2021)
Average	**669.25**	**5.21**				
SD	**334.82**	**2.61**				
St. Lawrence	52.2±51.57 **		90% pellet	0.4 to 2.16 mm	PE	Yang et al. (2021)
	832					Gao et al. (2023)
Average	**442.10**	**3.44**				
SD	**36.47**	**0.28**				
Global River (n=251)	**256.0**	**1.99**				Koutnik et al. (2021)
Global Stormwater (n=35)	**1691.0**	**13.17**				Koutnik et al. (2021)
Global Lake (n=228)	**268.1**	**2.09**				Koutnik et al. (2021)
Global Estuary (n=88)	**99.7**	**0.78**				Koutnik et al. (2021)

* Calculated values by assuming that mass per particle is equal to 0.0000294 (g) and that sediment depth is equal to 10 cm.

** Calculated value by assuming that sediment density is equal to 2650 kg/m3 and that sediment depth is equal to 10 cm.
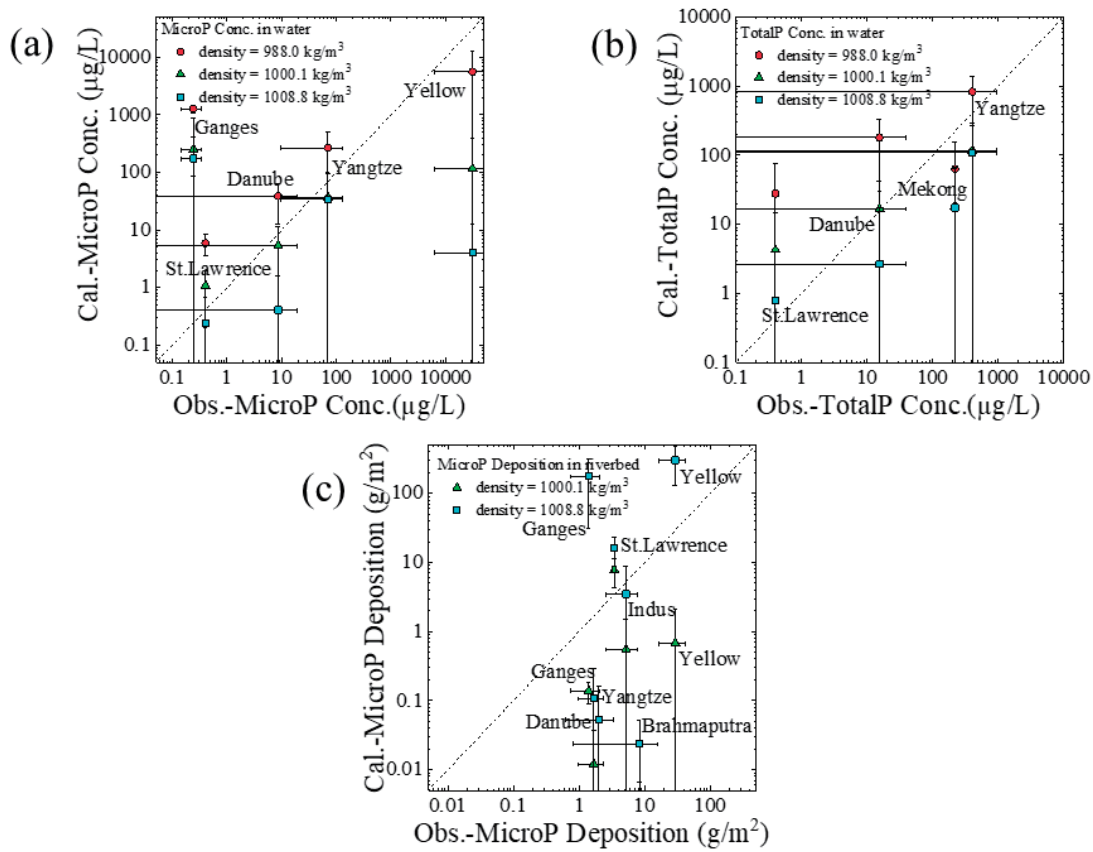
Figure 2.3 Comparison of (a) microplastic concentration in water, (b) total plastic concentration in water, and (c) microplastic deposition in riverbeds based on previously obtained data for global major rivers. In these figures, the error bar (solid line) shows the standard deviation of annual-averaged values simulated by the model.

2.4.2 Plastic Movement between Water and Riverbed Before and After Floods

Riverine plastic transport was also simulated by considering the effects of the settling and resuspension of plastic particles as an extension of previous studies (Nakayama and Osako, 2023a, 2023b). The model simulated changes in the plastic concentration and flux for plastics of different densities (1008.8, 1000.1, and 1000.001 kg/m³ under conditions that averaged all iterations of Monte Carlo model simulations, a density greater than that of water, and a density almost the same as that of water, respectively) in the Yangtze River. Generally, large-sized microplastics were distributed more in the riverbed than in the water under higher discharge or faster flow, where the influence of the estuary was relatively low, which is consistent with previous studies (Kooi et al., 2018; Liu et al., 2021). In particular, the results show that the number of large-sized microplastics in water decreased while that in the riverbed increased as the density increased. Moreover, settling and resuspension were almost equal under the mass budget in water and bed sediment, shown in equations (2.1) and (2.2) (Nizzetto et al., 2016; Koutnik et al., 2021). The concentration of plastic in the water and riverbed had a wider range of values depending on the river relative to the river discharge, which caused plastic transport to increase fivefold during floods (van Emmerik et al., 2019) and could even cause a 100-fold increase relative to non-flood conditions (van Emmerik et al., 2023). This phenomenon also

implies a shift in microplastics from sink to source between the beginning and end of a flood event, when the flow threshold is exceeded (Ockelfold et al., 2020).

The model also simulated the size distribution of microplastics in the water and riverbed sediment (density = 1000.1 kg/m^3) during the rising limb, falling limb, and normal flow in the Yangtze River (Fig. 2.4). Although the relative abundance across different size categories in water and sediment showed that more than 70% of plastics are smaller than 200 μm in water, which is similar to the findings of Treilles et al. (2022), the size distributions under low-flow conditions and during a flood event were different, which is contrary to the results of this previous study. While small microplastics are suspended in water and large microplastics are distributed in the riverbed under normal flow, floods disturb this equilibrium completely, with large microplastics becoming resuspended in the water. This reflects the fact that riverbed deposition increases during the rising limb and that horizontal transport increases after deposition starts to decrease in the falling limb, as suggested by Drummond et al. (2022). This is also related to the fact that microplastic sedimentation is promoted by the aggregation of microplastics mixed with organic minerals and sediments (Liu et al., 2021). Other studies have shown that most plastics in rivers are affected by biofouling, increasing their density (Kaiser et al., 2017; Kooi et al., 2017). Overall, the present modelling of this process represents a significant step because few previous studies have attempted to include settling and resuspension when modeling the fate and transport of plastics in global river basins (Jambeck et al., 2015; Lebreton et al., 2017; Schmidt et al., 2017; Meijer et al., 2021).
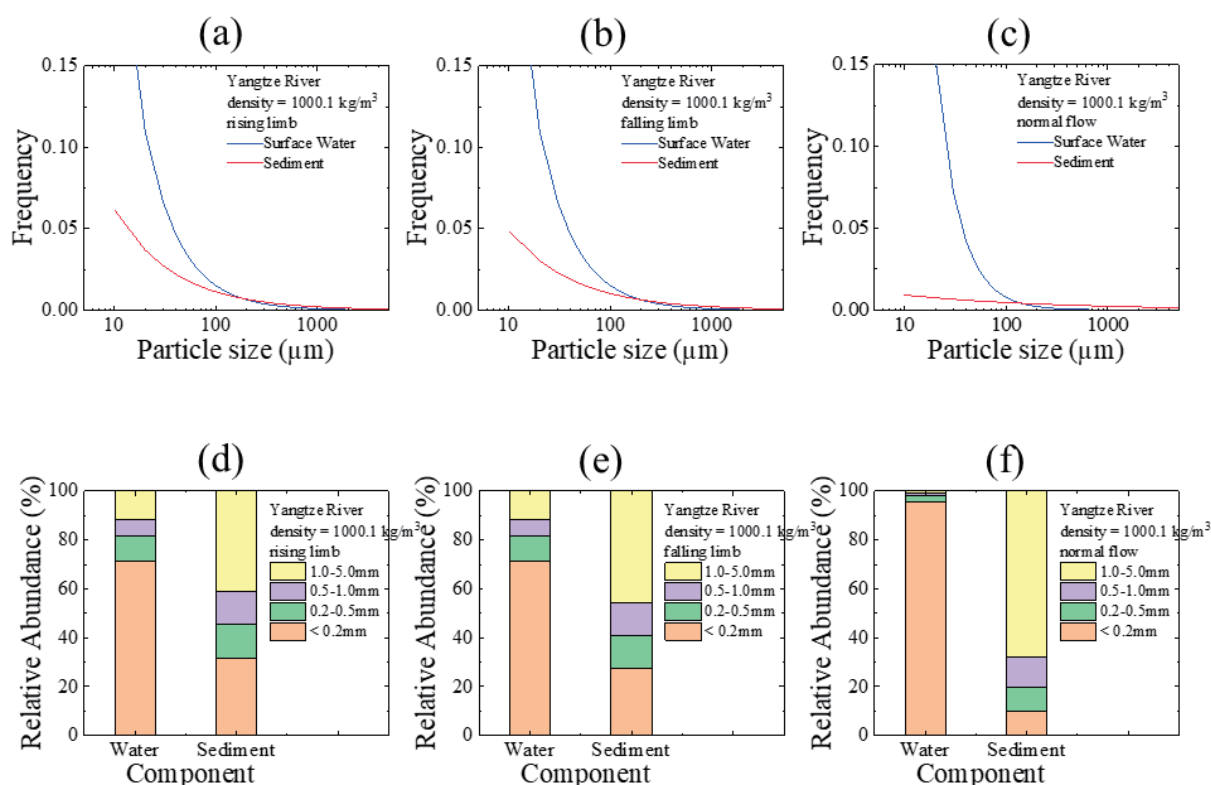
Figure 2.4 Size distribution of microplastics in water and riverbed sediment (density = 1000.1 kg/m^3 for a density slightly greater than that of water) during the rising limb, falling limb, and

normal flow in the Yangtze River. (a)-(c) Normal frequency distribution in water and sediment, and (d)-(f) relative abundance across different size categories in water and sediment.

2.4.3 Effect of Seasonality and Interannual Variability on Plastic Mobilization and Transport

The present model simulated the impact of seasonality and interannual variability on plastic mobilization and transport (Fig. 2.5). The findings revealed that most rivers in Asia, except for the Ganges and Indus Rivers, release large amounts of plastic from summer to autumn. In addition, the simulated results showed that the percentage of exported microplastic load stored on riverbeds during flood periods was relatively high, reaching 70–90% in certain major rivers worldwide (Fig. 2.6a). This finding is consistent with a previous report, which found that flooding exported approximately 70% of the microplastic load stored in riverbeds (Hurley et al., 2018). In contrast, the percentage of plastic load transported to the ocean during flood periods was not as high (Fig. 2.6b) as that reported in the study by Wagner et al. (2019), who indicated that 90% of the plastic load transported out of urban catchments during high-flow periods occurred only 20% of the time. Furthermore, the simulated total fluxes were within the range of the results reported by Roebroek et al. (2021), indicating potential plastic mobilization between non-flood conditions and the undefended 10-year return period. This result suggests that it is necessary to consider the effects of interannual variability when improving the accuracy of plastic flux estimation.
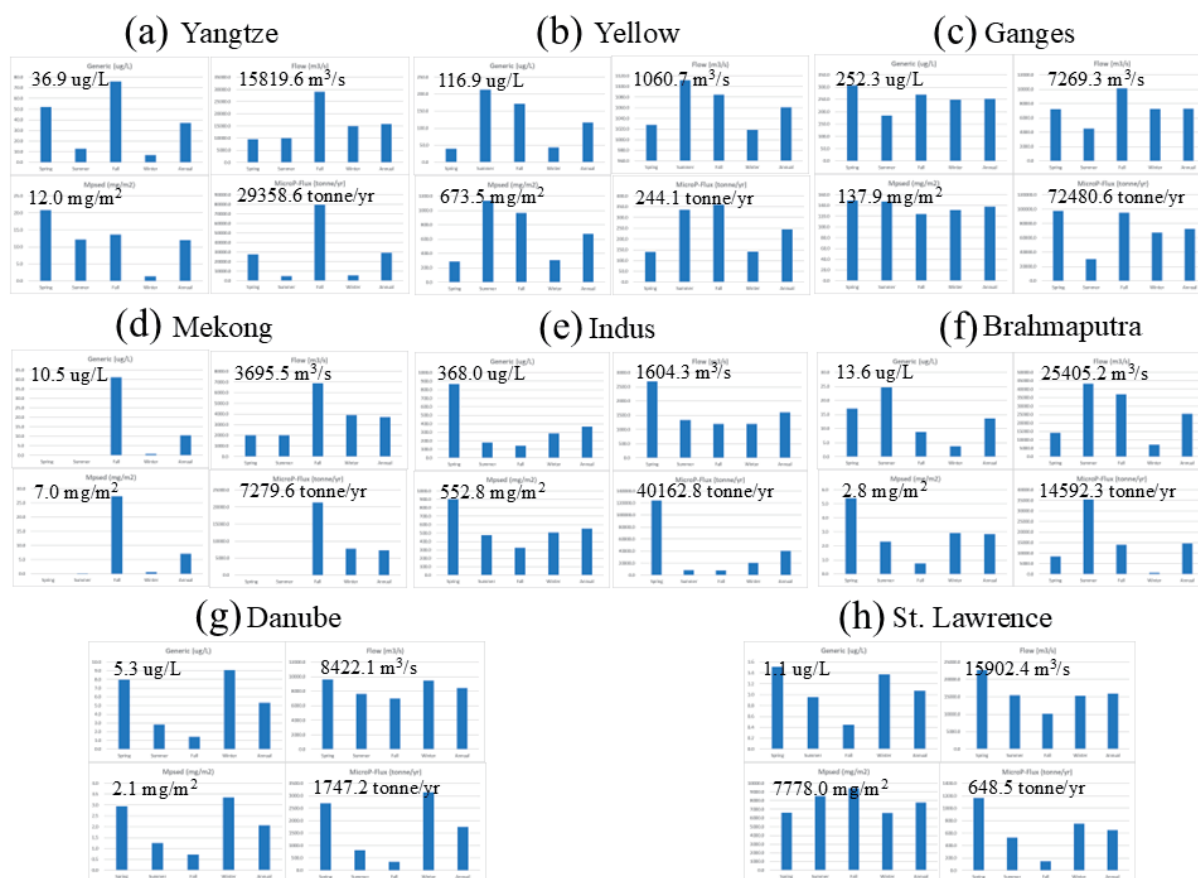
Figure 2.5 Seasonal variations of plastic concentration and flux (density = 1000.1 kg/m³) in some of the world's major rivers. Concentration in water, amount in riverbed, river discharge, and

horizontal flux in the (a) Yangtze, (b) Yellow, (c) Ganges, (d) Mekong, (e) Indus, (f) Brahmaputra, (g) Danube, and (h) St. Lawrence Rivers.
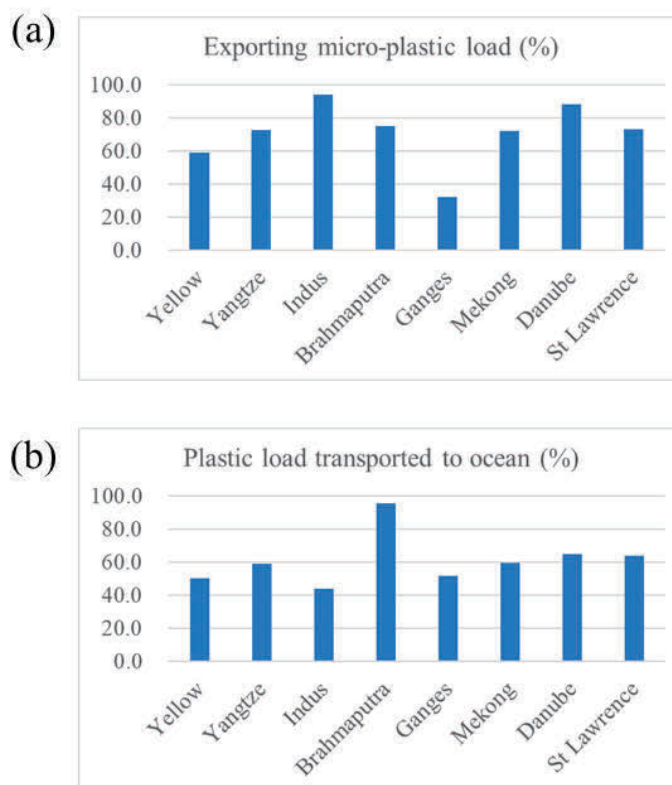
Figure 2.6 Percentages of (a) exported microplastic load stored in riverbeds and (b) plastic load transported to the ocean during flood periods for several of the world's major rivers.

The simulated results show that the distribution of plastic transport and deposition is heterogeneous and that Asia contributes a relatively large proportion of plastic transport on a global scale. Table 2.4 also shows the weighted average plastic budgets for the world's major rivers. The simulated results show that the sinking of plastics to riverbeds and lake and reservoir beds is difficult to ignore (Nakayama, 2024), although the amount of deposited plastics simulated by the model in this study (0.531 Tg/yr) was smaller than that in a previous case (3.1 Tg/yr) (OECD, 2022). Moreover, microplastics were retained to a greater extent (38.6%) by lakes, reservoirs, and riverbeds than were macroplastics (24.9%), which is consistent with the study by Chen et al. (2022), who showed that higher proportions of microplastics are preferentially retained by hydraulic sorting and that macroplastics are more easily evacuated by fluvial flooding. The riverine plastic transport to the ocean determined in the present study was 1.218±0.393 Tg/yr, with macroplastic flux of 0.793±0.305 Tg/yr and microplastic flux of 0.426±0.248 Tg/yr, which is within the range of previous values, i.e., 0.41–4.0 Tg/yr (Meijer et al., 2021).

Table 2.4 Weighted plastic budget average for global major rivers (153 basins/watersheds, 325 river channels). The range is also added for each averaged value. The error for the simulated value indicates the standard deviation for major rivers worldwide; + and - indicate increases and decreases of fluxes (horizontal transport, and vertical flux from water to bottom sediment) from the averaged values, respectively.

River	Macro P flux (Tg/yr)	Micro P flux (Tg/yr)	Total P flux (Tg/yr)
Riverine Transport to Ocean *	1.056±0.294	0.693±0.227	1.749±0.371
Reservoir Storage **	0.206±0.065	0.180±0.080	0.386±0.103
Lake Storage **	0.035±0.049	0.075±0.061	0.110±0.079
Net Transport to Ocean **	0.815±0.305	0.439±0.248	1.253±0.393
Riverbed Storage	0.022±0.010	0.013±0.004	0.035±0.011
Revised Net Transport to Ocean	0.793±0.305	0.426±0.248	1.218±0.393
* Nakayama & Osako (2023b)			
** Nakayama (2024)			

2.5 Conclusion

In this chapter, the process-based NICE-BGC model was extended to incorporate resuspension and bedload transport to evaluate global plastic dynamics in both lotic and lentic waters, including the amount of plastic flowing from land into rivers, and eventually into the ocean. This new model simulated the size distribution of plastics in water and riverbed sediments of major global rivers and showed that large microplastics are more abundantly distributed in the riverbed than in water. Although small-sized microplastics are distributed in water and large-sized microplastics are deposited on riverbeds under normal flow, flood events completely disturb this equilibrium and resuspend large-sized microplastics into the water. In addition, the model demonstrated seasonal variations in plastic flux for each continent and showed that flood events have a great impact on plastic mobilization, creating high intra-annual variability, mainly as a result of settling, resuspension, and bedload transport. In particular, the results showed that the percentage of the exported microplastic load stored on riverbeds during flood periods was relatively high in some of the world's major rivers, which explains why the amount of plastic deposited on riverbeds might be smaller than that found in lakes and dams. Riverine plastic transport to the ocean determined in the present study was 1.218±0.393 Tg/yr, with a macroplastic flux of 0.793±0.305 Tg/yr and microplastic flux of 0.426±0.248 Tg/yr, which is within the range of previous values, i.e., 0.41–4.0 Tg/yr. These results will aid in the development of solutions and measures for the reduction of plastic input to the ocean and help quantify the magnitude of plastic transport under climate change.

References

Best, J. (2018) Anthropogenic stresses on the world's big rivers. Nature Geoscience, 12, 7–21. doi:10.1038/s41561-018-0262-x

Brooks, A.L., Wang, S., Jambeck, J.R. (2018) The Chinese import ban and its impact on global plastic waste trade. Scientific Advances, 4(6), eaat0131. doi:10.1126/sciadv.aat0131

Burns, E.E., Boxall, A.B.A. (2018) Microplastics in the aquatic environment: Evidence for or against adverse impacts and major knowledge gaps. Environmental Toxicology and Chemistry, 37(11), 2776–2796. doi:10.1002/etc.4268

Cera, A., Cesarini, G., Scalici, M. (2020) Microplastics in freshwater: What is the news from the world ?. Diversity, 12, 276. doi:10.3390/d12070276

Chapra, S.C., Martin, J.L. (2012) LAKE2K: A modelling framework for simulating lake water quality (Version 1.4): Documentation and users manual. Civil and Environmental Engineering Dept., Tufts University, Medford, MA

Chen, Y., Gao, B., Xu, D., et al. (2022) Catchment-wide flooding significantly altered microplastics organization in the hydro-fluctuation belt of the reservoir. iScience, 25, 104401. doi:10.1016/j.isci.2022.104401

Climatic Research Unit (CRU). (2017) CRU TS3.24 of High Resolution Gridded Data of Month-by-month Variation in Climate. http://catalogue.ceda.ac.uk/

Drummond, J.D., Aquino, T., Davies-Colley, R.J., Krause, S. (2022) Modeling contaminant microbes in rivers during both baseflow and stormflow. Geophysical Research Letters, 49, e2021GL096514. doi:10.1029/2021GL096514

Eerkes-Medrano, D., Thompson, R.C., Aldridge, D.C. (2015) Microplastics in freshwater systems: A review of the emerging threats, identification of knowledge gaps and prioritisation of research needs. Water Research, 75, 63–82. doi:10.1016/j.watres.2015.02.012

ESRI. (2019) Overlay Layers. Portal for ArcGIS. https://gislab.depaul.edu/portal/portalhelp/en/portal/latest/use/geoanalytics-overlay-layers.htm

European Centre for Medium-Range Weather Forecasts (ECMWF). (2019) ERA-Interim. http://data-portal.ecmwf.int/data/d/interim_daily/

European Commission. (2012) Harmonized World Soil Database. http://eusoils.jrc.ec.europa.eu/ESDB_Archive/soil_data/global.htm

European Commission. (2015) Global Land Cover 2000. https://forobs.jrc.ec.europa.eu/products/glc2000/glc2000.php

Food and Agriculture Organization of the United Nations (FAO). (2016) Global Map of Irrigation Areas (GMIA). http://www.fao.org/nr/water/aquastat/irrigationmap/index.stm

Gao, B., Chen, Y., Xu, D., Sun, K., Xing, B. (2023) Substantial burial of terrestrial microplastics in the Three Gorges Reservoir, China. Communications Earth & Environment, 4, 32. doi:10.1038/s43247-023-00701-z

Haberstroh, C.J., Arias, M.E., Yin, Z., et al. (2021) Plastic transport in a complex confluence of the Mekong River in Cambodia. Environmental Research Letters, 16, 095009. doi:10.1088/1748-9326/ac2198

Han, M., Niu, X., Tang, M., et al. (2020) Distribution of microplastics in surface water of the lower Yellow River near estuary. Science of the Total Environment, 707, 135601. doi:10.1016/j.scitotenv.2019.135601

Hartmann, J., Moosdorf, N. (2012) The new global lithological map database GLiM: A representation of rock properties at the Earth surface. Geochemistry, Geophysics, Geosystems, 13, Q12004. doi:10.1029/2012GC004370

Huang, Q., Liu, M., Cao, X., Liu, Z. (2023) Occurrence of microplastics pollution in the Yangtze River: Distinct characteristics of spatial distribution and basin-wide ecological risk assessment. Water Research, 229, 119431. doi:10.1016/j.watres.2022.119431

Hurley, E., Woodward, J., Rothwell, J.J. (2018) Microplastic contamination of river beds significantly reduced by catchment-wide flooding. Nature Geoscience, 11, 251–257. doi:10.1038/s41561-018-0080-1

Jambeck, J.R., Geyer, R., Wilcox, C., et al. (2015) Plastic waste inputs from land into the ocean. Science, 347, 768–771. doi:10.1126/science.1260352

Jones, E.R., van Vliet, M.T.H., Qadir, M., Bierkens, M.F.P. (2021) Country-level and gridded estimates of wastewater production, collection, treatment and reuse. Earth System Science Data, 13, 237–254. doi:10.5194/essd-13-237-2021

Kaiser, D., Kowalski, N., Waniek, J.J. (2017) Effects of biofouling on the sinking behavior of microplastics. Environmental Research Letters, 12, 124003. doi:10.1088/1748-9326/aa8e8b

Kooi, M., van Nes, E.H., Scheffer, M., Koelmans, A.A. (2017) Ups and downs in the ocean: Effects of biofouling on vertical transport of microplastics. Environmental Science & Technology, 51, 7963–7971. doi:10.1021/acs.est.6b04702

Kooi, M., Besseling, E., Kroeze, C., et al. (2018) Modelling the fate and transport of plastic decries in freshwaters: review and guidance. In: Wagner, M., Lambert, S. [Eds] Freshwater Microplastics. The Handbook of Environmental Chemistry 58, Springer, pp.125–152

Kooi, M., Koelmans, A.A. (2019) Simplifying microplastic via continuous probability distributions for size, shape, and density. Environmental Science & Technology Letters, 6, 551–557. doi:10.1021/acs.est.9b00379

Koutnik, V.S., Leonard, J., Alkidim, S., et al. (2021) Distribution of microplastics in soil and freshwater environments: global analysis and framework for transport modelling. Environmental Pollution, 224, 116552. doi:10.1016/j.envpol.2021.116552

Kumar, R., Sharma, P., Verma, A., et al. (2021) Effect of physical characteristics and hydrodynamic conditions on transport and deposition of microplastics in riverine ecosystem. Water, 13, 2710. doi:10.3390/w13192710

Lebreton, L., Andrady, A. (2019) Future scenarios of global plastic waste generation and disposal. Palgrave Communications, 5, 6. doi:10.1057/s41599-018-0212-7

Lebreton, L, van der Zwet, J., Damsteeg, J.-W., et al. (2017) River plastic emissions to the world's oceans. Nature Communications, 8, 15611. doi:10.1038/ncomms15611

Lehner, B., Döll, P. (2004) Development and validation of a global database of lakes, reservoirs and wetlands. Journal of Hydrology, 296, 1–22. doi:10.1016/j.jhydrol.2004.03.028

Lehner, B., Reidy Liermann, C., Revenga, C., et al. (2011) High-resolution mapping of the world's reservoirs and dams for sustainable river-flow management. Frontiers in Ecology and the Environment, 9, 494–502. doi:10.1890/100125

Li, Y., Lu, Z., Zheng, H., et al. (2020) Microplastics in surface water and sediments of Chongming Island in the Yangtze Estuary, China. Environmental Sciences Europe, 32, 15. doi:10.1186/s12302-020-0297-7

Liu, Y., You, J., Li, Y., et al. (2021) Insights into the horizontal and vertical profiles of microplastics in a river emptying into the sea affected by intensive anthropogenic activities in Northern China. Science of the Total Environment, 779, 146589. doi:10.1016/j.scitotenv.2021.146589

Mai, L., Sun, X.-F., Xia, L.-L., Bao, L.-J., Liu, L.-Y., Zeng, E.Y. (2020) Global riverine plastic outflows. Environmental Science & Technology, 54, 10049–10056. doi:10.1021/acs.est.0c02273

Meijer, L.J.J., van Emmerik, T., van der Ent, R., et al. 2021. More than 1000 rivers account for 80% of global riverine plastic emissions into the ocean. Science Advances, 7, eaaz5803. doi:10.1126/sciadv.aaz5803

Ministry of Foreign Affairs of Japan. (2019) G20 Osaka Leader's Declaration. https://www.mofa.go.jp/policy/economy/g20_summit/osaka19/en/documents/final_g20_osaka_leaders_decl aration.html

Mueller, N.D., Gerber, J.S., Johnston, M., et al. (2012) Closing yield gaps through nutrient and water management. Nature, 490, 254–257. doi:10.1038/nature11420

Nakayama, T. (2017a) Development of an advanced eco-hydrologic and biogeochemical coupling model aimed at clarifying the missing role of inland water in the global biogeochemical cycle. Journal of Geophysical Research: Biogeosciences, 122, 966–988. doi:10.1002/2016JG003743

Nakayama, T. (2017b) Scaled-dependence and seasonal variations of carbon cycle through development of an advanced eco-hydrologic and biogeochemical coupling model. Ecological Modelling, 356, 151–161. doi:10.1016/j.ecolmodel.2017.04.014

Nakayama, T. (2022) Impact of anthropogenic disturbances on carbon cycle changes in terrestrial-aquatic-estuarine continuum by using an advanced process-based model. Hydrological Processes, 36(2), e14471. doi:10.1002/hyp.14471

Nakayama, T. (2023) Evaluation of global biogeochemical cycle in lotic and lentic waters by developing an advanced eco-hydrologic and biogeochemical coupling model. Ecohydrology, 17(4), e2555. doi:10.1002/eco.2555

Nakayama, T., Pelletier, G. (2018) Impact of global major reservoirs on carbon cycle changes by using an advanced eco-hydrologic and biogeochemical coupling model. Ecological Modelling, 387, 172–186. doi:10.1016/j.ecolmodel.2018.09.007

Nakayama, T., Osako, M. (2023a) Development of a process-based eco-hydrology model for evaluating the spatio-temporal dynamics of macro- and micro-plastics for the whole of Japan. Ecological Modelling, 476, 110243. doi:10.1016/j.ecolmodel.2022.110243

Nakayama, T., Osako, M. (2023b) The flux and fate of plastic in the world's major rivers: Modeling spatial and temporal variability. Global and Planetary Change, 221, 104037. doi:10.1016/j.gloplacha.2023.104037

Nakayama, T. (2024) Impact of global major reservoirs and lakes on plastic dynamics by using a process-based eco-hydrology model. Lakes & Reservoirs: Science, Policy and Management for Sustainable Use, 29, e12463. doi:10.1111/lre.12463

NASA. (2013) GLDAS vegetation class. http://ldas.gsfc.nasa.gov/gldas/GLDASvegetation.php

NASA. (2018) Gridded Population of the World, Version 4 (GPWv4). https://sedac.ciesin.columbia.edu/data/set/gpw-v4-population-count-adjusted-to-2015-unwpp-country-totals-rev11

Nizzetto, L., Bussi, G., Futter, M.N., et al. (2016) A theoretical assessment of microplastic transport in river catchments and their retention by soils and river sediments. Environmental Science: Processes & Impacts, 18, 1050–1059. doi:10.1039/c6em00206d

Ockelford, A., Cundy, A., Ebdon, J.E. (2020) Storm response of fluvial sedimentary microplastics. Scientific Reports, 10, 1865. doi:10.1038/s41598-020-58765-2

OECD. (2022) Global Plastics Outlook: Economic Drivers, Environmental Impacts and Policy Options, OECD Publishing, Paris. https://doi.org/10.1787/de747aef-en

Pojar, I., Stanica, A., Stock, F., et al. (2021) Sedimentary microplastic concentrations from the Romanian Danube River to the Black Sea. Scientific Reports, 11, 2000. doi:10.1038/s41598-021-81724-4

Portmann, F.T., Siebert, S., Döll, P. (2010) MIRCA2000 – Global monthly irrigated and rainfed crop areas around the year 2000: A new high-resolution data set for agricultural and hydrological modelling. Global Biogeochemical Cycles, 24, GB 1011. doi:10.1029/2008GB003435

Praetorius, A., Scheringer, M., Hungerbühler, K. (2012) Development of environmental fate models for engineered nanoparticles - A case study of TiO2 nanoparticles in the Rhine River. Environmental Science & Technology, 46, 6705–6713. doi:10.1021/es204530n

Qian, Y., Shang, Y., Zheng, Y., et al. (2023) Temporal and spatial variation of microplastics in Baotou section of Yellow River, China. Journal of Environmental Management, 338, 117803. doi:10.1016/j.jenvman.2023.117803

Roebroek, C.T.J., Harrigan, S., van Emmerik, T.H.M., et al. (2021) Plastic in global rivers: are floods making it worse? Environmental Research Letters, 16, 025003. doi:10.1088/1748-9326/abd5df

Schmidt, C., Krauth, T., Wagner, S. (2017) Export of plastic debris by rivers into the sea. Environmental Science & Technology, 51, 12246–12253. doi:10.1021/acs.est.7b02368

Schwarz, A.E., Ligthart, T.N., Boukris, E., van Harmelen, T. (2019) Sources, transport, and accumulation of different types of plastic litter in aquatic environments: A review study. Marine Pollution Bulletin, 143, 92–100. doi:10.1016/j.marpolbul.2019.04.029

Siebert, S., Döll, P. (2010) Quantifying blue and green virtual water contents in global crop production as well as potential production losses without irrigation. Journal of Hydrology, 384, 198–217

Siegfried, M., Koelmans, A.A., Besseling, E., Kroeze, C. (2017) Export of microplastics from land to sea. A modelling approach. Water Research, 127, 249–257. doi:10.1016/j.watres.2017.10.011

Singh, N., Mondal, A., Bagri, A., et al. (2021) Characteristics and spatial distribution of microplastics in the lower Ganga River water and sediment. Marine Pollution Bulletin, 163, 111960. doi:10.1016/j.marpolbul.2020.111960

Strokal, M., Bai, Z., Franssen, W., et al. (2021) Urbanization: an increasing source of multiple pollutants to rivers in the 21st century. Urban Sustainability, 1, 24. doi:10.1038/s42949-021-00026-w

Thompson, R.C., Olsen, Y., Mitchell, R.P., et al. (2004) Lost at sea: Where is all the Plastic? Science, 304, 838. doi:10.1126/science.1094559

Tian, H., Yang, J., Lu, C., et al. (2018) The global N2O model intercomparison project. Bulletin of the American Meteorological Society, 99(6), 1231–1251. doi:10.1175/bams-d-17-0212.1

Treilles, R., Gasperi, J., Tramoy, R., et al. (2022) Microplastic and microfiber fluxes in the Seine River: Flood events versus dry periods. Science of the Total Environment, 805, 150123. doi:10.1016/j.scitotenv.2021.150123

Tsering, T., Sillanpaa, M., Sillanpaa, M., Viitala, M., Reinkainen, S.-P. (2021) Microplastics pollution in the Brahmaputra River and the Indus River of the Indian Himalaya. Science of the Total Environment, 789, 147968. doi:10.1016/j.scitotenv.2021.147968

UNESCO. (2022) IHP-IX: Strategic Plan of the Intergovernmental Hydrological Programme: Science for a Water Secure World in a Changing Environment, ninth phase 2022–2029. https://unesdoc.unesco.org/ark:/48223/pf0000381318.locale=en

U.S. Geological Survey (USGS). (1996a) GTOPO30 Global 30 Arc Second Elevation Data Set. USGS. http://www1.gsi.go.jp/geowww/globalmap-gsi/gtopo30/gtopo30.html

U.S. Geological Survey (USGS). (1996b) HYDRO1K. USGS. https://lta.cr.usgs.gov/HYDRO1K

U.S. Geological Survey (USGS). (2018) Shuttle Radar Topography Mission (SRTM) 1 Arc-Second Global. USGS. doi:10.5066/F7PR7TFT

van Emmerik, T., Strady, E., Kieu-Le, T.-C., Nguyen, L., Gratiot, N. (2019) Seasonality of riverine macroplastic transport. Scientific Reports, 9, 13549. doi:10.1038/s41598-019-50096-1

van Emmerik, T., Frings, R.M., Schreyers, L.J., Hauk, R., de Lange, S.I., Mellink, Y.A.M. (2023) River plastic transport and deposition amplified by extreme flood. Nature Water, 1, 514–522. doi:10.1038/s44221-023-00092-7

van Wijnen, J., Ragas, A.M.J., Kroeze, C. (2019) Modelling global river export of microplastics to the marine environment: Sources and future trends. Science of the Total Environment, 673, 392–401. doi:10.1016/j.scitotenv.2019.04.078

Wagner, S., Klöckner, P., Stier, B., Römer, M., Seiwert, B., Reemtsma, T., Schmidt, C. (2019) Relationship between discharge and river plastic concentrations in a rural and an urban catchment. Environmental Science & Technology, 53, 10082–10091. doi:10.1021/acs.est.9b03048

Waldschläger, K., Schüttrumpf, H. (2019) Erosion behavior of different microplastic particles in comparison to natural sediments. Environmental Science & Technology, 53, 13219–13227. doi:10.1021/acs.est.9b05394

Waldschläger, K., Lechthaler, S., Stauch, G., Schuttrumpf, H. (2020) The way of microplastic through the environment – Application of the source-pathway-receptor model (review). Science of the Total Environment, 713, 136584. doi:10.1016/j.scitotenv.2020.136584

Weiss, L., Ludwig, W., Heussner, S., et al. (2021) The missing ocean plastic sink: Gone with the rivers. Science, 373, 107–111. doi:10.1126/science.abe0290

Xiong, X., Wu, C., Elser, J.J., Mei, Z., Hao, Y. (2019) Occurrence and fate of microplastic debris in middle and lower reaches of the Yangtze River – From inland to the sea. Science of the Total Environment, 659, 66–73. doi:10.1016/j.scitotenv.2018.12.313

Yang, L., Zhang, Y., Kang, S., Wang, Z., Wu, C. (2021) Microplastics in freshwater sediment: A review on methods, occurrence, and sources. Science of the Total Environment, 754, 141948. doi:10.1016/j.scitotenv.2020.141948

Zhang, B., Tian, H., Lu, C., et al. (2017) Global manure nitrogen production and application in cropland during 1860–2014; a 5 arcmin gridded global dataset for Earth system modelling. Earth System Science Data, 9, 667–678. doi:10.5194/essd-9-667-2017

Zhao, H., Zhou, Y., Han, Y., et al. (2022) Pollution status of microplastics in the freshwater environment of China: a mini review. Water Emerging Contaminations & Nanoplastics, 1, 5. doi:10.20517/wecn.2021.05

Zhao, S., Wang, T., Zhu, L., et al. (2019) Analysis of suspended microplastics in the Changjiang Estuary: Implications for riverine plastic load to the ocean. Water Research, 161, 560–569. doi:10.1016/j.watres.2019.06.019

- 37 -

Chapter 3

Evaluation of Plastic Flux and Fate in Terrestrial-Aquatic-Estuarine Continuum Using an Advanced Process-Based Model

Abstract

In recent decades, environmental contamination by plastics has received considerable attention from scientists, policymakers, and the public. Although models have successfully simulated the transport and fate of plastic debris in freshwater systems, a complete model is currently being developed to clarify the dynamic characteristics of the plastic budget on a continental scale. Recently, the author linked two process-based eco-hydrology models, the National Integrated Catchment-based Eco-hydrology and BioGeochemical Cycle (NICE-BGC), to a plastic debris model that accounts for both the transport and fate of plastic debris (advection, dispersion, diffusion, settling, dissolution, and biochemical degradation by light and temperature) and applied these models at a regional scale and a global scale. The present study modified this model to incorporate plastic dynamics in estuaries by extending previous studies. The model was employed to conduct a 2-year global simulation aimed at evaluating changes in plastic dynamics in major global rivers, including 130 tidal estuaries. The model simulated the impact of estuaries on the plastic budget and its seasonal variability caused by settling, resuspension, and bedload transport during 2014–2015. The model showed that plastics with smaller particle sizes accumulated to a greater degree in the water in estuaries than in rivers, while plastics with larger particle sizes accumulated more in riverbeds. The simulated results also showed that estuaries trap more plastic than lakes and riverbeds (0.218±0.053 Tg/yr), although not as much as reservoirs (0.386±0.103 Tg/yr). More than 40% of plastics were retained by lakes, reservoirs, riverbeds, and estuaries, and riverine plastic transport to the ocean was revised from 1.749±0.371 Tg/yr in the author's previous study to 1.000±0.397 Tg/yr in the present study. These results support the development of solutions and measures for reducing plastic input to the ocean and help quantify the magnitude of plastic transport under climate change.

Keywords: Eco-hydrology model; estuaries; plastic budget; riverine plastic transport

3.1 Introduction

Plastic pollution is considered a main environmental problem, and such pollutants in streams, rivers, and oceans pose potential risks to human health and the environment (Siegfried et al., 2017). Once plastic is released into the environment, it is gradually degraded by physical, chemical, and biological processes, leading to its further subdivision into an enormous number of forms that are impossible to remove and remain indefinitely in the environment. Previous studies on the origin and fate of plastic waste in freshwater systems have suggested that land-derived plastics are among the primary sources of marine plastic pollution (Thompson et al., 2004). Subsequent studies (Jambeck et al., 2015; Lebreton et al., 2017; Schmidt et al., 2017) estimated the distribution of global riverine plastic emissions into the ocean using empirical indicators representative of waste generation (mismanaged plastic waste: MPW) inside a river basin. Recently, Meijer et al. (2021) applied a probabilistic approach to more accurately analyze the spatial distribution of plastic waste generation (Lebreton and Andrady, 2019) and the climatological/geographical differences within river basins. Other studies (Siegfried et al., 2017; van Wijnen et al., 2019; Strokal et al., 2021) adapted process-oriented models to estimate plastic transport to the ocean by extending the existing non-dynamic nutrient export model.

In contrast, tidal estuaries are affected by both rivers and oceans. Although the land-ocean aquatic continuum is known to play an important role in biogeochemical cycles, the quantitative contributions of inland waters, estuaries, and continental shelves to carbon and nutrient budgets and the plastic cycle remain largely uncertain (Laruelle et al., 2013; Vermeiren et al., 2016; Pinheiro et al., 2021; Biltcliff-Ward et al., 2022; Wang et al., 2022; Schreyers et al., 2024). Because the hydrodynamics in tidal rivers and estuaries are influenced by tides and freshwater discharge, available observations suggest that plastics can be retained in such water bodies for long periods, especially during periods of low net discharge (Schreyers et al., 2024). Their results showed that net plastic transport accounts for approximately 27–32% of the total plastic transport and that plastic transport is also governed by factors other than water flow, such as wind, plastic concentration, and plastic entrapment, because of diurnal inequality in the tidal cycle. This also shows that the transformation of microplastics can be enhanced within frontal systems due to strong turbulence and interactions with sediment and biological particles, which exacerbate potential ecosystem impacts (Wang et al., 2022). These studies indicate that global plastic transport models should be developed by demonstrating the ability of estuaries to trap large quantities of microplastic debris (Biltcliff-Ward et al., 2022). From the viewpoint of temporal plastic dynamics, research has focused on the flow threshold above which rivers move from a sink to a source of microplastics (Ockelfold et al., 2020) and the characteristics of deposition and remobilization between rising and falling limbs (Drummond et al., 2022). This phenomenon becomes more complex in estuaries, and source-sink patterns vary among estuary types and with local-scale processes because of the spatial context of plastic–organism interactions, chemical behavior of plastics in estuaries, effects of wind on plastic suspension-deposition cycles, and the relative importance of processes affecting the position in the water column (Vermeiren et al., 2016). The estuarine plastic cycle is also poorly understood because most previous studies used "species" as an ecological unit rather than trophic/functional guilds and ontogenetic shifts in feeding behavior to understand communities and intraspecific relationships (Pinheiro et al., 2021). Thus, the effects of human disturbances on plastic cycle changes must be quantified in the terrestrial-aquatic-estuarine continuum on a global scale.

In terms of biogeochemical cycles, river estuaries are net heterotrophic ecosystems that show significant supersaturation of CO_2, and the magnitude of emissions is sensitive to anthropogenic disturbances, as reflected by increases in nutrient load, carbon supply,

deoxygenation, and ocean acidification (Frankignoulle et al., 1998; Regnier et al., 2013; Laruelle et al., 2014; Nakayama, 2022). While the outer part of an estuary with high salinity behaves as a carbon sink because of intense primary production, the inner part with low salinity acts as a carbon source because of the high turbidity and associated hypoxia (Guo et al., 2009; Chen et al., 2012). Regarding the behavior of microplastics, larger plastic particles are distributed more efficiently in bed sediments than in the water column because the aggregation of microplastics mixed with organic minerals is one of the mechanisms responsible for microplastic sedimentation (Kooi et al., 2018; Koutnik et al., 2021; Liu et al., 2021). In estuaries, Li et al. (2021) showed that large microplastics are relatively conserved and significantly correlated with salinity, while small microplastics are influenced by more complicated factors. Studies have also focused on the vertical and horizontal plastic litter distribution in a tidal river (Blondel and Buschman, 2022), and they showed that more plastic litter was present lower in the water column than in the surface water and that this flux may follow the transport of organic matter such as aquatic plants. In addition, a recent study evaluated the potential of plastispheres for biotic and abiotic denitrification and nitrous oxide (N_2O) production in estuaries (Su et al., 2022).

Thus, these studies show that multivariate analysis and robust models are necessary to predict the fate and transport of plastics in estuarine environments (Pinheiro et al., 2021). Great progress has been made in the modeling of plastics in estuaries over the last few years (Atwood et al., 2019; Cohen et al., 2019; Defontaine et al., 2020; Díez-Minguito et al., 2020; López et al., 2021). Díez-Minguito et al. (2020) used an idealized 2D-vertical model to elucidate the relative importance of river discharge and wind-driven and density-driven circulation and indicated that winds dominate the circulation in the outer part of the estuary and that gravitational circulation dominates the net flow near the head. Another study used a 3D model to show that neutrally buoyant microplastics are easily flushed out while heavier microplastics are prone to entrapment in estuaries, particularly under low discharge conditions (Defontaine et al., 2020). Atwood et al. (2019) compared remote sensing and hydrodynamic modelling to estimate the coastal accumulation of microplastic particles emitted from an Italian river and revealed that discharged particle amounts were only semi-coupled to beaching rates with strong mouth dependence and occurred within the first ten days. Other studies also used 3D simulation to reveal that particle size is not important while particle density significantly influences the overall data and mean duration in the water column (López et al., 2021). Moreover, buoyant particles have been shown to quickly organize in patchy, highly inhomogeneous distributions, thus creating "hot spots" of microplastics (Cohen et al., 2019). The development of a framework to reverse global water resource degradation and plastic pollution is vital for achieving Sustainable Development Goals (SDGs) (UNESCO, 2022). The G20 Osaka Summit in 2019 shared the "Osaka Blue Ocean Vision" (Ministry of Foreign Affairs of Japan, 2019), which is positioned alongside the Conference of the Parties (COP) as part of global warming countermeasures. Quantitative assessment of the fate and transport of plastics will be necessary to realize this vision because countries around the world have decided on concrete future measures for dealing with plastics based on scientific results. Because extreme events such as floods and droughts are expected to increase further with climate change, it is also important to evaluate the impact of flood events on plastic mobilization and its high variability in estuaries.

The author developed a process-based model that couples eco-hydrology with the biogeochemical cycle (National Integrated Catchment-based Eco-hydrology-BioGeochemical Cycle (NICE-BGC) (Nakayama, 2017a, 2017b) and incorporates complex terrestrial-aquatic linkages in the hydrological–biogeochemical cycle. Recently, this process-based NICE-BGC was extended by coupling it with a plastic debris (engineered materials) model and applied to

the evaluation of spatiotemporal variations of plastic debris on a regional scale for the entirety of Japan (Nakayama and Osako, 2023a) and on a global scale for the world's major rivers (Nakayama and Osako, 2023b, 2024). Based on this background, three basic issues were addressed: (i) How is the movement of plastic particles between the water and riverbed sediment affected by estuaries? (ii) What is the impact of estuaries on the plastic balance? (iii) Does the incorporation of estuarine dynamics improve the estimates of plastic flux to the ocean? To clarify these issues, the author incorporated plastic dynamics in estuaries by extending previous studies (Nakayama and Osako, 2023a, 2023b, 2024). This model was employed to conduct a 2-year global simulation aimed at evaluating the changes in plastic dynamics in major rivers, including 130 tidal estuaries (Fig. 3.1). The model simulated the impact of estuaries on the plastic budget and its seasonal variability caused by settling, resuspension, and bedload transport during 2014–2015. The present study represents an important step not only for qualifying the various processes but also for identifying the driver hierarchy in a range of river catchments.
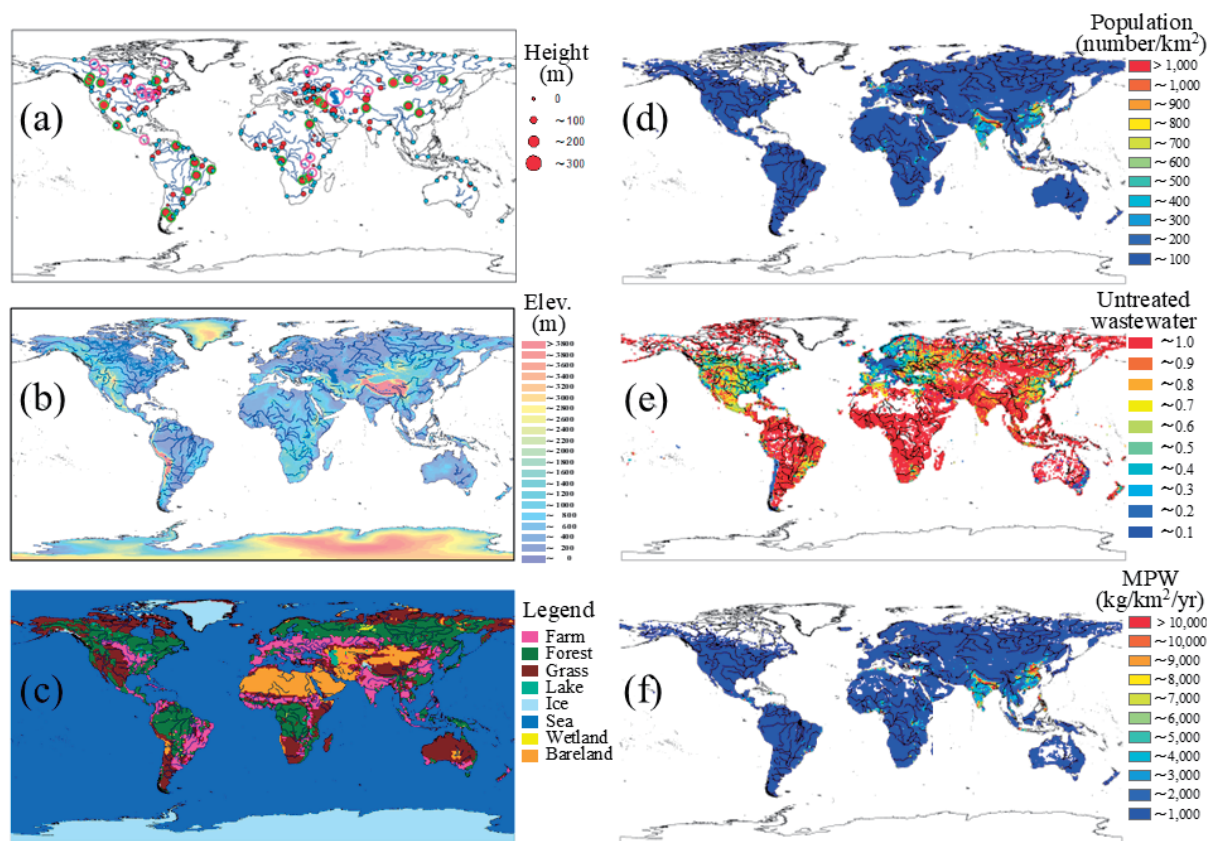
Figure 3.1 Location of the study area in the terrestrial-aquatic-estuarine continuum on a global scale. (a) World's major rivers (153 basins, 325 river channels) with 82 major reservoirs (red circle), 19 lakes (blue mesh), and 130 tidal estuaries (light blue circle), (b) elevation, (c) land cover, (d) population density, (e) untreated wastewater calculated from wastewater treatment and wastewater production, and (f) mismanaged plastic waste (MPW). In the figure, line shows the world's major rivers in HYDRO1K.

3.2 Methods

3.2.1 Modeling Fate and Transport of Plastics by Incorporating Resuspension and Bedload Transport

The process-based NICE-BGC coupled with a plastic debris model (Nakayama and Osako, 2023a, 2023b, 2024) includes advection, dispersion, diffusion, settling, dissolution and deterioration due to light and temperature; however, it assumes no interaction with suspended matter (heteroaggregation) (Praetorius et al., 2012), biofouling (Kooi et al., 2017, 2018), and wind effects. The model also incorporates resuspension and bedload transport in addition to settling, by extension of previous studies (Nakayama, 2025) (Fig. 3.2). Although the transport/diffusion models of macro- and microplastics applied the same equations, the settling velocities and resuspension differed depending on the size. Furthermore, the author assumed that the deterioration of macroplastics due to light and temperature eventually transitioned to microplastics, and this disappearance term in the equation for macroplastics was added to the equation for microplastics (Nakayama and Osako, 2023a, 2023b). The model now includes the mass budget in the water and bed sediments of any given reach, which is consistent with previous studies (Nizzetto et al., 2016; Koutnik et al., 2021). Thus, the model can simulate the concentration of plastics in both the water and bed sediment and evaluate the hydrograph for plastic transport under various shear stresses during storm events, as proposed by Kumar et al. (2021).

Recently, Nakayama (2023) coupled NICE-BGC with LAKE2K in a stratified water quality model (Chapra and Martin, 2012). LAKE2K simulates a lake as a one-dimensional system consisting of three vertical layers (epilimnion, metalimnion, and hypolimnion). The model inputs the hypsographic information of the reservoir and lake in the form of an elevation-area curve (Chapra and Martin, 2012) (Fig. 3.2) and simulates the associated hydrodynamics of horizontal and vertical transport. In this study, the coupled model was extended to simulate the plastic dynamics in both lotic and lentic waters by extending previous studies (Nakayama and Osako, 2023a, 2023b) (Fig. 3.2). After simulating plastic transport on a hillslope, the estimated rate of conversion of macroplastics to microplastics (3%/yr) was determined based on van Wijnen et al. (2019), and the conversion rate was based on Jambeck et al. (2015) (Fig. 3.2). This model has been applied to the world's major rivers (153 basins and 325 river channels), with 82 major reservoirs, 19 lakes, and 130 tidal estuaries (Alder, 2003) (Fig. 3.1).
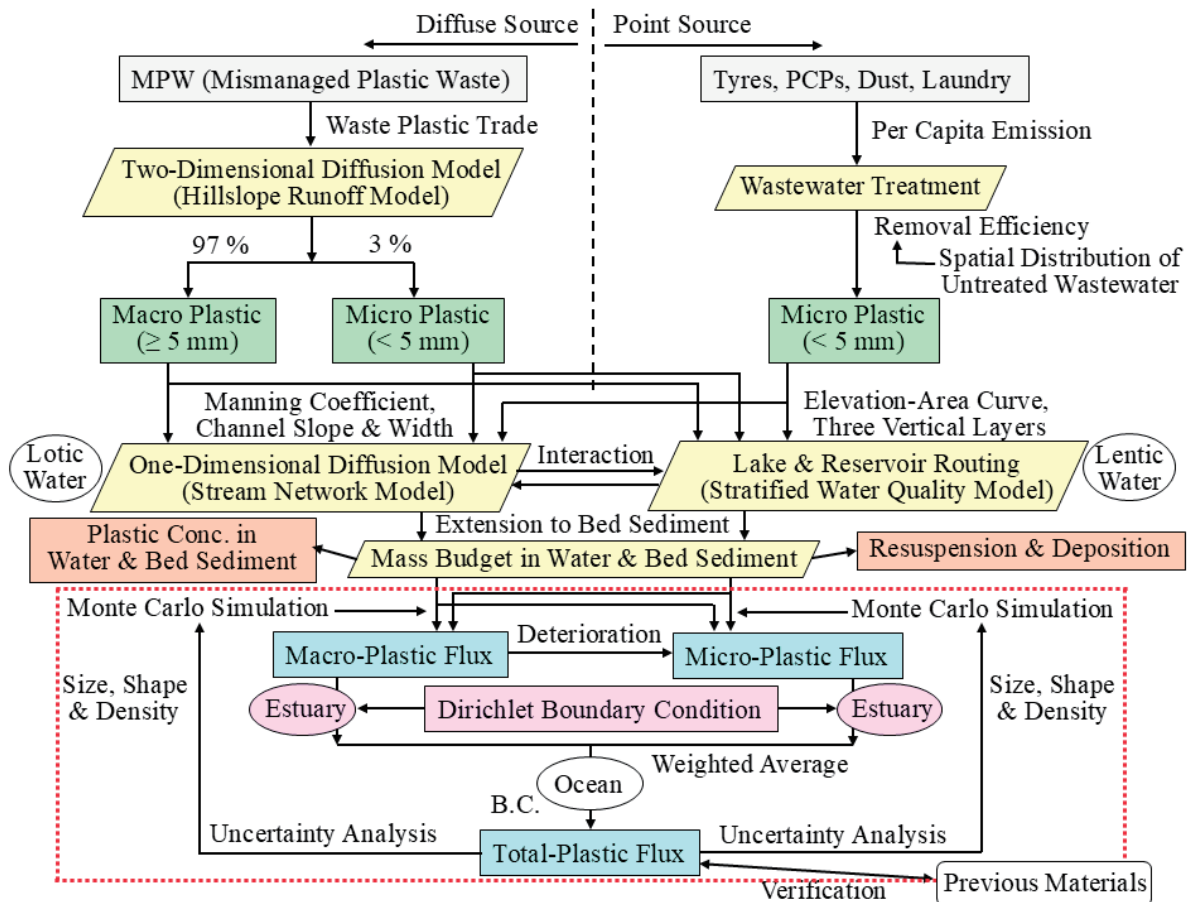
Figure 3.2 Flow diagram showing the transport of macro- and microplastics in the terrestrial-aquatic-estuarine continuum obtained by extending the NICE-BGC model. Red dotted frames indicate the newly developed processes in the current model, which include the effect of estuaries on plastic cycles based on the author's previous studies. "B.C." means boundary conditions for the model simulation.

3.2.2 Extension of NICE-BGC to Include Plastic Dynamics in Estuaries

To calculate the hydrological and biogeochemical cycles in tidal estuaries, the author incorporated the 'Dirichlet boundary condition' into the original QUAL2Kw (Pelletier et al., 2006) for 130 global tidal estuaries as sea boundaries (Nakayama, 2022) (Fig. 3.2). The length, width, and depth of the estuaries of major global rivers were estimated from the Global Estuary Database (Alder, 2003), Global Delta Maps (Ericson et al., 2006; Tessler et al., 2015), Global Coastal Typology (Dürr et al., 2011), and MARCATS (MARgins and CATchments Segmentation) (Laruelle et al., 2013) using ArcGIS software (Table 3.1). First, the length of the estuary was calculated by overlaying the river channel line and estuary polygon using ArcGIS. The width of the estuary was then calculated by averaging the channel widths estimated using Google Earth in the overlaid channel (Fig. 3.3). The tidally averaged dispersion coefficient EL (m2/s) for all estuaries was also calculated, as suggested by Fischer et al. (1979):

$$E_L = 0.011 \frac{U^2 w^2}{H u_*} \tag{3.1}$$

where U is the longitudinal flow velocity (m/s); w is the estuary width (m); H is the flow depth (m); and u_* is the shear (friction) velocity (m/s). This enabled the model to calculate the tidal propagation of water quality upstream, starting at the downstream boundary conditions, which represents the so-called 'mixing intensity of dissolved constituents' (Regnier and O'Kane, 2004) on a regional/continental scale. The variables (in monthly time steps) for the downstream boundary conditions included water temperature, conductivity, dissolved oxygen (DO), nitrate, and phosphate obtained from the World Ocean Atlas 2013 (WOA2013) (NOAA, 2013); alkalinity obtained from Lee et al. (2006); pH obtained from Jiang et al. (2019); and plastic concentration obtained from Kandorp et al. (2023). Other variables related to the carbon cycle for the downstream boundary conditions were assumed to be half the values simulated by the model upstream from the lowest reach in the estuary of each river because these concentrations generally decrease across an estuarine salinity gradient along a theoretical dilution line (Vanderborght et al., 2002; Regnier and O'Kane, 2004; Bauer and Bianchi, 2011). Details are described in the author's previous study (Nakayama, 2022), excluding the plastic cycles. These modifications indicate that the extension of the NICE-BGC to include estuaries allows for the simulation of biogeochemical and plastic cycle changes in the terrestrial-aquatic-estuarine continuum.

Table 3.1 List of input datasets for the NICE-BGC model.

Data set	Original resolution	Year	Source and reference
Climatology	1.0°	2014-2015	ERA-interim; ECMWF (2019)
Elevation	1.0km	around 1996	GTOPO30; U.S. Geological Survey (1996a)
Land cover	1.0km	around 2000	GLC2000; European Commission (2015)
Soil texture	1.0km	around 1970-2000	HWSD; European Commission (2012)
Vegetation type	0.25°	around 2000	GLDAS Vegetation Class; NASA (2013)
River networks	1.0km	around 1996	HYDRO1K; U.S. Geological Survey (1996b)
Lakes and wetlands	0.5 min	around 1990-2000	GLWD; Lehner and Döll (2004)
Reservoirs and Dams	point	around 2010	GRanD; Lehner et al. (2011)
Geological structures	0.5°	around 1970-2000	GLiM; Hartmann and Moosdorf (2012)
Crop type	5 min	around 2000	MIRCA2000; Portmann et al. (2010)
Irrigation type	5 min	2000-2008	GMIA; FAO (2016)
Irrigation water use	5 min	1998-2002	GCWM; Siebert and Döll (2010)
Fertilizer use	5 min	around 2000	Earth Stat; Mueller et al. (2012)
Manure use	5 min	1998-2014	Zhang et al. (2017)
Atmospheric N deposition	0.5°	1998-2015	ISIMIP2a; Tian et al. (2018)
Estuary	polygon	around 2000	Global Estuary Database; Alder (2003)
Estuary type	0.5°	around 2000	Global Coastal Typology; Dürr et al. (2011)
Coastal line	0.5°	around 2000	MARCATS; Laruelle et al. (2013)
Water level	point	1992-2021	G-REALM; USDA (2022)
Population	1.0km	2015	NASA (2018)
Wastewater production and treatment	5 min	2015	Jones et al. (2021)
Mismanaged plastic waste	1.0 km	2015	Lebreton and Andrady (2019)
Ocean water quality	1.0°	1995-2012	WOA2013; NOAA (2013)
Ocean alkalinity	1.0°	around 2000	Lee et al. (2006)
Ocean pH	1.0°	1990, 2000, 2010	Jiang et al. (2019)
Ocean plastic concentration	average hexagon edge length of 22 km	2015	Kaandorp et al. (2023)

Figure 3.3 Averaged length and width of inland water (a)-(b) and estuary (c)-(d) input to the model. Each value is displayed as a contour for each basin.

3.3 Input Data and Boundary Conditions for Simulation

3.3.1 Model Input Data

The input data at hybrid spatial resolution were prepared and arranged to calculate a spatially averaged 1° × 1° grid using the Spatial Analyst Tools in ArcGIS v10.3 for the global simulation (Fig. 3.1 and Table 3.1). Elevation, land cover, soil texture, vegetation type, river networks, lakes and wetlands, reservoirs and dams, geological structures, crop type, irrigation type, irrigation water use, fertilizer use, and manure use were categorized based on the global datasets. Although data on plastics are scarce, the author simulated global plastic debris based on gridded population data at 1 km resolution from 2015 global data (NASA, 2018); wastewater production, collection, treatment, and reuse data at 5 arcmin (approximately 10 km) resolution (Jones et al., 2021), and MPW data at 1 km resolution (Lebreton and Andrady, 2019) as a diffuse source (Table 3.1). The plastic concentrations of macro- and microplastics in the ocean surface water (from 0 to 5 m) were also used as the downstream boundary conditions of each river mouth (Kandorp et al., 2023) (Fig. 3.4). To reasonably create grid data from point, polyline,

and polygon data for different sources with different spatial resolutions, an overlay analysis was conducted using GIS tools (intersect, union, and identity) (ESRI, 2019).

In addition, the per capita emissions of microplastics in each economic region were determined based on a previous study (van Wijnen et al., 2019). Generally, micro-plastics at point sources originate from four sources: personal care products (PCPs) (0.0007–0.0055 kg/cap. /yr), laundry fibers (0.007–0.11 kg/cap. /yr), car tire wear (0.0072–0.18 kg/cap. /yr), and macroplastic fragmentation (8.5–27 kg/cap. /yr) for each region (Nakayama and Osako, 2023a, 2023b). We estimated the potential fluxes of microplastics by multiplying their per capita emissions and population distribution for each catchment flow into wastewater treatment plants (WWTPs) in the NICE-BGC simulation (Fig. 3.2). We also applied "untreated wastewater" and converted it to estimate the efficiency of microplastic removal, the former being calculated by subtracting the ratio of wastewater treatment and wastewater production at 5 arcmin resolution (Jones et al., 2021). This revealed that the efficiency of microplastic removal in WWTPs in developed countries was much higher than that in developing countries (Fig. 3.1c) because almost all treatments are secondary and tertiary (Nakayama and Osako, 2023a). Microplastic concentrations on hillslopes were also assumed to be constant (Wagner et al., 2019), and the time series proportional to hillslope runoff was calculated at each time step. The details are described in the author's previous studies (Nakayama and Osako, 2023a, 2023b).

The author previously showed that both macro- and microplastic fluxes into the ocean simulated by the models were generally consistent with previous data for major global rivers and closely related to population density (Nakayama and Osako, 2023b). Moreover, all available previous data were compile, the average values and standard deviations of plastic concentration in the water were calculated (Eerkes-Medrano et al., 2015; Lebreton et al., 2017; Schmidt et al., 2017; van Wijnen et al., 2019; Xiong et al., 2019; Han et al., 2020; Li et al., 2020; Mai et al., 2020; Waldschläger et al., 2020; Haberstroh et al., 2021; Singh et al., 2021; Weiss et al., 2021; Zhao et al., 2022; Huang et al., 2023; Qian et al., 2023) the average values and standard deviations of plastic deposition in the riverbed were calculated (Pojar et al., 2021; Singh et al., 2021; Tsering et al., 2021; Yang et al., 2021; Zhao et al., 2022; Gao et al., 2023; Qian et al., 2023; Nakayama, 2025). Because most previous data were expressed as the number of plastics (items), these values were converted to plastic weight, assuming that the mass per particle would be 0.0000294 (g), which is the value averaged from Schmidt et al. (2017) and Zhao et al. (2019). For simplicity, the author also assumed that the sediment density was equal to 2,650 kg/m^3 and the sediment depth was equal to 10 cm for the calculation of plastic deposition in the riverbed.
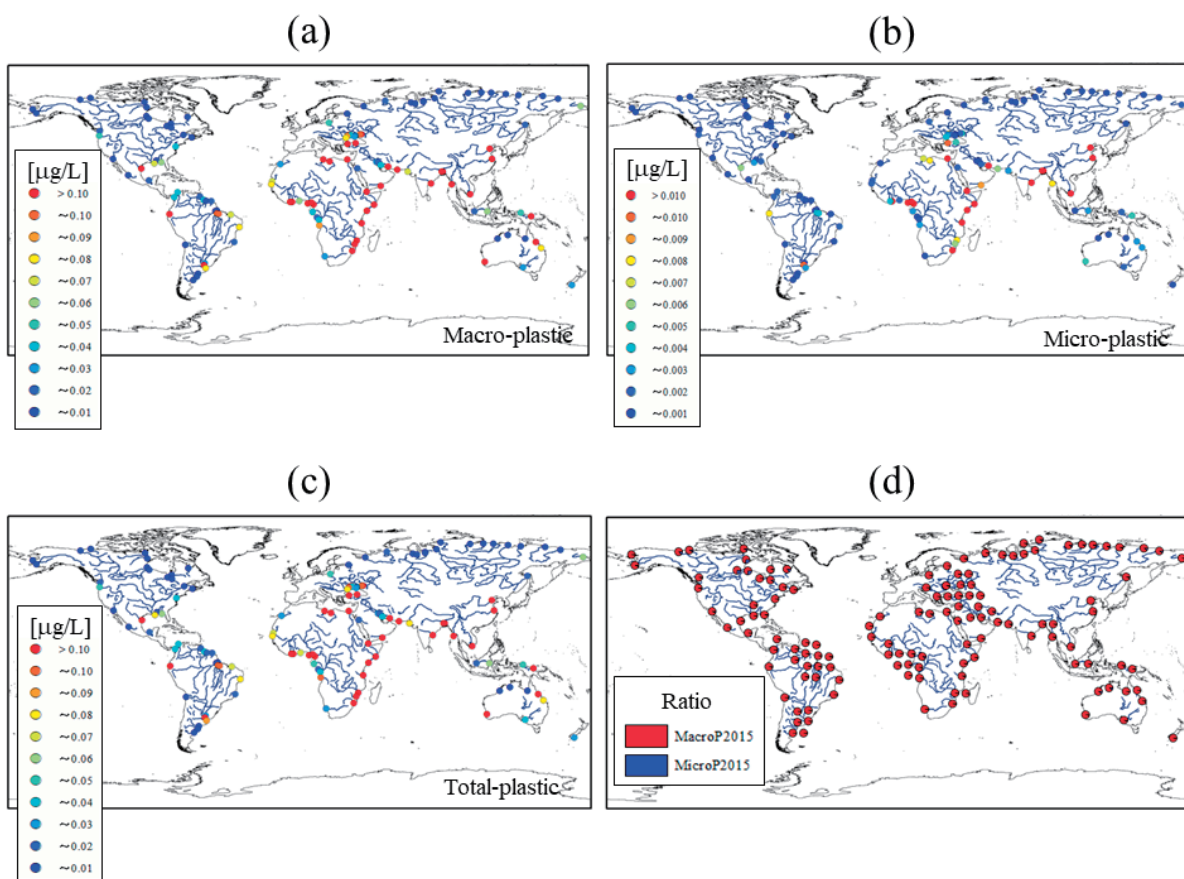
Figure 3.4 Concentrations of (a) macroplastic, (b) microplastic, and (c) total plastic, and (d) ratio of each plastic in the ocean surface water (from 0 to 5 m) in 2015 input to the model as the downstream boundary condition of each river mouth.

3.3.2 Boundary Conditions and Simulation Process

The simulation was conducted at a $1° × 1°$ resolution in the horizontal direction and in the same layers in the vertical direction (Nakayama and Osako, 2023b) (Fig. 3.1). The NICE-BGC simulation for terrestrial ecosystems was conducted at the same spatial resolution with a time step of $\Delta t = 1$ day for two years during 2014–2015 by iteratively inputting values simulated by NICE after calculating the daily averaged data from 1-hourly data (Fig. 2). The author used previous data on per capita emissions of microplastics into rivers (PCPs, dust, laundry fibers, and tires) and the removal efficiency of WWTPs as a point source. The two-dimensional diffusion (hillslope runoff) submodel of the NICE-BGC simulated the outflow of macroplastics originating from MPW (Lebreton and Andrady, 2019) as a diffuse source (Fig. 3.2). The rate of release of mismanaged and littered plastic into the aquatic environment varies from a few percent to at most 10% (OECD, 2022), and the yield ratio is <1% in global major rivers, such as the Yangtze, Indus, Yellow, Nile, and Ganges Brahmaputra (Peng et al., 2021). In contrast, the simulated value from NICE-BGC was a few percent at most and the distribution was spatially uneven, with greater retention of plastic waste in agricultural soils, although the results were somewhat consistent with Nakayama and Osako (2023b). The NICE-BGC simulation for aquatic ecosystems was then conducted by inputting the simulated results for land into a stream

network model. The simulation, which included estuaries, became more unstable because of the Dirichlet boundary conditions, as described in section 3.2.2. The simulation required a smaller time step between Δt = 0.044 min and 0.70 min than that without estuaries to ensure the stability of the model. The hydrological cycle and plastic transport in rivers were simulated and verified using previous datasets and materials on a continental scale (Nakayama and Osako, 2023b; Nakayama, 2025).

To simulate the plastic flux, the weighted average value was calculated by multiplying each probability by each flux and their summation. This was based on the assumption that both micro- and macroplastics are pure and totally inert polymers with a continuous probability distribution of size, shape, and density (Kooi and Koelmans, 2019), which is consistent with Nakayama and Osako (2023b). Uncertainty and sensitivity analyses were conducted by ranking the model parameters according to their contribution to prediction uncertainty using Monte Carlo model simulations. Details are described in a previous study (Nakayama and Osako, 2023b, 2024). The results yielded quantitative measures of model performance in terms of reproducing the seasonality and intraannual variability in the hydrologic cycle and plastic transport.

3.4 Results and Discussion

3.4.1 Evaluation of Plastic Concentrations and Fluxes for the World's Major Rivers

The model compared the plastic concentration in the water and plastic deposition in the riverbed of estuaries with previous data on global major rivers (Fig. 3.5). The results show that the plastic concentration in the water simulated by the model was reasonably consistent with the observed data (Fig. 3.5a-b), although the microplastic deposition in the riverbed in estuaries was slightly underestimated relative to the observed values (Fig. 3.5c). This trend is similar to in the results for inland water in Nakayama (2025) because when plastic is lighter than water, the simulation is overestimated relative to observations (density = 988.0 kg/m^3 for floating condition), and when the plastic density is relatively higher than that of water, the simulation is more consistent with observations (density = 1000.1 kg/m^3 for a density slightly higher than that of the water). This is supported by previous research indicating that PP and PE are the dominant polymers in freshwater (Burns and Boxall, 2018). However, most observations have been performed for the downstream sections of these rivers, which are sometimes influenced by estuaries, where PP tends to be most prevalent in water and PE is more prevalent in sediment (Koutnik et al., 2021).
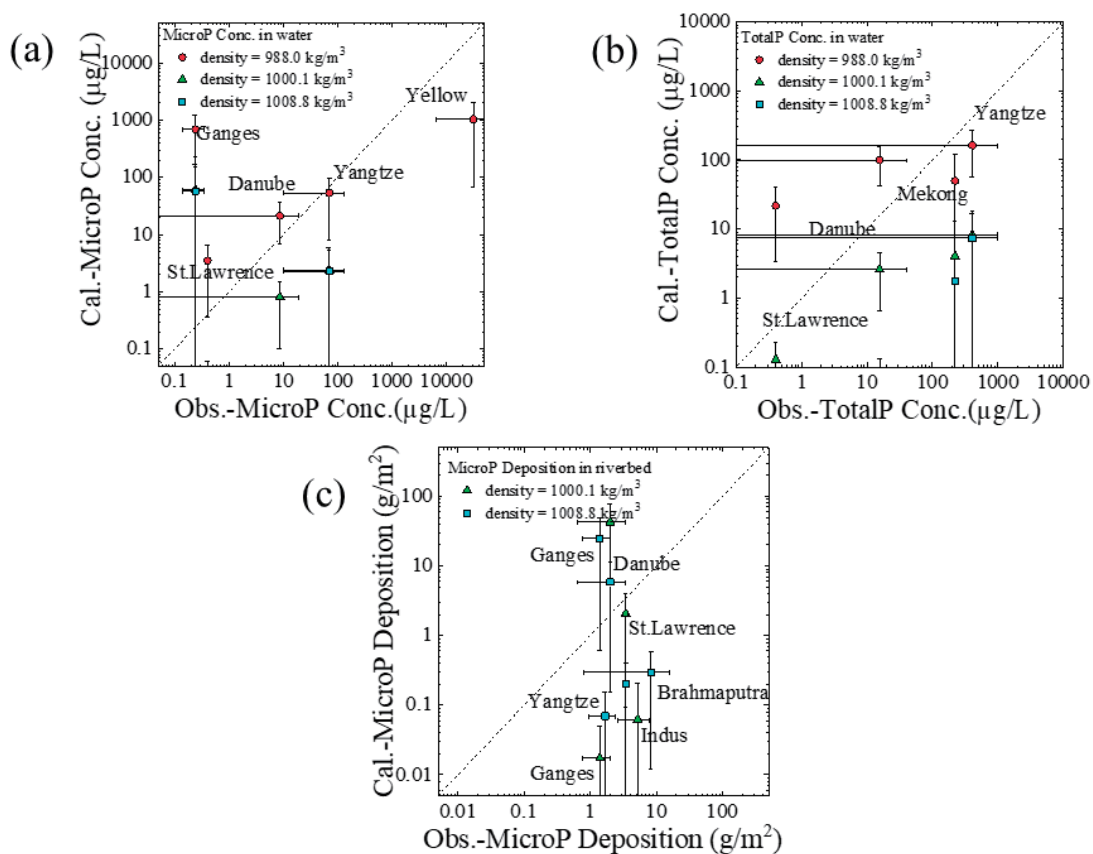
Figure 3.5 Comparison of simulated (a) microplastic concentrations in water, (b) total plastic concentrations in water, and (c) microplastic deposition in the riverbed in estuaries with previous data obtained for global major rivers. In these figures, the error bar (solid line) shows the standard deviation of annually averaged values simulated by the model.

3.4.2 Change of Plastic Movement between Water and Riverbed in Estuaries

The author also simulated riverine plastic transport by considering the effects of the settling and resuspension of plastic particles as an extension of previous studies (Nakayama and Osako, 2023a, 2023b, 2024). The model simulated changes in the plastic concentration and flux for plastics of different densities (1008.8, 1000.1, and 988.0 kg/m^3 under conditions in which all iterations were averaged by Monte Carlo model simulations, with these values indicating a density slightly than that of water, a density almost the same as that of water, and a density less than that of water, respectively). The author's previous study showed that coarser particles are accumulated to a greater degree in the riverbed than in water under higher discharge or faster flow, where the influence of an estuary is relatively small (Nakayama, 2025), which is consistent with previous studies (Kooi et al., 2018; Liu et al., 2021).

The model simulated the size distribution of microplastics in the water and sediment of the Yangtze, Mekong, and Ganges Rivers (density = 1000.1 kg/m^3, which is slightly higher than that of water) (Fig. 3.6). The results show that the movement of plastic between the water and riverbed changed greatly in the estuary, which is inconsistent with the results of a previous study on inland water (Nakayama and Osako, 2024). Although the relative abundance across different size categories in the water and sediment showed that more than 70% of the plastics

were smaller than 200 μm in the water, which is consistent with Treilles et al. (2022), the size distributions in estuaries differed, which is inconsistent with Trielles et al. The results also show that plastics with smaller particle sizes accumulate more in the water of estuaries than in most rivers and that plastics with larger particle sizes accumulate more on the riverbed than in rivers. This is because the concentrations of plastic in the water and riverbed of estuaries have a narrower range of values depending on the river compared with the concentrations in inland water, which is caused by the buffer effect in estuaries that weakens the effects of flooding. This also implies that estuaries can trap large quantities of microplastic debris (Biltcliff-Ward et al., 2022).
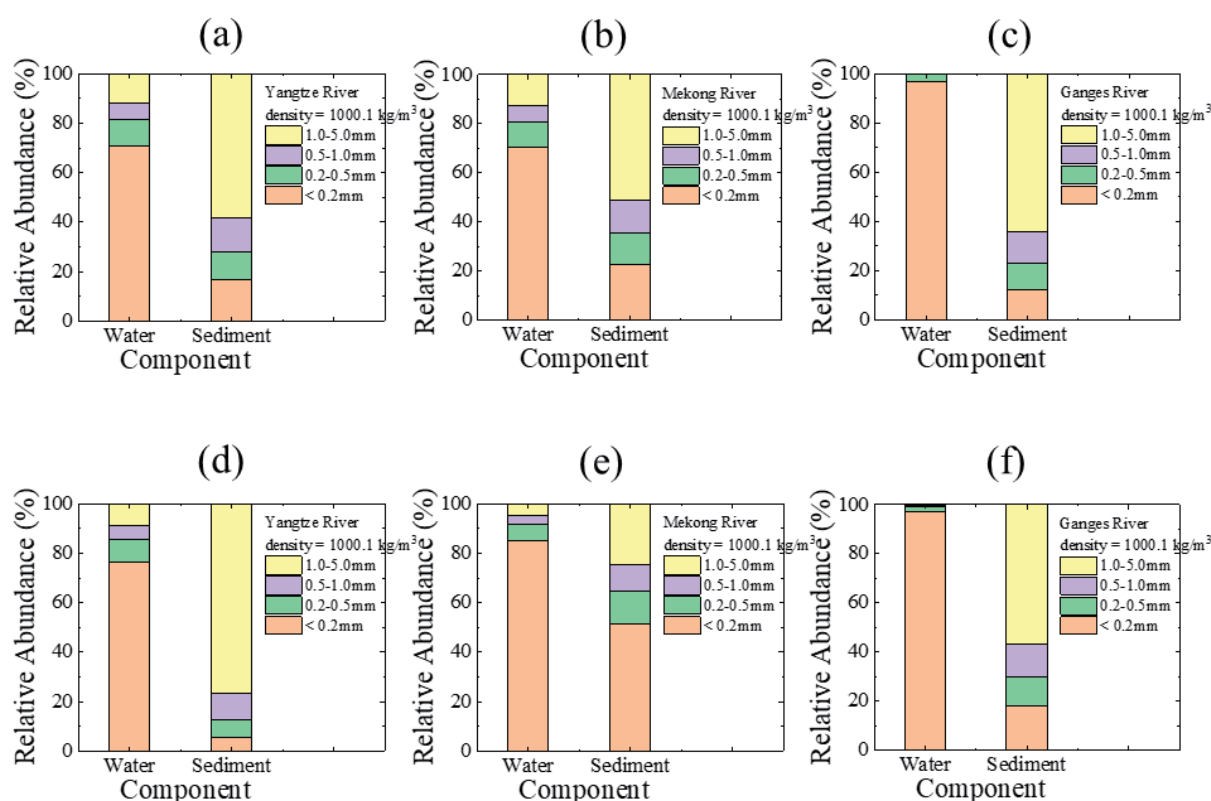
Figure 3.6 Relative abundance across different size categories in water and riverbed sediment (density = 1000.1 kg/m³, which is slightly higher than that of water) in the inland waters and estuaries in the Yangtze, Mekong, and Ganges Rivers. (a)-(c) Relative abundance in inland waters, and (d)-(f) relative abundance in estuaries.

In addition, riverbeds at the mouth of the Yangtze River (Fig. 3.6a and d) have more large-sized plastics than the rivers, while the opposite trend was observed in the Mekong and Ganges Rivers (Fig. 3.6b-c and e-f). This is also related to the fact that microplastic sedimentation is promoted by the aggregation of microplastics mixed with organic minerals and sediments in some rivers (Liu et al., 2021). Other studies have shown that most plastics in most rivers and estuaries are affected by biofouling, increasing their density (Kaiser et al., 2017; Kooi et al., 2017). Overall, the modelling of this process presented here represents a significant step because few previous studies have attempted to include settling and resuspension when

modeling the fate and transport of plastics in both inland waters and estuaries of global river basins.

3.4.3 Change of Plastic Budget in Terrestrial-Aquatic-Estuarine Continuum

The simulated results show that the distribution of total-plastic transport and deposition is heterogeneous and that Asia and Africa contribute to a relatively large proportion of plastic transport on a global scale (Fig. 3.7). In particular, the storage of both macro- and microplastics in reservoirs and estuaries, as well as lakes and riverbeds, greatly affects plastic transport to the ocean. Moreover, macroplastics are more susceptible to this effect than microplastics because the inflow of the former is greater than that of the latter.
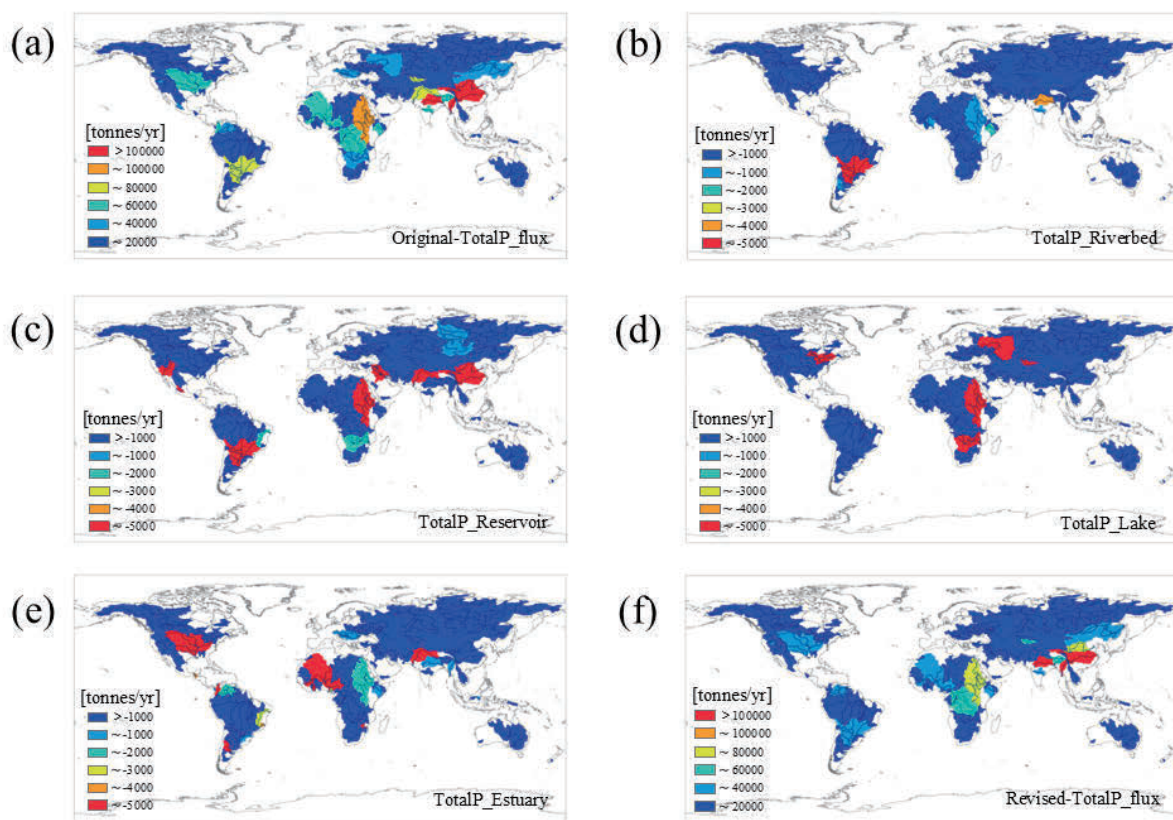
Figure 3.7 Spatial distribution of total-plastic transport and deposition in major rivers worldwide. (a) Horizontal transport to the ocean without deposition, (b) riverbed storage, (c) reservoir storage, (d) lake storage, (e) estuarine storage, and (f) net horizontal transport to the ocean.

Table 3.2 also shows the weighted average plastic budgets for major global rivers. The simulated results show that the sinking of plastics in estuaries, riverbeds, lakes, and reservoir beds should not be ignored (Nakayama, 2024, 2025), although the amount of deposited plastics in estuaries simulated by the model here (0.749 Tg/yr) was lower than that in a previous case (3.1 Tg/yr) (OECD, 2022). In particular, the result shows that estuaries trap more plastic than lakes and riverbeds (0.218±0.053 Tg/yr), although not as much as reservoirs (0.386±0.103 Tg/yr). Moreover, microplastics accumulate more (50.6%) in lakes, reservoirs, riverbeds, and

estuaries than macroplastics (37.7%), which is consistent with Chen et al. (2022), who showed that higher proportions of small-sized plastics are preferentially retained by hydraulic sorting and that large-sized plastics are more easily evacuated by fluvial transport. Riverine plastic transport to the ocean simulated in the present study was 1.000±0.397 Tg/yr, with macroplastic flux at 0.657±0.309 Tg/yr and microplastic flux at 0.343±0.249 Tg/yr, which was within the range of previous values, i.e., 0.41–4.0 Tg/yr (Meijer et al., 2021).

Table 3.2 Weighted plastic budget average for global major rivers (153 basins/watersheds, 325 river channels), including 130 tidal estuaries. The range is also added for each averaged value. The error in simulated value means the standard deviation for the major rivers worldwide; + and - mean the increase and decrease of fluxes (horizontal transport, and vertical flux from water to bottom sediment) from the averaged values, respectively.

River	Macro P flux (Tg/yr)	Micro P flux (Tg/yr)	Total P flux (Tg/yr)
Riverine Transport to Ocean *	1.056±0.294	0.693±0.227	1.749±0.371
Reservoir Storage **	0.206±0.065	0.180±0.080	0.386±0.103
Lake Storage **	0.035±0.049	0.075±0.061	0.110±0.079
Riverbed Storage ***	0.022±0.010	0.013±0.004	0.035±0.011
Estuarine Storage	0.135±0.048	0.083±0.022	0.218±0.053
Net Transport to Ocean	0.657±0.309	0.343±0.249	1.000±0.397
* Nakayama & Osako (2023b)			
** Nakayama (2024)			
*** Nakayama (2025)			

3.5 Conclusion

In this chapter, the process-based NICE-BGC was modified to incorporate plastic dynamics in estuaries by extending previous studies. This model was employed to conduct a 2-year global simulation aimed at evaluating changes in plastic dynamics in major rivers, including 130 tidal estuaries. The model simulated the impact of estuaries on the plastic budget and its seasonal variability caused by settling, resuspension, and bedload transport during 2014–2015. The model showed that plastics with smaller particle sizes showed greater accumulation in the water of estuaries than in rivers, while plastics with larger particle sizes accumulated more on the riverbed. The model also simulated the spatial distribution of plastic transport and deposition, which showed that Asia and Africa contributed a relatively large proportion of plastic transport on a global scale. In particular, the simulated results showed that estuaries trap more plastic than lakes and riverbeds (0.218±0.053 Tg/yr), although not as much as reservoirs (0.386±0.103 Tg/yr). More than 40% of the plastics were retained by lakes, reservoirs, riverbeds, and estuaries, and riverine plastic transport to the ocean was revised from 1.749±0.371 Tg/yr in the author's previous study to 1.000±0.397 Tg/yr in the present study. These results will aid in the development of solutions and measures for reducing plastic input to the ocean and help quantify the magnitude of plastic transport under climate change.

References

Alder, J. (2003) Putting the coast in the "Sea Around Us". The Sea Around Us Newsletter, 15, 1–2. http://data.unep-wcmc.org/datasets/23

Atwood, E.C., Falcieri, F.M., Piehl, S., et al. (2019) Coastal accumulation of microplastic particles emitted from the Po River, Northern Italy: Comparing remote sensing and hydrodynamic modelling with in situ sample collections. Marine Pollution Bulletin, 138, 561–574. doi:10.1016/j.marpolbul.2018.11.045

Bauer, J.E., Bianchi, T.S. (2011) Dissolved organic carbon cycling and transformation. In: Wolanski, E., McLusky, D.S. (Eds.), Treatise on Estuarine and Coastal Science. Academic Press, Waltham, Vol. 5, pp. 7–67

Biltcliff-Ward, A., Stead, J.L., Hudson, M.D. (2022) The estuarine plastics budget: A conceptual model and meta-analysis of microplastic abundance in estuarine systems. Estuarine, Coastal and Shelf Science, 275, 107963. doi:10.1016/j.ecss.2022.107963

Blondel, E., Buschman, F.A. (2022) Vertical and horizontal plastic litter distribution in a bend of a tidal river. Frontiers in Environmental Science, 10, 861457. doi:10.3389/fenvs.2022.861457

Brooks, A.L., Wang, S., Jambeck, J.R. (2018) The Chinese import ban and its impact on global plastic waste trade. Scientific Advances, 4(6), eaat0131. doi:10.1126/sciadv.aat0131

Burns, E.E., Boxall, A.B.A. (2018) Microplastics in the aquatic environment: Evidence for or against adverse impacts and major knowledge gaps. Environmental Toxicology and Chemistry, 37(11), 2776–2796. doi:10.1002/etc.4268

Chapra, S.C., Martin, J.L. (2012) LAKE2K: A modelling framework for simulating lake water quality (Version 1.4): Documentation and users manual. Civil and Environmental Engineering Dept., Tufts University, Medford, MA

Chen, C.T.A., Huang, T.H., Fu, Y.H., et al. (2012) Strong sources of CO2 in upper estuaries become sinks of CO2 in large river plumes. Current Opinion in Environmental Sustainability, 4 (2), 179–185. doi:10.1016/j.cosust.2012.02.003

Chen, Y., Gao, B., Xu, D., et al. (2022) Catchment-wide flooding significantly altered microplastics organization in the hydro-fluctuation belt of the reservoir. iScience, 25, 104401. doi:10.1016/j.isci.2022.104401

Climatic Research Unit (CRU). (2017) CRU TS3.24 of High Resolution Gridded Data of Month-by-month Variation in Climate. http://catalogue.ceda.ac.uk/

Cohen, J.H., Internicola, A.M., Mason, R.A., et al. (2019) Observations and simulations for microplastic debris in a tide, wind, and freshwater-driven estuarine environment: the Delaware Bay. Environmental Science & Technology, 53, 14204–14211. doi:10.1021/acs.est.9b04814

Defontaine, S., Sous, D., Tesan, J., et al. (2020) Microplastics in a salt-wedge estuary: Vertical structure and tidal dynamics. Marine Pollution Bulletin, 160, 111688. doi:10.1016/j.marpolbul.2020.111688

Díez-Minguito, M., Bermúdez, M., Gago, J., et al. (2020) Observations and idealized modelling of microplastic transport in estuaries: The exemplary case of an upwelling systems (Ria de Vigo, NW Spain). Marine Chemistry, 222, 103780. doi:10.1016/j.marchem.2020.103780

Drummond, J.D., Aquino, T., Davies-Colley, R.J., Krause, S. (2022) Modeling contaminant microbes in rivers during both baseflow and stormflow. Geophysical Research Letters, 49, e2021GL096514. doi:10.1029/2021GL096514

Dürr, H.H., Laruelle, G.G., van Kempen, C.M., et al. (2011) Worldwide typology of nearshore coastal systems: Defining the estuarine filter of river inputs to the oceans. Estuaries and Coasts, 34(3), 441–458. doi:10.1007/s12237-011-9381-y

Eerkes-Medrano, D., Thompson, R.C., Aldridge, D.C. (2015) Microplastics in freshwater systems: A review of the emerging threats, identification of knowledge gaps and prioritisation of research needs. Water Research, 75, 63–82. doi:10.1016/j.watres.2015.02.012

Ericson, J.P., Vorosmarty, C.J., Dingman, S.L., et al. (2006) Effective sea-level rise and deltas: Causes of change and human dimension implications. Global and Planetary Change, 50, 63–82. doi:10.1016/j.gloplacha.2005.07.004

ESRI. (2019) Overlay Layers. Portal for ArcGIS. https://gislab.depaul.edu/portal/portalhelp/en/portal/latest/use/geoanalytics-overlay-layers.htm

European Centre for Medium-Range Weather Forecasts (ECMWF). (2019) ERA-Interim. http://data-portal.ecmwf.int/data/d/interim_daily/

European Commission. (2012) Harmonized World Soil Database. http://eusoils.jrc.ec.europa.eu/ESDB_Archive/soil_data/global.htm

European Commission. (2015) Global Land Cover 2000. https://forobs.jrc.ec.europa.eu/products/glc2000/glc2000.php

Fischer, H.B., List, E.J., Koh, R.C.Y., et al. (1979) Mixing in rivers. In: Fischer, H.B., Koh, R.C.Y., Brooks, N.H. (Eds.), Mixing in Inland and Coastal Waters. Academic Press, New York, pp. 104–147. doi:10.1016/C2009-0-22051-4

Food and Agriculture Organization of the United Nations (FAO). (2016) Global Map of Irrigation Areas (GMIA). http://www.fao.org/nr/water/aquastat/irrigationmap/index.stm

Frankignoulle, M., Abril, G., Borges, A., Bourge, I., Canon, C., Delille, B., Libert, E., Theate, J.-M. (1998) Carbon dioxide emission from European estuaries. Science, 282, 434–436. doi:10.1126/science.282.5388.434

Gao, B., Chen, Y., Xu, D., Sun, K., Xing, B. (2023) Substantial burial of terrestrial microplastics in the Three Gorges Reservoir, China. Communications Earth & Environment, 4, 32. doi:10.1038/s43247-023-00701-z

Guo, X., Dai, M., Zhai, W., et al. (2009) CO2 flux and seasonal variability in a large subtropical estuarine system, the Pearl River Estuary, China. Journal of Geophysical Research, 114, G03013. doi:10.1029/2008JG000905

Haberstroh, C.J., Arias, M.E., Yin, Z., et al. (2021) Plastic transport in a complex confluence of the Mekong River in Cambodia. Environmental Research Letters, 16, 095009. doi:10.1088/1748-9326/ac2198

Han, M., Niu, X., Tang, M., et al. (2020) Distribution of microplastics in surface water of the lower Yellow River near estuary. Science of the Total Environment, 707, 135601. doi:10.1016/j.scitotenv.2019.135601

Hartmann, J., Moosdorf, N. (2012) The new global lithological map database GLiM: A representation of rock properties at the Earth surface. Geochemistry, Geophysics, Geosystems, 13, Q12004. doi:10.1029/2012GC004370

Huang, Q., Liu, M., Cao, X., Liu, Z. (2023) Occurrence of microplastics pollution in the Yangtze River: Distinct characteristics of spatial distribution and basin-wide ecological risk assessment. Water Research, 229, 119431. doi:10.1016/j.watres.2022.119431

Hurley, E., Woodward, J., Rothwell, J.J. (2018) Microplastic contamination of river beds significantly reduced by catchment-wide flooding. Nature Geoscience, 11, 251–257. doi:10.1038/s41561-018-0080-1

Jambeck, J.R., Geyer, R., Wilcox, C., et al. (2015) Plastic waste inputs from land into the ocean. Science, 347, 768–771. doi:10.1126/science.1260352

Jiang, L.-Q., Carter, B.R., Feely, R.A., et al. (2019) Surface ocean pH and buffer capacity: past, present and future. Scientific Reports, 9, 18624. doi:10.1038/s41598-019-55039-4

Jones, E.R., van Vliet, M.T.H., Qadir, M., Bierkens, M.F.P. (2021) Country-level and gridded estimates of wastewater production, collection, treatment and reuse. Earth System Science Data, 13, 237–254. doi:10.5194/essd-13-237-2021

Kaandorp, M.L.A., Lobelle, D., Kehl, C., et al. (2023) Global mass of buoyant marine plastics dominated by large long-lived debris. Nature Geoscience, 16, 189–694. doi:10.1038/s41561-023-01216-0

Kaiser, D., Kowalski, N., Waniek, J.J. (2017) Effects of biofouling on the sinking behavior of microplastics. Environmental Research Letters, 12, 124003. doi:10.1088/1748-9326/aa8e8b

Kooi, M., van Nes, E.H., Scheffer, M., Koelmans, A.A. (2017) Ups and downs in the ocean: Effects of biofouling on vertical transport of microplastics. Environmental Science & Technology, 51, 7963–7971. doi:10.1021/acs.est.6b04702

Kooi, M., Besseling, E., Kroeze, C., et al. (2018) Modelling the fate and transport of plastic decries in freshwaters: review and guidance. In: Wagner, M., Lambert, S. [Eds] Freshwater Microplastics. The Handbook of Environmental Chemistry 58, Springer, pp. 125–152

Kooi, M., Koelmans, A.A. (2019) Simplifying microplastic via continuous probability distributions for size, shape, and density. Environmental Science & Technology Letters, 6, 551-557. doi:10.1021/acs.est.9b00379

Koutnik, V.S., Leonard, J., Alkidim, S., et al. (2021) Distribution of microplastics in soil and freshwater environments: global analysis and framework for transport modelling. Environmental Pollution, 224, 116552. doi:10.1016/j.envpol.2021.116552

Kumar, R., Sharma, P., Verma, A., et al. (2021) Effect of physical characteristics and hydrodynamic conditions on transport and deposition of microplastics in riverine ecosystem. Water, 13, 2710. doi:10.3390/w13192710

Laruelle, G.G., Dürr, H.H., Lauerwald, R., et al. (2013) Global multi-scale segmentation of continental and coastal waters from the watersheds to the continental margins. Hydrology and Earth System Sciences, 17, 2029–2051. doi:10.5194/hess-17-2029-2013

Laruelle, G., Lauerwald, R., Pfeil, B., Regnier, P. (2014) Regionalized global budget of the CO2 exchange at the air-water interface in continental shelf seas. Global Biogeochemical Cycles, 28, 1199–1214. doi:10.1002/2014GB004832

Lebreton, L., Andrady, A. (2019) Future scenarios of global plastic waste generation and disposal. Palgrave Communications, 5, 6. doi:10.1057/s41599-018-0212-7

Lebreton, L, van der Zwet, J., Damsteeg, J.-W., et al. (2017) River plastic emissions to the world's oceans. Nature Communications, 8, 15611. doi:10.1038/ncomms15611

Lee, K., Tong, L.T., Millero, F.J., et al. (2006) Global relationships of total alkalinity with salinity and temperature in surface waters of the world's oceans. Geophysical Research Letters, 33, L19605. doi:10.1029/2006GL027207

Lehner, B., Döll, P. (2004) Development and validation of a global database of lakes, reservoirs and wetlands. Journal of Hydrology, 296, 1–22. doi:10.1016/j.jhydrol.2004.03.028

Lehner, B., Reidy Liermann, C., Revenga, C., et al. (2011) High-resolution mapping of the world's reservoirs and dams for sustainable river-flow management. Frontiers in Ecology and the Environment, 9, 494–502. doi:10.1890/100125

Li, Y., Lu, Z., Zheng, H., et al. (2020) Microplastics in surface water and sediments of Chongming Island in the Yangtze Estuary, China. Environmental Sciences Europe, 32, 15. doi:10.1186/s12302-020-0297-7

Li, Y., Liu S., Liu, M., et al. (2021) Mid-level riverine outflow matters: A case of microplastic transport in the Jiulong River, China. Frontiers in Marine Science, 8, 712727. doi:10.3389/fmars.2021.712727

Liu, Y., You, J., Li, Y., et al. (2021) Insights into the horizontal and vertical profiles of microplastics in a river emptying into the sea affected by intensive anthropogenic activities in Northern China. Science of the Total Environment, 779, 146589. doi:10.1016/j.scitotenv.2021.146589

López, A.G., Najjar, R.G., Friedrichs, M.A.M., et al. (2021) Estuaries as filters for riverine microplastics: Simulations in a large, coastal-plain estuary. Frontiers in Marine Science, 8, 715924. doi:10.3389/fmars.2021.715924

Mai, L., Sun, X.-F., Xia, L.-L., Bao, L.-J., Liu, L.-Y., Zeng, E.Y. (2020) Global riverine plastic outflows. Environmental Science & Technology, 54, 10049–10056. doi:10.1021/acs.est.0c02273

Meijer, L.J.J., van Emmerik, T., van der Ent, R., et al. (2021) More than 1000 rivers account for 80% of global riverine plastic emissions into the ocean. Science Advances, 7, eaaz5803. doi:10.1126/sciadv.aaz5803

Ministry of Foreign Affairs of Japan. (2019) G20 Osaka Leader's Declaration. https://www.mofa.go.jp/policy/economy/g20_summit/osaka19/en/documents/final_g20_osaka_leaders_declaration.html

Mueller, N.D., Gerber, J.S., Johnston, M., et al. (2012) Closing yield gaps through nutrient and water management. Nature, 490, 254–257. doi:10.1038/nature11420

Nakayama, T. (2017a) Development of an advanced eco-hydrologic and biogeochemical coupling model aimed at clarifying the missing role of inland water in the global biogeochemical cycle. Journal of Geophysical Research: Biogeosciences, 122, 966-988. doi:10.1002/2016JG003743

Nakayama, T. (2017b) Scaled-dependence and seasonal variations of carbon cycle through development of an advanced eco-hydrologic and biogeochemical coupling model. Ecological Modelling, 356, 151–161. doi:10.1016/j.ecolmodel.2017.04.014

Nakayama, T. (2020) Inter-annual simulation of global carbon cycle variations in a terrestrial-aquatic continuum. Hydrological Processes, 34(3), 662–678. doi:10.1002/hyp.13616

Nakayama, T. (2022) Impact of anthropogenic disturbances on carbon cycle changes in terrestrial-aquatic-estuarine continuum by using an advanced process-based model. Hydrological Processes, 36(2), e14471. doi:10.1002/hyp.14471

Nakayama, T. (2023) Evaluation of global biogeochemical cycle in lotic and lentic waters by developing an advanced eco-hydrologic and biogeochemical coupling model. Ecohydrology, 17(4), e2555. doi:10.1002/eco.2555

Nakayama, T., Pelletier, G. (2018) Impact of global major reservoirs on carbon cycle changes by using an advanced eco-hydrologic and biogeochemical coupling model. Ecological Modelling, 387, 172–186. doi:10.1016/j.ecolmodel.2018.09.007

Nakayama, T., Osako, M. (2023a) Development of a process-based eco-hydrology model for evaluating the spatio-temporal dynamics of macro- and micro-plastics for the whole of Japan. Ecological Modelling, 476, 110243. doi:10.1016/j.ecolmodel.2022.110243

Nakayama, T., Osako, M. (2023b) The flux and fate of plastic in the world's major rivers: Modeling spatial and temporal variability. Global and Planetary Change, 221, 104037. doi:10.1016/j.gloplacha.2023.104037

Nakayama, T., Osako, M. (2024) Plastic trade-off: Impact of export and import of waste plastic on plastic dynamics in Asian region. Ecological Modelling, 489, 110624. doi:10.1016/j.ecolmodel.2024.110624

Nakayama, T. (2024) Impact of global major reservoirs and lakes on plastic dynamics by using a process-based eco-hydrology model. Lakes & Reservoirs: Science, Policy and Management for Sustainable Use, 29, e12463. doi:10.1111/lre.12463

Nakayama, T. (2025) Impact of settling and resuspension on plastic dynamics during extreme flow and their seasonality in global major rivers. Hydrological Processes, 39(2), e70072, doi:10.1002/hyp.70072

NASA. (2013) GLDAS vegetation class. http://ldas.gsfc.nasa.gov/gldas/GLDASvegetation.php

NASA. (2018) Gridded Population of the World, Version 4 (GPWv4). https://sedac.ciesin.columbia.edu/data/set/gpw-v4-population-count-adjusted-to-2015-unwpp-country-totals-rev11

National Oceanic and Atmospheric Administration (NOAA). (2013) World Ocean Atlas 2013 ver.2. https://www.nodc.noaa.gov/OC5/woa13/

Nizzetto, L., Bussi, G., Futter, M.N., et al. (2016) A theoretical assessment of microplastic transport in river catchments and their retention by soils and river sediments. Environmental Science: Processes & Impacts, 18, 1050–1059. doi:10.1039/c6em00206d

Ockelford, A., Cundy, A., Ebdon, J.E. (2020) Storm response of fluvial sedimentary microplastics. Scientific Reports, 10, 1865. doi:10.1038/s41598-020-58765-2

OECD. (2022) Global Plastics Outlook: Economic Drivers, Environmental Impacts and Policy Options, OECD Publishing, Paris. https://doi.org/10.1787/de747aef-en

Pelletier, G.J., Chapra, S.C., Tao, H. (2006) QUAL2Kw – A framework for modeling water quality in streams and rivers using a genetic algorithm for calibration. Environmental Modelling and Software, 21, 419–425. doi:10.1016/j.envsoft.2005.07.002

Peng, Y., Wu, P., Schartup, A.T., Zhang, Y. (2021) Plastic waste release caused by COVID-19 and its fate in the global ocean. Proceedings of the National Academy of Sciences of the United States America, 118(47), e2111530118. doi:10.1073/pnas.2111530118

Pinheiro, L.M., Agostini, V.O., Lima, A.R.A., et al. (2021) The fate of plastic litter within estuarine compartments: An overview of current knowledge for the transboundary issue to guide future assessments. Environmental Pollution, 279, 116908. doi:10.1016/j.envpol.2021.116908

Pojar, I., Stanica, A., Stock, F., et al. (2021) Sedimentary microplastic concentrations from the Romanian Danube River to the Black Sea. Scientific Reports, 11, 2000. doi:10.1038/s41598-021-81724-4

Portmann, F.T., Siebert, S., Döll, P. (2010) MIRCA2000 – Global monthly irrigated and rainfed crop areas around the year 2000: A new high-resolution data set for agricultural and hydrological modelling. Global Biogeochemical Cycles, 24, GB 1011. doi:10.1029/2008GB003435

Praetorius, A., Scheringer, M., Hungerbühler, K. (2012) Development of environmental fate models for engineered nanoparticles - A case study of TiO2 nanoparticles in the Rhine River. Environmental Science & Technology, 46, 6705-6713. doi:10.1021/es204530n

Qian, Y., Shang, Y., Zheng, Y., et al. (2023) Temporal and spatial variation of microplastics in Baotou section of Yellow River, China. Journal of Environmental Management, 338, 117803. doi:10.1016/j.jenvman.2023.117803

Regnier, P., O'Kane, J.P. (2004) On the mixing processes in estuaries: The fractional freshwater method revisited. Estuaries and Coasts, 27(4), 571–582

Regnier, P., Friedlingstein, P., Ciais, P., et al. (2013) Anthropogenic perturbation of the carbon fluxes from land to ocean. Nature Geoscience, 6, 597–607. doi:10.1038/ngeo1830

Schmidt, C., Krauth, T., Wagner, S. (2017) Export of plastic debris by rivers into the sea. Environmental Science & Technology, 51, 12246–12253. doi:10.1021/acs.est.7b02368

Schreyers, L.D.M., van Emmerik, T.H.M., Bui, K., et al. (2024) River plastic transport affected by tidal dynamics. Hydrology and Earth System Sciences, 28, 589–610. doi:10.5194/egusphere-2022-1495

Siebert, S., Döll, P. (2010) Quantifying blue and green virtual water contents in global crop production as well as potential production losses without irrigation. Journal of Hydrology, 384, 198–217

Siegfried, M., Koelmans, A.A., Besseling, E., Kroeze, C. (2017) Export of microplastics from land to sea. A modelling approach. Water Research, 127, 249–257. doi:10.1016/j.watres.2017.10.011

Singh, N., Mondal, A., Bagri, A., et al. (2021) Characteristics and spatial distribution of microplastics in the lower Ganga River water and sediment. Marine Pollution Bulletin, 163, 111960. doi:10.1016/j.marpolbul.2020.111960

Strokal, M., Bai, Z., Franssen, W., et al. (2021) Urbanization: an increasing source of multiple pollutants to rivers in the 21st century. Urban Sustainability, 1, 24. doi:10.1038/s42949-021-00026-w

Su, X., Yang, L., Yang, K., et al. (2022) Estuarine plastisphere as an overlooked source of N2O production. Nature Communications, 13, 3884. doi:10.1038/s41467-022-31584-x

Tessler, Z.D., Vorosmarty, C.J., Grossberg, M., et al. (2015) Profiling risk and sustainability in coastal deltas of the world. Science, 349(6248), 638–643. doi:10.1126/science.aab3574

Thompson, R.C., Olsen, Y., Mitchell, R.P., et al. (2004) Lost at sea: Where is all the Plastic? Science, 304, 838. doi:10.1126/science.1094559

Tian, H., Yang, J., Lu, C., et al. (2018) The global N2O model intercomparison project. Bulletin of the American Meteorological Society, 99(6), 1231–1251. doi:10.1175/bams-d-17-0212.1

Treilles, R., Gasperi, J., Tramoy, R., et al. (2022) Microplastic and microfiber fluxes in the Seine River: Flood events versus dry periods. Science of the Total Environment, 805, 150123. doi:10.1016/j.scitotenv.2021.150123

Tsering, T., Sillanpaa, M., Sillanpaa, M., Viitala, M., Reinkainen, S.-P. (2021) Microplastics pollution in the Brahmaputra River and the Indus River of the Indian Himalaya. Science of the Total Environment, 789, 147968. doi:10.1016/j.scitotenv.2021.147968

UNESCO. (2022) IHP-IX: Strategic Plan of the Intergovernmental Hydrological Programme: Science for a Water Secure World in a Changing Environment, ninth phase 2022–2029. https://unesdoc.unesco.org/ark:/48223/pf0000381318.locale=en

U. S. Department of Agriculture (USDA). (2022) Global Reservoirs and Lakes Monitor (G-REALM). Foreign Agricultural Service. https://ipad.fas.usda.gov/cropexplorer/global_reservoir/

U.S. Geological Survey (USGS). (1996a) GTOPO30 Global 30 Arc Second Elevation Data Set. USGS. http://www1.gsi.go.jp/geowww/globalmap-gsi/gtopo30/gtopo30.html

U.S. Geological Survey (USGS). (1996b) HYDRO1K. USGS. https://lta.cr.usgs.gov/HYDRO1K

U.S. Geological Survey (USGS). (2018) Shuttle Radar Topography Mission (SRTM) 1 Arc-Second Global. USGS. doi:10.5066/F7PR7TFT

van Emmerik, T., Strady, E., Kieu-Le, T.-C., Nguyen, L., Gratiot, N. (2019) Seasonality of riverine macroplastic transport. Scientific Reports, 9, 13549. doi:10.1038/s41598-019-50096-1

van Wijnen, J., Ragas, A.M.J., Kroeze, C. (2019) Modelling global river export of microplastics to the marine environment: Sources and future trends. Science of the Total Environment, 673, 392–401. doi:10.1016/j.scitotenv.2019.04.078

Vanderborght, J.P., Wollast, R., Loijen, M., Regnier, P. (2002) Application of a transport-reaction model to the estimation of biogas fluxes in the Scheldt estuary. Biogeochemistry, 59, 207–237

Vermeiren, P., Muñoz, C.C., Ikejima, K. (2016) Sources and sinks of plastic debris in estuaries: A conceptual model integrating biological, physical and chemical distribution mechanisms. Marine Pollution Bulletin, 113, 7–16. doi:10.1016/j.marpolbul.2016.10.002

Wagner, S., Klöckner, P., Stier, B., Römer, M., Seiwert, B., Reemtsma, T., Schmidt, C. (2019) Relationship between discharge and river plastic concentrations in a rural and an urban catchment. Environmental Science & Technology, 53, 10082–10091. doi:10.1021/acs.est.9b03048

Waldschläger, K., Schüttrumpf, H. (2019) Erosion behavior of different microplastic particles in comparison to natural sediments. Environmental Science & Technology, 53, 13219–13227. doi:10.1021/acs.est.9b05394

Waldschläger, K., Lechthaler, S., Stauch, G., Schuttrumpf, H. (2020) The way of microplastic through the environment – Application of the source-pathway-receptor model (review). Science of the Total Environment, 713, 136584. doi:10.1016/j.scitotenv.2020.136584

Wang, T., Zhao, S., Zhu, L., et al. (2022) Accumulation, transformation and transport of microplastics in estuarine fronts. Nature Reviews Earth & Environment, 3(11), 795–805. doi:10.1038/s43017-022-00349-x

Weiss, L., Ludwig, W., Heussner, S., et al. (2021) The missing ocean plastic sink: Gone with the rivers. Science, 373, 107–111. doi:10.1126/science.abe0290

Xiong, X., Wu, C., Elser, J.J., Mei, Z., Hao, Y. (2019) Occurrence and fate of microplastic debris in middle and lower reaches of the Yangtze River – From inland to the sea. Science of the Total Environment, 659, 66–73. doi:10.1016/j.scitotenv.2018.12.313

Yang, L., Zhang, Y., Kang, S., Wang, Z., Wu, C. (2021) Microplastics in freshwater sediment: A review on methods, occurrence, and sources. Science of the Total Environment, 754, 141948. doi:10.1016/j.scitotenv.2020.141948

Zhang, B., Tian, H., Lu, C., et al. (2017) Global manure nitrogen production and application in cropland during 1860-2014; a 5 arcmin gridded global dataset for Earth system modelling. Earth System Science Data, 9, 667-678. doi:10.5194/essd-9-667-2017

Zhao, H., Zhou, Y., Han, Y., et al. (2022) Pollution status of microplastics in the freshwater environment of China: a mini review. Water Emerging Contaminations & Nanoplastics, 1, 5. doi:10.20517/wecn.2021.05

Zhao, S., Wang, T., Zhu, L., et al. (2019) Analysis of suspended microplastics in the Changjiang Estuary: Implications for riverine plastic load to the ocean. Water Research, 161, 560–569. doi:10.1016/j.watres.2019.06.019

- 60 -

Chapter 4

Improvement in the Simulation of Plastic Dynamics and Their Relation to Biogeochemical Cycles in Global Rivers by Considering the Effect of the Interaction Processes of Biofouling and Heteroaggregation

Abstract

Recent research has shown that inland waters act as important transport pathways for both water and dissolved substances and play a significant role in continental biogeochemical cycling. In the present study, the coupled National Integrated Catchment-based Eco-hydrology-BioGeochemical Cycle (NICE-BGC) model was extended to evaluate biogeochemical cycles and their relationship with plastic dynamics in the terrestrial-aquatic continuum on a global scale. The new model showed the effect of different grid resolutions on hydrological and carbon cycle changes. The model also simulated different speciation states of microplastics to indicate the impact of interaction processes, heteroaggregation, and biofouling on plastic dynamics. In particular, the model could estimate attached algal growth as a function of the encounter kernel rate. The results showed that microplastics might quickly aggregate with suspended particulate matter to form heteroaggregates in rivers containing large amounts of microplastics. The dominance of heteroaggregates was related to the higher concentration of both suspended particles and total organic carbon (TOC). Furthermore, the dynamic rate of biofouling simulated by the model showed that algal growth affects the diurnal and seasonal fluctuations of different speciation states of microplastics in some rivers, with the proportion of biofouled plastic increasing in waters where the flow is slower and the retention time is longer. Finally, the plastic budgets of major global rivers were estimated by including storage within reservoirs, lakes, riverbeds, estuaries, and interaction processes. These findings provide valuable insights for improving our understanding of the plastic cycle associated with carbon cycle variations to minimize the range of uncertainty in combined lotic and lentic waters.

Keywords: Carbon cycle; coupling model; grid resolution; interaction processes; plastic cycle

4.1 Introduction

Recent studies have indicated that inland waters, including rivers, lakes, and groundwater, may act as important transport pathways for both water and dissolved substances and play a globally significant role in continental biogeochemical cycling, or the so-called 'boundless carbon cycle' (Cole et al., 2007; Battin et al., 2009; Drake et al., 2018). Comprehensive analysis has revealed a global CO_2 evasion (degassing) rate of 1.2–2.1 PgC/year from inland waters (Tranvik et al., 2009; Aufdenkampe et al., 2011; Raymond et al., 2013). Other studies have also indicated that carbon budgets are diverse in various basins/catchments and that dissolved organic carbon (DOC), dissolved inorganic carbon (DIC), and particulate organic carbon (POC) are also important for the evaluation of CO_2 flux and sediment storage in the global carbon cycle (Cole et al., 2007; Tranvik et al., 2009; Aufdenkampe et al., 2011; Raymond et al., 2013). To bridge the gap between vertical flux and horizontal carbon transport, the author developed an advanced model coupling eco-hydrology and the biogeochemical cycle (i.e., National Integrated Catchment-based Eco-hydrology-Biogeochemical Cycle, NICE-BGC) (Nakayama, 2022), which incorporates the complex coupling of the hydrologic-carbon cycle in terrestrial-aquatic-estuarine linkages. In addition, other studies focusing on inland waters undergoing eutrophication have shown that CO_2 sources sometimes become net sinks because of CO_2 disequilibrium caused by nutrient-driven primary production, as reflected by high oxygen concentrations (Balmer and Downing, 2011; Heathcote and Downing, 2012; Pacheco et al., 2013).

Plastic pollution is considered a main environmental problem, and such pollutants in streams, rivers, and oceans pose potential risks to human health and the environment (Siegfried et al., 2017). Humans are exposed to microplastics via oral intake, inhalation, and skin contact, which can cause organ dysfunction, metabolic disorders, immune responses, and chronic diseases (Li et al., 2023). Once plastics are released into the environment, they are gradually degraded by physical, chemical, and biological processes, leading to further disaggregation into an enormous number of forms, which are impossible to remove and remain indefinitely in the environment. Previous studies on the origin and fate of plastic waste in freshwater systems have suggested that land-derived plastics are among the main sources of marine plastic pollution (Jambeck et al., 2015). Subsequent studies (Lebreton et al., 2017; Schmidt et al., 2017) estimated the distribution of global riverine emissions of plastic into the ocean using empirical indicators representative of waste generation (mismanaged plastic waste, MPW) inside a river basin. Recently, Meijer et al. (2021) performed a more accurate analysis to account for the spatial distribution of plastic waste generation (Lebreton and Andrady, 2019) and climatological/geographical differences within river basins using a probabilistic approach. Other studies (Siegfried et al., 2017; van Wijnen et al., 2019; Strokal et al., 2021) adapted process-oriented models to estimate plastic transport to the ocean by extending existing non-dynamic nutrient export models. The process-based NICE-BGC was also extended by coupling it with a plastic debris (engineered materials) model and applied to evaluate spatiotemporal variations in plastic debris on a regional scale throughout Japan (Nakayama and Osako, 2023a) and on a global scale for the world's major rivers (Nakayama and Osako, 2023b).

Plastic debris in inland waters is subject to weathering by mechanical abrasion, ultraviolet light, photochemical dissolution, and biodegradation, which results in fragmentation and chemical degradation over time; moreover, this debris aggregates with suspended particle matter (SPM) and is colonized by biofilms (Domercq et al., 2022). While weathering, dissolution, and degradation have been considered in previous model development (Siegfried et al., 2017; van Wijnen et al., 2019; Strokal et al., 2021; Nakayama and Osako, 2023a, 2023b),

heteroaggregation and biofouling and the resulting retention of plastics have rarely been incorporated in existing river models (except in laboratory and experimental studies) because of the lack of on-site observation data on the heterogeneous effects of different speciation states of plastics. Previous studies have shown that the proportion of biofouled plastic increases more in lentic waters and estuaries and that the salinity and temperature of water influence biofilm colonization (D'Avignon et al., 2022; Elagami et al., 2022). Aggregation with SPM also affects the surface modification of plastics by the adsorption of suspended matter in natural waters and stabilizes it to be dispersed in suspension. In contrast, homoaggregation is negligible in aquatic environments because of the high dilution of plastic particles in the environment and their low concentrations relative to natural suspended sediment concentrations (Domercq et al., 2022). These interaction processes affect the settling velocity and resuspension rate of microplastics, resulting in changes in the fate and transport of plastics in inland waters (Koutnik et al., 2021).

Therefore, the impact of biofouling and heteroaggregation on plastic cycle changes must be quantified via robust hybrid modelling that considers plastic and biogeochemical linkages between land and aquatic systems. This highlights the need to incorporate the effects of different grid resolutions in global biogeochemical and plastic cycle models to minimize the range of uncertainty in the model (Cole et al., 2007; Battin et al., 2009; Regnier et al., 2013). Based on this background, three basic issues were addressed: (i) How do different grid resolutions affect variations in biogeochemical and plastic cycles in global river basins? (ii) How do biofouling and heteroaggregation affect temporal variations in the plastic cycle of global river basins? (iii) How is the global plastic budget affected by these interaction processes in the terrestrial-aquatic continuum? To clarify these issues, the present study extended the NICE-BGC model to incorporate the effect of the interaction processes of heteroaggregation (Praetorius et al., 2012) and biofouling (Kooi et al., 2017, 2018) on plastic dynamics in global major rivers and to evaluate the relationship between plastic cycles and biogeochemical dynamics in the terrestrial-aquatic continuum (Fig. 4.1, and Table 4.1). The model results show the effects of different grid resolutions on hydrologic and carbon cycle changes in the major global rivers. The new model can simulate different speciation states of microplastics (pristine, heteroaggregated, biofouled, and biofouled & heteroaggregated) in inland water. In addition, the model can estimate the attached algal growth as a function of the encounter kernel rate. This improvement is important for evaluating the plastic cycle associated with carbon cycle variations to minimize the range of uncertainty in actual combined lotic and lentic waters. Such evaluations may help ensure that the questions addressed by the model are meaningful, tangible, and specific, and recognize the importance of identifying key decision points within the system from a holistic perspective towards enhancing and scaling up the practice of accurate modelling (Jakeman et al., 2024).
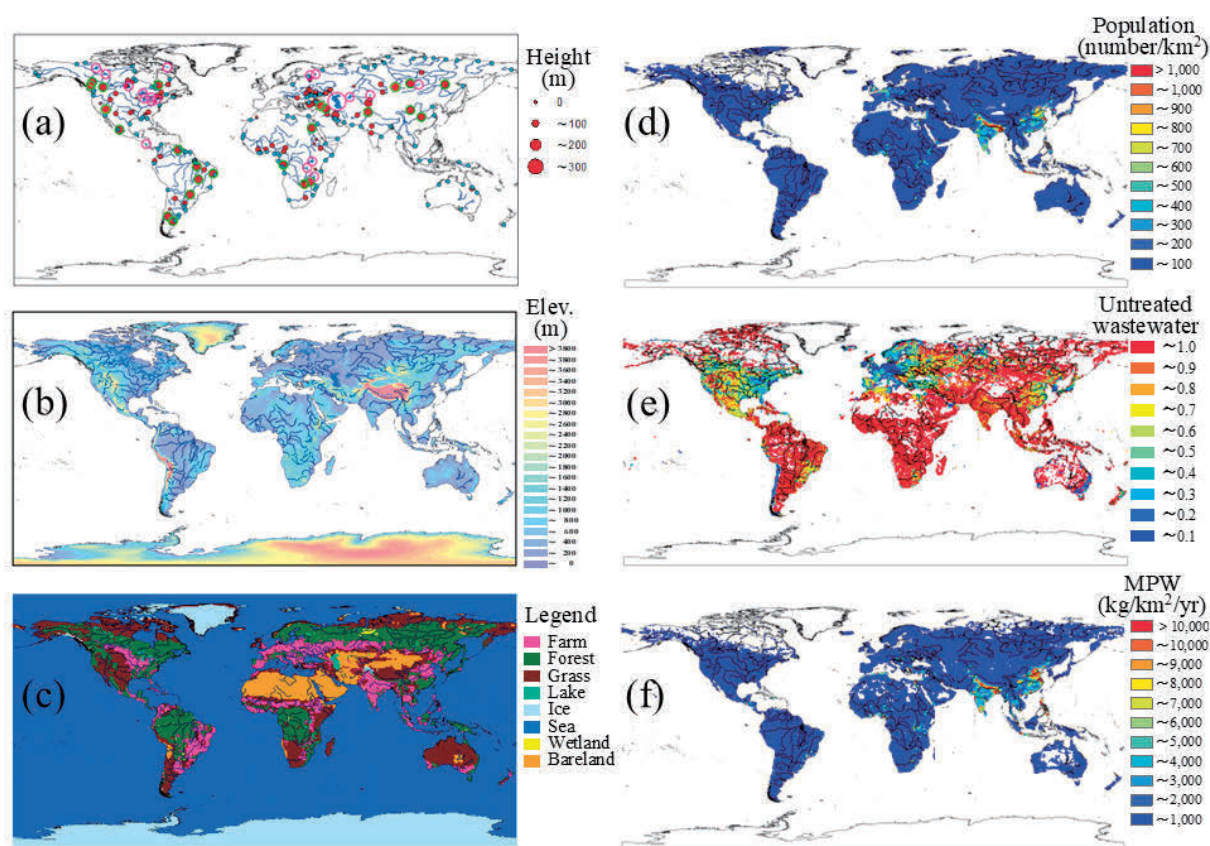
Figure 4.1 Location of the study area on a global scale. (a) World's major rivers (153 basins, 325 river channels) with 82 major reservoirs (red circle) and 19 lakes (blue mesh), including 130 tidal estuaries (light blue circle), (b) elevation, (c) land cover, (d) population density, (e) untreated wastewater calculated from wastewater treatment and wastewater production, and (f) mismanaged plastic waste (MPW). In the figure, the line shows the world's major rivers in HYDRO1K.

Table 4.1 List of input datasets for NICE simulation.

Data set	Original resolution	Year	Source and reference
Climatology	1.0°	2014-2015	ERA-interim; ECMWF (2019)
Elevation	1.0km	around 1996	GTOPO30; U.S. Geological Survey (1996a)
Land cover	1.0km	around 2000	GLC2000; European Commission (2015)
Soil texture	1.0km	around 1970-2000	HWSD; European Commission (2012)
Vegetation type	0.25°	around 2000	GLDAS Vegetation Class; NASA (2013)
River networks	1.0km	around 1996	HYDRO1K; U.S. Geological Survey (1996b)
Lakes and wetlands	0.5 min	around 1990-2000	GLWD; Lehner and Döll (2004)
Reservoirs and Dams	point	around 2010	GRanD; Lehner et al. (2011)
Geological structures	0.5°	around 1970-2000	GLiM; Hartmann and Moosdorf (2012)
Crop type	5 min	around 2000	MIRCA2000; Portmann et al. (2010)
Irrigation type	5 min	2000-2008	GMIA; FAO (2016)
Irrigation water use	5 min	1998-2002	GCWM; Siebert and Döll (2010)
Fertilizer use	5 min	around 2000	Earth Stat; Mueller et al. (2012)
Manure use	5 min	1998-2014	Zhang et al. (2017)
Atmospheric N deposition	0.5°	1998-2015	ISIMIP2a; Tian et al. (2018)
Estuary	polygon	around 2000	Global Estuary Database; Alder (2003)
Estuary type	0.5°	around 2000	Global Coastal Typology; Dürr et al. (2011)
Coastal line	0.5°	around 2000	MARCATS; Laruelle et al. (2013)
Water level	point	1992-2021	G-REALM; USDA (2022)
Population	1.0km	2015	NASA (2018)
Wastewater production and treatment	5 min	2015	Jones et al. (2021)
Mismanaged plastic waste	1.0 km	2015	Lebreton and Andrady (2019)
Ocean water quality	1.0°	1995-2012	WOA2013; NOAA (2013)
Ocean alkalinity	1.0°	around 2000	Lee et al. (2006)
Ocean pH	1.0°	1990, 2000, 2010	Jiang et al. (2019)
Ocean plastic concentration	average hexagon edge length of 22 km	2015	Kaandorp et al. (2023)

4.2 Methods

4.2.1 Extension of the Microplastic Submodel by Including Interaction Processes

In this chapter, the microplastic submodel of the NICE-BGC model was newly extended to couple with the interaction processes of heteroaggregation, breakup, and biofouling, thus representing an extension of the author's previous studies (Nakayama and Osako, 2023a, 2023b) (Fig. 4.2). The source and sink terms for constituent S can be extended to the following four speciation states (pristine, heteroaggregated, biofouled, biofouled, and heteroaggregated) due to the reactions and mass transfer mechanisms of microplastics (Praetorius et al., 2012; Domercq et al., 2022):

$$S_{P\_pris} = -\frac{v_{Pmic}}{h}P_{pris} - k_{Pmic}(T)P_{pris} - \alpha_{Pmic}\frac{I(0)/24}{k_e h}(1 - e^{-k_e h})P_{pris}$$
$$- k_{hetAgg}P_{pris} - k_{biof}P_{pris} + k_{hetAgg-breakup}P_{het} + k_{defoul}P_{biof} \quad (4.1)$$

$$S_{P\_het} = -\frac{v_{Phet}}{h}P_{het} - k_{Phet}(T)P_{pris} - \alpha_{Phet}\frac{I(0)/24}{k_e h}(1 - e^{-k_e h})P_{het}$$
$$+ k_{hetAgg}P_{pris} - k_{hetAgg-breakup}P_{het} - k'_{biof}P_{het} + k'_{defoul}P_{comp} \quad (4.2)$$

$$S_{P\_biof} = -\frac{v_{Pbiof}}{h}P_{biof} - k_{Pbiof}(T)P_{biof} - \alpha_{Pbiof}\frac{I(0)/24}{k_e h}(1 - e^{-k_e h})P_{biof}$$
$$+ k_{biof}P_{pris} - k_{defoul}P_{biof} - k'_{hetAgg}P_{biof} + k'_{hetAgg-breakup}P_{comp} \quad (4.3)$$

$$S_{P\_comp} = -\frac{v_{Pcomp}}{h}P_{comp} - k_{Pcomp}(T)P_{comp} - \alpha_{Pcomp}\frac{I(0)/24}{k_e h}(1 - e^{-k_e h})P_{comp}$$
$$+ k'_{hetAgg}P_{biof} + k'_{biof}P_{het} - k_{hetAgg-breakup}P_{comp} - k'_{defoul}P_{comp} \quad (4.4)$$

where P_{pris} (µg/l), P_{het} (µg/l), P_{biof} (µg/l), and P_{comp} (µg/l) are the concentrations of pristine, heteroaggregated, biofouled, and biofouled & heteroaggregated microplastics, respectively; T is the water temperature; v_{Pmic} is the settling velocities of microplastic (m/d); $k_{Pmic}(T)$ is the temperature-dependent plastic dissolution rates (/d); α_{Pmic} is the light efficiency factors (-); k_{hetAgg}, k_{biof}, $k_{hetAgg-breakup}$, and k_{defoul} are rate constants for heteroaggregation, biofouling, heteroaggregation break-up, and defouling of pristine plastic, respectively; and k'_{hetAgg}, k'_{biof}, $k'_{hetAgg-breakup}$, and k'_{defoul} are rate constants for heteroaggregation, biofouling, heteroaggregation break-up, and defouling of heteroaggregated or biofouled plastic, respectively. The effective sizes of the heteroaggregated and biofouled microplastics ($r_{micro-SPM}$ and $r_{micro-biof}$) were calculated to account for the effect of the added volume of SPM and biofilm based on the method of Domercq et al. (2022):

$$r_{micro-SPM} = \sqrt[3]{\frac{3 \times (V_{micro} + V_{SPM})}{4 \times \pi}} \quad (4.5)$$

$$r_{micro-biof} = r_{micro} + T_{biof} \quad (4.6)$$

where r_{micro} is the radius of microplastics (m); V_{micro} is the volume of plastic particle (m^3); V_{SPM} is the volume of SPM particle (m^3); and T_{biof} is the thickness of biofilm layer (m). The effective densities of heteroaggregated and biofouled microplastics ($\rho_{micro-SPM}$ and $\rho_{micro-biof}$) are also calculated via the same method:

$$\rho_{micro-SPM} = \rho_{micro} \times \frac{V_{micro}}{V_{micro} + V_{SPM}} + \rho_{SPM} \times \frac{V_{SPM}}{V_{micro} + V_{SPM}} \quad (4.7)$$

$$\rho_{micro-biof} = \frac{r_{micro}^3 \times \rho_{micro} + ((r_{micro} + T_{biof})^3 - r_{micro}^3) \times \rho_{biof}}{(r_{micro} + T_{biof})^3} \quad (4.8)$$

where ρ_{micro} is the density of plastic particles (kg/m^3); ρ_{SPM} is the density of SPM particles (kg/m^3); and ρ_{biof} is the density of biofilm (kg/m^3). The biofilm layer was assumed to have a thickness of 5 µm and a density of 1388 kg/m^3 for the biofouled particle, whereas the SPM was assumed to have a spherical shape, a diameter of 0.5 µm, and a density of 2000 kg/m^3, as indicated by previous studies (Praetorius et al., 2012; Domercq et al., 2022).

The rate constants in the above equations (4.1)-(4.4) are given as follows:

$$k_{biof} = \frac{1}{(t_{biof-growth})} \quad (4.9)$$

$$k_{hetAgg} = \alpha_{hetAgg} \times k_{coll} \times C_{SPM} \quad (4.10)$$

$$k_{coll} = \frac{2k_B T}{3\mu} \frac{(r_{micro}+r_{SPM})^2}{r_{micro} \times r_{SPM}} + \frac{4}{3} G(r_{micro} + r_{SPM})^3 + \pi(r_{micro} + r_{SPM})^2 \times \left| v_{set}^{micro} - v_{set}^{SPM} \right|$$

(4.11)

$$C_{SPM} = m_i / \left(\frac{4}{3} \pi \rho_{SPM} r_{SPM}^3 \right)$$

(4.12)

$$k_{hatAgg-breakup} = \frac{1}{10} k_{hetAgg}$$

(4.13)

where k_{biof} and k'_{biof} are the rate constants for biofouling (these were given as constant values assuming that biofilm formation uses a first-order rate constant as indicated by previous studies (Praetorius et al., 2012; Domercq et al., 2022) because advection becomes predominant in fast flowing rivers; $t_{biof-growth}$ is time for the biofilm coverage to grow (day) (equals to 30 days for pristine and heteroaggregated plastics)); α_{hetAgg} represents the heteroaggregation attachment efficiency (equal to 0.01 for pristine plastic and 0.02 for biofouled plastic); k_{coll} is the rate of collision between microplastic and SPM (m^3/s); C_{SPM} is the number of SPM per volume ($1/m^3$); k_B is the Boltzmann constant (equals to 1.38×10^{-20} m^2g/s^2/K); T, G, and μ are the absolute temperature (K), shear rate (1/s), and dynamic viscosity of water (g/m/s), respectively; r_{micro} and r_{SPM} are the radii of microplastics and SPM (mm), respectively; v_{set}^{micro} and v_{set}^{SPM} are the settling velocities of microplastic and SPM calculated by Stokes' formula (m/s) (Nakayama and Osako, 2023b), respectively; ρ_{SPM} is the density of SPM (equals to 2000 kg/m^3); and m_i represents inorganic suspended solids (mg/L) calculated by NICE-BGC at each time step (Nakayama, 2022), thus representing an extension of the use of constant values in previous studies (Praetorius et al., 2012; Domercq et al., 2022). The rate constants for defouling (k_{defoul} and k'_{defoul}) were set to zero.
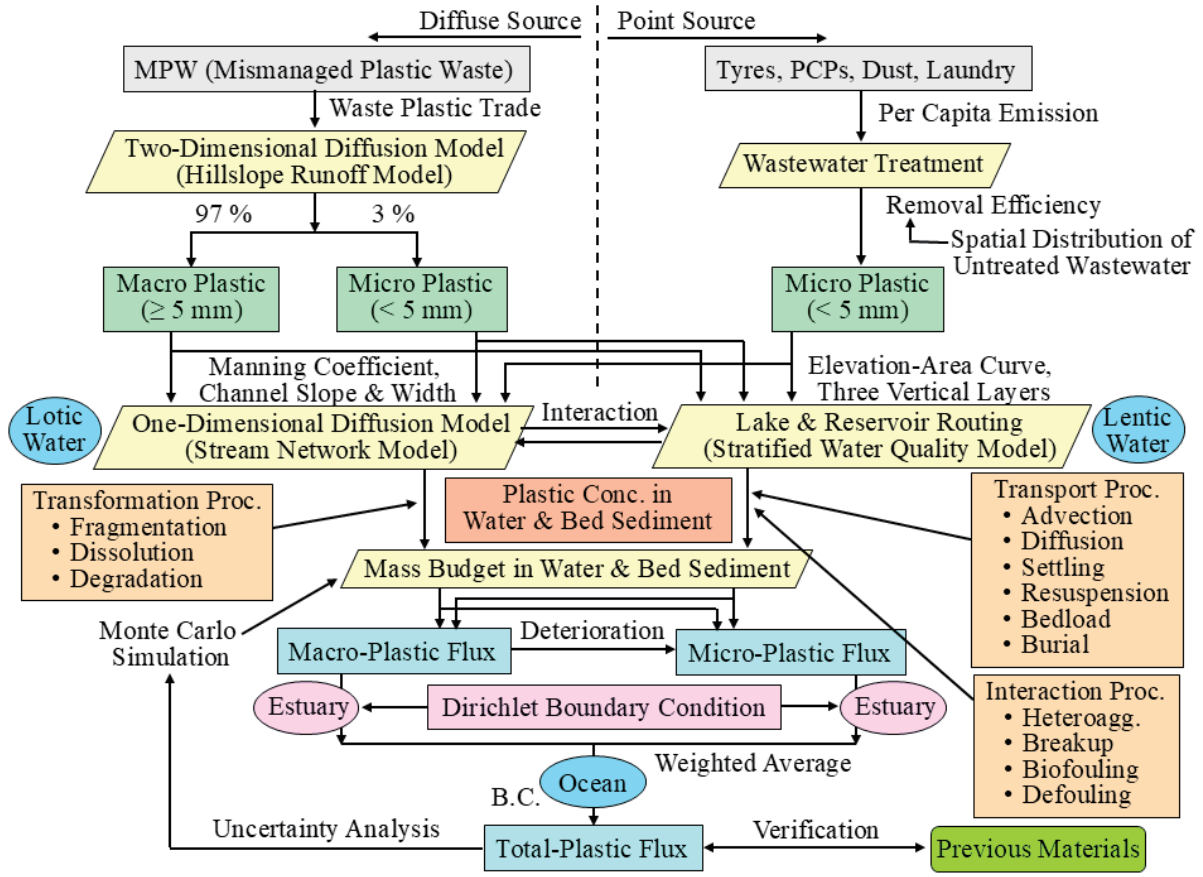
Figure 4.2 Flow diagram showing the transport of macro- and microplastics by extending the NICE-BGC model to include the effect of heteroaggregation and biofouling on plastic dynamics on the global scale. The newly developed model includes the interaction processes of heteroaggregation and biofouling on plastic cycles by extension of the author's previous studies. "B.C." means boundary conditions for the model simulation.

In equations (4.1)–(4.4), the total microplastic concentration P_{micro} (μg/l) is expressed as the sum of the four speciation states of the microplastic concentrations, as shown in equation (4.14).

$$P_{micro} = P_{pris} + P_{het} + P_{biof} + P_{comp} \tag{4.14}$$

where $P_{pris} = P_{het} = P_{biof} = P_{comp} = 0$ represents the upstream inflow plastic in each river channel. Plastic inflowing from hillslope was set to P_{pris} and $P_{het} = P_{biof} = P_{comp} = 0$ at each time step, assuming that no aggregation or biofouling occurs when microplastics flow from land to rivers.

4.2.2 Extension of the Microplastic Submodel by Including Biofouling

This study further extended the rate constant for biofouling at a constant value to a variable rate (Fig. 4.2). The proportion of biofouled plastics shows greater increases in lentic waters and estuaries (D'Avignon et al., 2022; Elagami et al., 2022). Therefore, NICE-BGC was extended

to estimate attached algal growth as a function of the encounter kernel rate (Kooi et al., 2017) because plastic dynamics are closely related to carbon cycles, such as flocculation, heteroaggregation, and biofouling.

$$S_{a\_total} = BotAlgPhoto - BotAlgResp - BotAlgDeath \tag{4.15}$$

$$S_{a\_attached} = BotAlgPhoto - BotAlgResp - BotAlgDeath + \beta_A a_p/(4\pi r_{micro}{}^2) \tag{4.16}$$

where a_{total}, a_{pris}, and $a_{attached}$ are the concentrations of total, pristine, and attached algae (mgA/m^2), respectively; a_p is the phytoplankton concentration calculated by NICE-BGC at each time step (µgA/L is equal to mgA/m^3); r_micro is the radius of the microplastic (mm); and β_A is the encounter kernel rate (m^3/s) and is defined as a combination of three terms as follows:

$$\beta_A = \beta_{A_{brownian}} + \beta_{A_{settling}} + \beta_{A_{shear}} \tag{4.17}$$

$$\beta_{A_{Brownian}} = 4\pi(D_{mic} + D_A)(r_{attached} + r_A) \tag{4.18}$$

$$\beta_{A_{settling}} = \frac{1}{2}\pi r_{attached}^2 v_{set} \tag{4.19}$$

$$\beta_{A_{shear}} = 1.3G(r_{attached} + r_A)^3 \tag{4.20}$$

$$D_{micro} = \frac{k_B(T+273.16)}{6\pi\mu r_{attached}} \tag{4.21}$$

$$D_A = \frac{k_B(T+273.16)}{6\pi\mu r_A} \tag{4.22}$$

$$r_{attached} = r_{micro} + t_{bf} \tag{4.23}$$

where $\beta_{ABrownian}$, $\beta_{Asettling}$ and β_{Ashear} are the Brownian motion, differential settling, and advective shear collision frequencies (Kooi et al., 2017), respectively; D_{micro} and D_A are the diffusivities of the plastic particle and the algae cells (m^2/s), respectively; $r_{attached}$ and r_A are the radii of plastic attached to algae and algae (mm), respectively; t_{bf} is the biofilm thickness (= 5 µm); G is the shear rate (1/s); k_B is the Boltzmann constant (m^{2}kg/s^2/K); and μ is the dynamic viscosity of water (g/m/s). r_A was calculated assuming a spherical particle with an algal shape.

In equations (4.15)–(4.16), the total algae concentration α_{total} (mgA/m^2) is expressed as the sum of the two speciation states of algae concentrations, as shown in equation (4.24).

$$a_{total} = a_{pris} + a_{attached} \tag{4.24}$$

where a_{pris} and $a_{attached}$ are the concentrations of pristine and attached algae (mgA/m^2), respectively. a_{pris} was used as the biomass of bottom plants calculated by NICE-BGC, and $a_{attached}$ equals 0 as the upstream inflow algae in each river channel. The dynamic rate of biofouling (k_{biof}) was calculated at each time step in the extension of equation (4.9) as follows:

$$k_{biof}(t) = \frac{\ln[a_{attached}(t)] - \ln[a_{attached}(t-1)]}{\Delta t} \tag{4.25}$$

In this equation, the reaction kinetics are assumed to be of the first order, as in Kooi et al. (2017). Generally, the rate constant (k_{biof}) has a constant value for inland water in equation (4.9) as a first approximation. However, to include spatiotemporal variations in biofilm formation, such as seasonal or local differences, it is valuable to calculate the variable rate in equation (4.25), assuming that the value varies depending on the compartment depth from a day to a full month.

4.3 Input Data and Boundary Conditions for Simulation

4.3.1 Model Input Data

The input data at various spatial resolutions were prepared and arranged to calculate spatially averaged 1° × 1° and 0.5° × 0.5° grids using the Spatial Analyst Tools in ArcGIS v10.8 software for the global simulation (Fig. 4.1, and Table 4.1). Elevation, land cover, soil texture, vegetation type, river networks, lakes and wetlands, reservoirs and dams, estuaries, coastal typology, geological structures, crop type, irrigation type, irrigation water use, fertilizer use, and manure use were categorized on the basis of the global datasets. To consider the terrestrial-aquatic-estuarine continuum, the length, width, and depth of estuaries for global major rivers were estimated from the Global Estuary Database (Alder, 2003), Global Coastal Typology (Dürr et al., 2011), and MARCATS (MARgins and CATchments Segmentation) (Laruelle et al., 2013) using ArcGIS software (Table 4.1). Although data on plastics are scarce, the following data were used to simulate global plastic debris: gridded population data at 1 km resolution from 2015 global data (NASA, 2018); wastewater production, collection, treatment, and reuse data at 5 arcmin (approximately 10 km) resolution (Jones et al., 2021); and MPW at 1 km resolution (Lebreton and Andrady, 2019) as a diffuse source (Table 4.1). To reasonably create grid data from point, polyline, and polygon data for different sources with different spatial resolutions, an overlay analysis was conducted using GIS tools (intersect, union, and identity) (ESRI, 2019).

4.3.2 Boundary Conditions and Running the Simulation

The simulation was conducted at 1° × 1° and 0.5° × 0.5° resolutions in the horizontal direction and in the same layers in the vertical direction (Nakayama and Osako, 2023b). NICE-BGC simulation for terrestrial ecosystems was conducted at the same spatial resolution with a time step of Δt, which is equal to 1 day for two years during 2014–2015, by iteratively inputting values simulated by NICE after calculating the daily averaged data from 1-hourly data. Previous data were used for per capita emissions of microplastics into rivers (personal care products, dust, laundry fibers, and tires) and the removal efficiency in wastewater treatment plants (WWTPs) as a point source (Fig. 4.2). The model also simulated the outflow of macroplastics originating from MPW (Lebreton and Andrady, 2019) as a diffuse source. A NICE-BGC simulation for aquatic ecosystems was then conducted by inputting the simulated results for land into a stream network model. In particular, the new model can simulate different speciation states of microplastics, including the interaction processes of heteroaggregation and biofouling in inland water, as shown in equations (4.1)–(4.4). Because the simulation including estuaries became more unstable under the Dirichlet boundary condition (Fig. 4.2), the simulation required a smaller time step between Δt at 0.044 min and 0.70 min than that without estuaries to ensure the stability of the model. The hydrological cycle, carbon dynamics, and plastic

transport in rivers were simulated and verified using previous datasets and materials on a continental scale (Nakayama and Osako, 2023b).

It is important to evaluate the uncertainty of plastic transport and its sensitivity to various factors because insufficient data are available on the characteristics of plastics at continental and global scales. In the present study, both micro- and macroplastics were assumed to have continuous probability distributions of size, shape, and density (Kooi and Koelmans, 2019), which is consistent with the author's previous study (Nakayama and Osako, 2023b). Uncertainty and sensitivity analyses were also conducted to evaluate the effects of various factors on plastic transport by ranking the model parameters according to their contribution to prediction uncertainty using Monte Carlo model simulations. Finally, the weighted average value was calculated by multiplying each probability by each flux and their sum (Fig. 4.2). The details were previously described (Nakayama and Osako, 2023b). The results yielded quantitative measures of model performance in terms of reproducing the seasonality and intraannual variability in the hydrologic cycle and plastic transport.

4.4 Results and Discussion

4.4.1 Changes of Hydrologic, Carbon, and Plastic Cycles at Different Grid Resolutions

A comparison of the annually averaged water and carbon fluxes from terrestrial to aquatic ecosystems simulated by NICE-BGC with different grid resolutions is shown in Fig. 4.3. Runoff and carbon transport are clearly correlated, with higher runoff having a significant effect on the transport of DOC and POC fluxes from terrestrial to aquatic ecosystems (Leach et al., 2016; Nakayama, 2022). In particular, this effect is dominant in the northern boreal and peatlands, where DOC predominantly originates. The results also show that South America, Africa, and Asia have a dominant effect on hydrological and carbon cycles on a global scale. In addition, the detailed flow of the water and carbon cycles was clarified by increasing the resolution of the model (Fig. 4.3d-f). This is especially true in humid, water-rich regions.
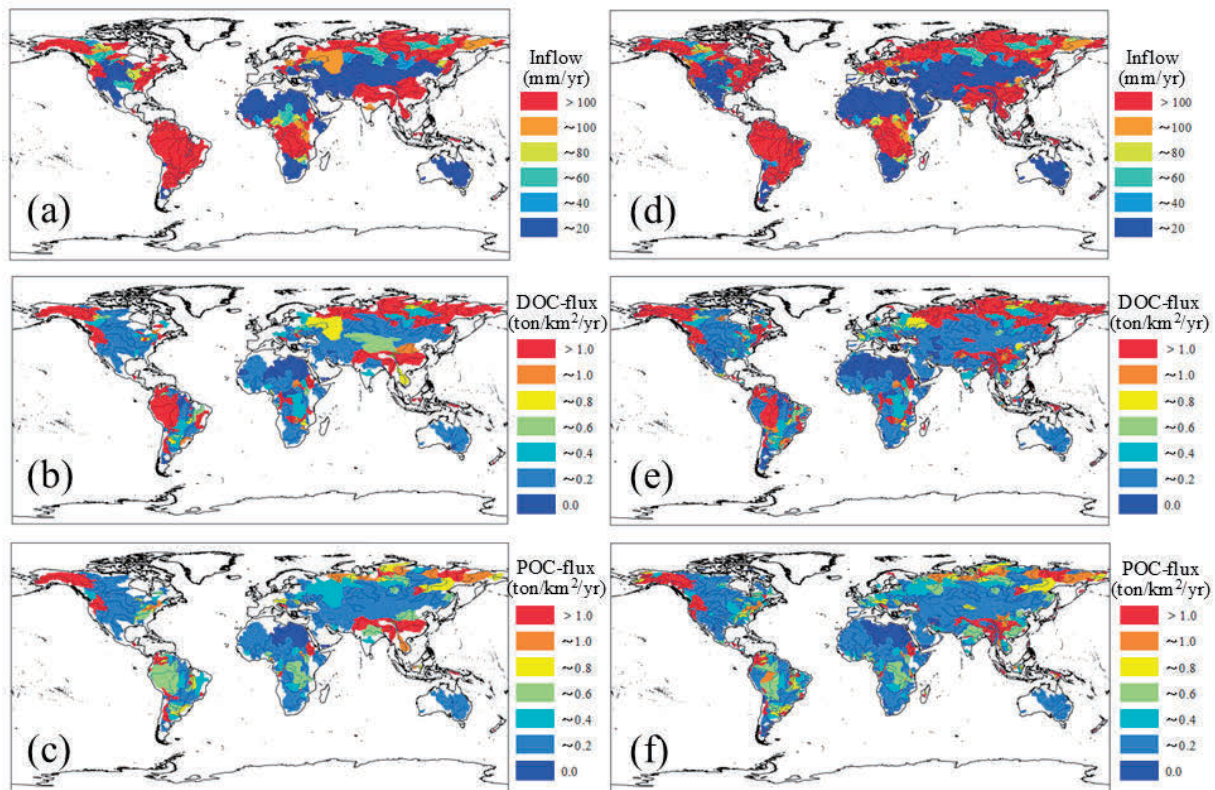
Figure 4.3 Comparison of annually averaged water and carbon fluxes from terrestrial into aquatic ecosystems simulated by NICE-BGC with different grid resolutions. (a)-(c) Total inflow (equal to surface water plus groundwater), DOC flux, and POC flux in 325 river channels (at 1° × 1° resolution), and (d)-(f) total inflow, DOC flux, and POC flux in 929 river channels (at 0.5° × 0.5° resolution), respectively.

Fig. 4.4 shows a comparison of the annually averaged plastic flux from terrestrial to aquatic ecosystems simulated by NICE-BGC with different grid resolutions. The results shows that the heterogeneous distribution of the plastic cycles were clarified by increasing the resolution of the model in the same manner as the water and carbon cycles (Fig. 4.3). This indicates that it is possible to calculate the spatial variability of each flux by increasing the spatial resolution of the model, although it is difficult to verify the calculated values of each flux in each basin on a global scale. The macroplastic, microplastic, and total plastic fluxes also increased from 325 river channels (1.53, 1.15, and 2.68 Tg/yr) (Nakayama and Osako, 2023b) to 929 river channels (2.31, 1.44, and 3.75 Tg/yr) by increasing the number of sub-basins in finer resolutions. This indicates that it is possible to more accurately reproduce spatial hotspots of land-based points and diffuse sources of plastic at finer resolutions and that the macroplastic, microplastic, and total plastic fluxes flowing down the slope into the river channel become greater as a result. Furthermore, Asia and Africa play important roles in plastic transport to the ocean because human activity has a clear impact on the plastic cycle through point sources (personal care products, dust, laundry fibers, car tire wear, and macroplastic fragmentation) (Siegfried et al., 2017; van Wijnen et al., 2019; Strokal et al., 2021) and diffuse sources (mismanaged plastic waste) (Lebreton and Andrady, 2019), which is inconsistent with the carbon cycle.
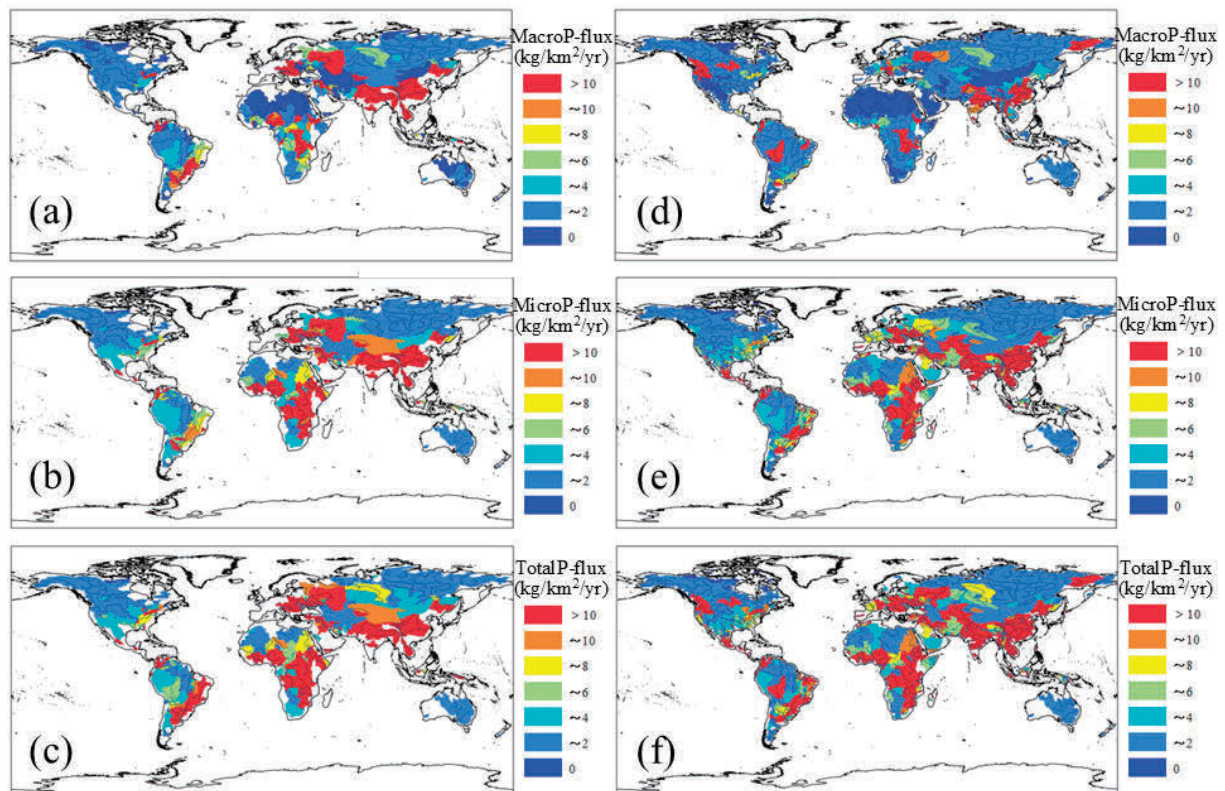
Figure 4.4 Comparison of annually averaged plastic fluxes from terrestrial into aquatic ecosystems simulated by NICE-BGC with different grid resolutions. (a)-(c) Macroplastic, microplastic, and total plastic fluxes in 325 river channels (at 1° × 1° resolution), and (d)-(f) macroplastic, microplastic, and total plastic fluxes in 929 river channels (at 0.5° × 0.5° resolution), respectively.

4.4.2 Impact of Biofouling and Heteroaggregation on Microplastic Dynamics in Global Major Rivers

Fig. 4.5 shows a comparison of carbon and plastic fluxes with different resolutions for some major global rivers. The results show that macro- and microplastic fluxes are heavily influenced by human activities and are prevalent in Asia and Africa (Lebreton et al., 2017; Meijer et al., 2021) (Fig. 4.5a and 4.5b), whereas the total organic carbon (TOC) flux is greatly affected by peat and precipitation and is abundant in South America and Asia (Raymond et al., 2013; Nakayama, 2022) (Fig. 4.5c). The higher resolution decreases the fluxes in these regions, but the results show that the trends are very different for plastic and carbon fluxes (Fig. 4.5d-f). Plastic transport differed significantly depending on the grid resolutions (Fig. 4.5a-b and d-e), whereas carbon fluxes were not significantly reduced at finer resolutions (Fig. 4.5c and 4.5f). This characteristic is more effective in terms of the calculated difference of model results at the two different resolutions (Fig. 4.6). Therefore, using a finer resolution increases the likelihood of plastics being retained or accumulated within the river channel and ultimately reduces the flux that flows out from the end of the river channel, despite the greater amount of plastic

contributed by the slope. This result also implies that the transport mechanism of plastic is more complex than that of the carbon cycle because of the complexity of plastic properties, such as the size, shape, and density, and the effects of settling, resuspension, bedload transport, dissolution, deterioration, heteroaggregation, and biofouling (Windsor et al., 2019).
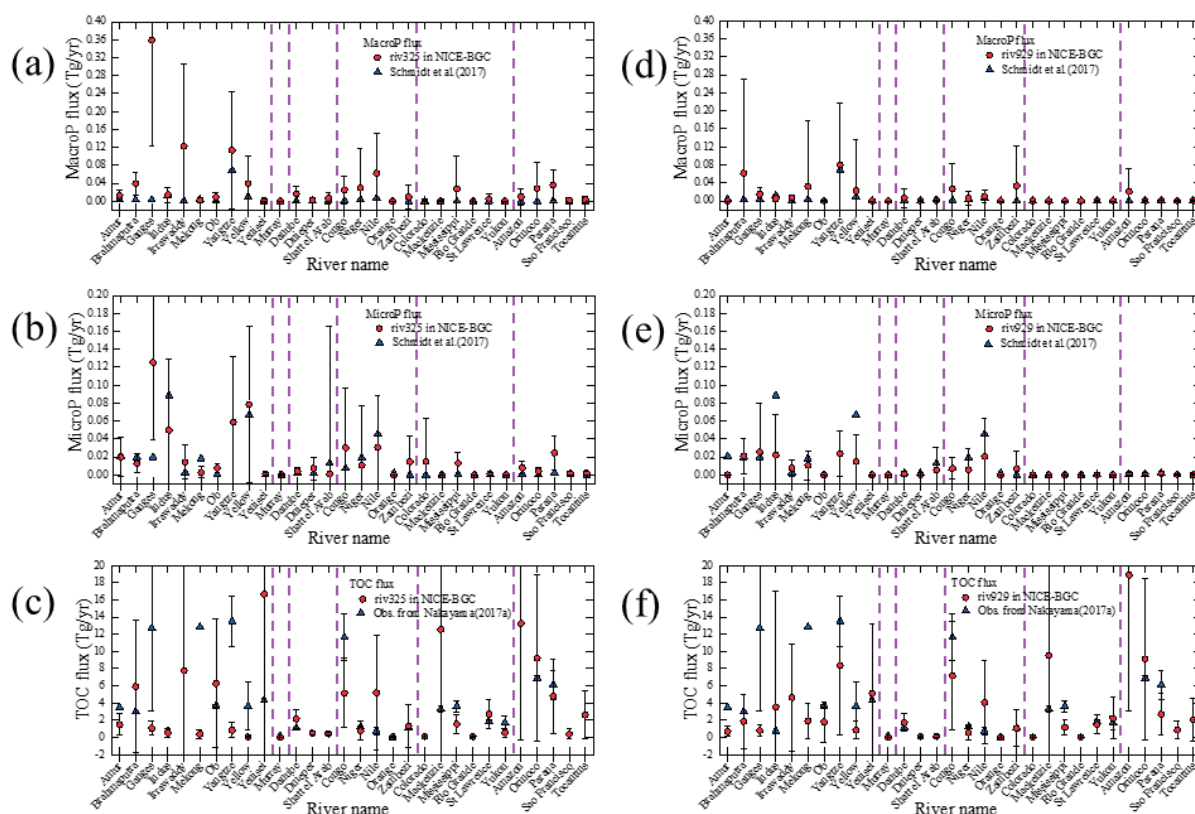
Figure 4.5 Comparison of carbon and plastic fluxes with different resolutions in global major rivers. (a)-(c) Macroplastic, microplastic, and TOC fluxes in 325 river channels (at 1° × 1° resolution), and (d)-(f) macroplastic, microplastic, and TOC fluxes in 929 river channels (at 0.5° × 0.5° resolution). The error bar with the solid line shows the standard deviation of simulated values, and the purple dashed line shows the boundaries of each continent (Asia, Oceania, Europe, Africa, North America, and South America).
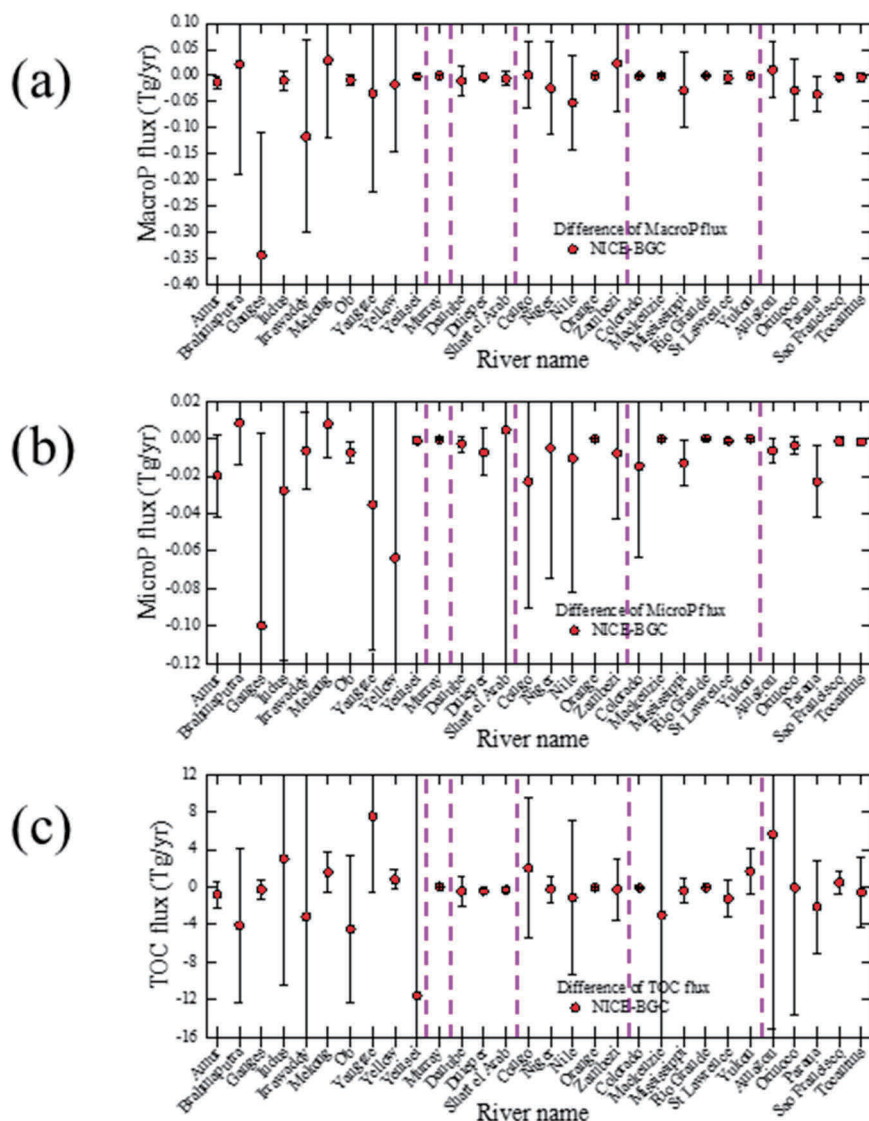
Figure 4.6 Calculated differences in the model results of carbon and plastic fluxes at two different resolutions in the global major rivers. (a) Macroplastic, (b) microplastic, and (c) TOC fluxes. The error bar with the solid line shows the standard deviation of simulated values, and the purple dashed line shows the boundaries of each continent (Asia, Oceania, Europe, Africa, North America, and South America).

Fig. 4.7 shows the horizontal microplastic transport in global major rivers (0.693±0.227 Tg/yr) (Nakayama and Osako, 2023b) and proportions of pristine, heteroaggregated, biofouled, and biofouled & heteroaggregated microplastics in horizontal microplastic transport. The results show that the microplastic concentration decreased owing to these interaction processes (Fig. 4.7a). The results also show that microplastic might quickly aggregate with SPM to form heteroaggregates in rivers with large amounts of microplastics, which is similar to accounting for 60.5–73.6 % of microplastic in the generic river system (Domercq et al., 2022) (Fig. 4.7b). Although microplastics remain the same as pristine microplastics in rivers with small amounts of microplastics, the dominance of heteroaggregates is related to the higher concentrations of both suspended particles (Fig. 4.7c) and TOC (Fig. 4.7d) (Liu et al., 2021). In contrast, the proportion of biofouled microplastic was slightly larger in some rivers with slower flow and

longer residence times (Amur, Yellow, Volta, and Colorado Rivers). This result implies that plastics are affected in a complicated manner by biogeochemical cycles in inland waters.
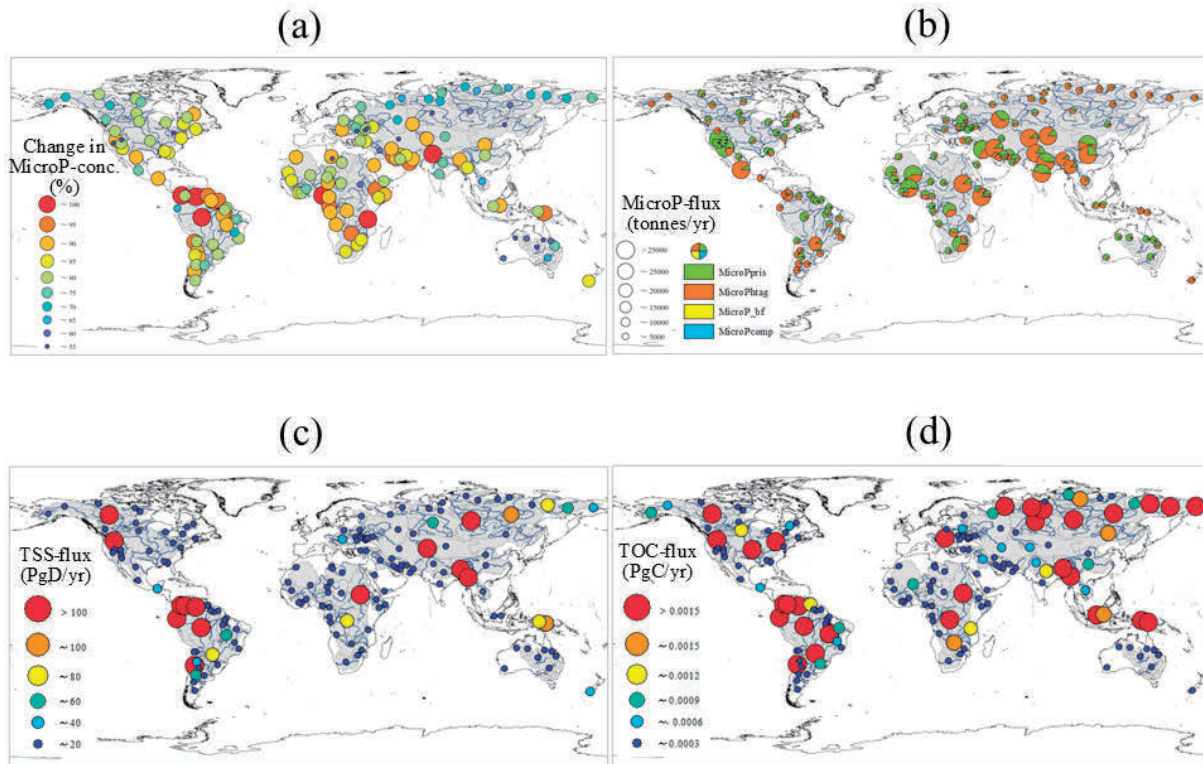
Figure 4.7 Impact of biofouling and heteroaggregation on microplastic dynamics in global major rivers simulated at 1° × 1° resolution. (a) Change in microplastic concentration by these interaction processes, (b) horizontal microplastic transport, (c) TSS (total suspended solid) flux, and (d) TOC flux. The continents shaded in grey show the major river basins (153 basins, 325 river channels) considered in this study. In panel a, the value was obtained by calculating the ratio of the microplastic concentration without interaction processes to that with interaction processes in the water. In panel b, the circle size means the magnitude of fluxes, and each pie chart shows the proportions of pristine, heteroaggregated, biofouled, and biofouled & heteroaggregated microplastics.

4.4.3 Variations of Different Speciation States of Micro-Plastic by Interaction Processes

Fig. 4.8 shows the relationship between the carbon cycle and biofouling in the Yangtze River. Phytoplankton, detritus, and algae are the key components of the carbon cycle in inland waters. The results showed that the biofouling rate had daily and seasonal variations that were greatly affected by the attached algal growth (Fig. 4.8b). The biofouling rate has a much larger value in early summer than the constant value, which is 1/30 (/day), assumed as the biofilm coverage rate to grow in equation (4.9). The rate also has a diurnal cycle that increases during the day owing to photosynthesis and decreases to a negative value at night owing to respiration (Kooi et al., 2017). As a result, P_{biof} and P_{comp} exhibited a sharp spike during the day and

fluctuated more or less at night when considering the dynamic rate of biofouling (Fig. 4.8d). The simulation also shows that the concentration of heteroaggregated plastic became much higher when the concentration of suspended solids was higher (the order of the vertical axis of P_{het} was larger than that of the other three items in Fig. 4.8c and 4.8d). Although the proportion of biofouled microplastics was much smaller than that of heteroaggregated microplastics, the results showed that algal growth affects the fluctuations in the different speciation states of microplastics in some rivers, particularly in lakes and slower rivers with longer residence times.
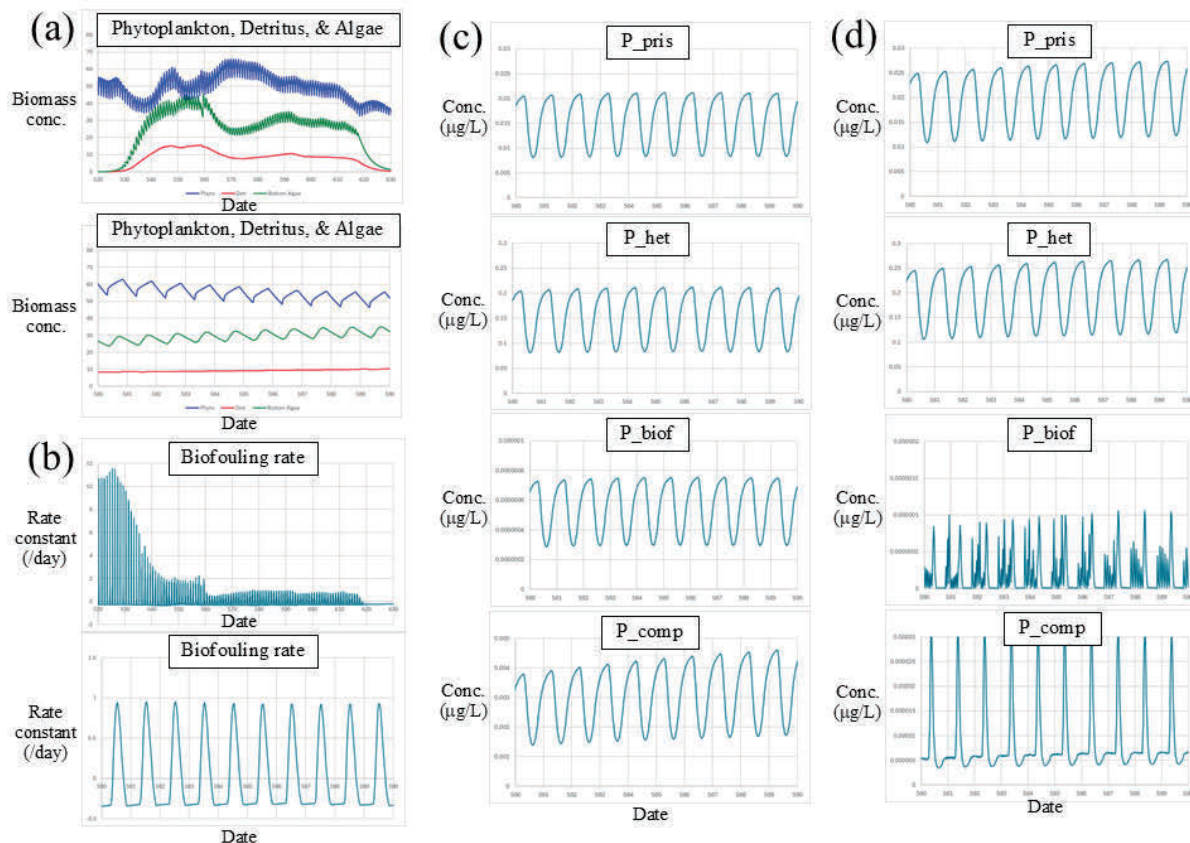
Figure 4.8 Relation between the carbon cycle and biofouling in the Yangtze River. (a) Biomass concentrations of phytoplankton, detritus, and algae, (b) biofouling rate calculated by attached algae, (c) microplastic concentration of different speciation states simulated at a constant rate equal to 1/30 (/day), and (d) microplastic concentration of different speciation states simulated at a dynamic rate, respectively. The date equal to 0 in the horizontal axis means January 1, 2014. In panels a and b, the top figure shows the values during the dates between 520 and 630, and the bottom figure shows an enlarged view during the dates between 580 and 590.

The model also simulated the change in microplastic concentration of different diameters (10 μm, 100 μm, and 1000 μm equal to 1 mm) in the water and riverbed sediment (density equals to 1000.1 kg/m³) during the rising limb, falling limb, and normal flow in the Yangtze River (Fig. 4.9). The results show that the average plastic concentration in the water decreased and that in the riverbed increased as the particle size of the plastic increased (Fig. 4.9a-b). In particular, the plastic concentration in the water decreased substantially during the rising limb, whereas that in the riverbed increased markedly during the falling limb. This tendency is

qualitatively consistent with previous results that floods completely disturb this equilibrium, coarser plastics become resuspended in the water, finer plastics are deposited within the water, and coarser plastics are distributed along the riverbed under normal flow (Drummond et al., 2022; Nakayama, 2025). In addition, the model could simulate changes in the different speciation states of microplastics in the water and riverbed sediment, which showed that the ratios were similar between water and riverbed sediment (Fig. 4.9c-d). Heteroaggregated plastics accounted for a large proportion, particularly during the rising limb, whereas pristine and biofouled & heteroaggregated plastics accounted for a slightly larger proportion depending on the particle size and runoff conditions. This result indicates that different speciation states of microplastics exhibit seasonal variations, the impact of flood events on plastic mobilization is dominated by trapping, retention, and resuspension during storm events, and a relatively larger fraction of plastic litter retained in the bottom sediment is efficiently flushed from riverbeds during flooding (Nizzetto et al., 2016; Hurley et al., 2018; van Emmerik et al., 2019; Roebroek et al., 2021).
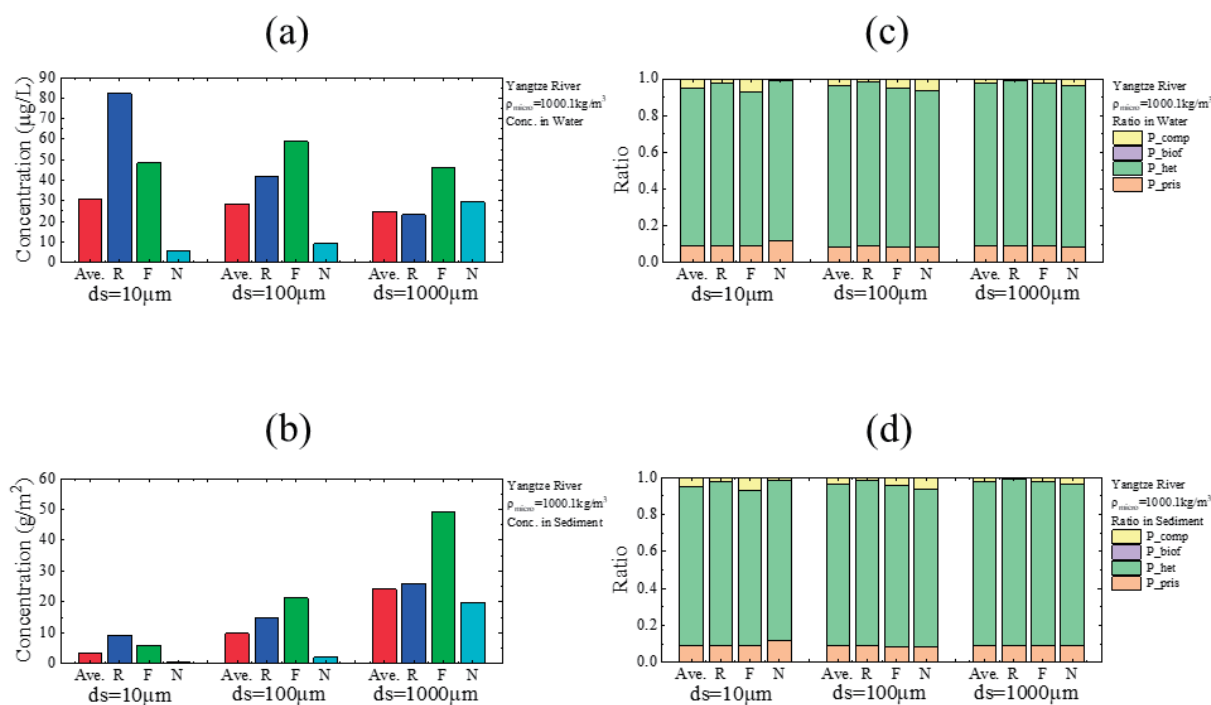
Figure 4.9 Change of microplastic concentration of different diameters (10 µm, 100 µm, and 1000 µm equals 1 mm) in the water and riverbed sediment (density equals 1000.1 kg/m³) during the rising limb (R), falling limb (F), normal flow (N), and averaged values (Ave.) in the Yangtze River. (a) Microplastic concentration in the water, (b) microplastic concentration in the riverbed sediment, (c) different speciation states of microplastic in the water, and (d) different speciation states of microplastic in the riverbed sediment.

4.4.4 Global Plastic Budget Affected by Biofouling and Heteroaggregation

The simulated results show the distribution of various deposits and total plastic transport to the ocean (Fig. 4.10). Asia and Africa account for a large proportion of plastic deposition on a global scale. In particular, the results show that the interaction processes of heteroaggregation, breakup, and biofouling heterogeneously affect the plastic cycle on a global scale (Fig. 4.10f). The total amount of microplastic deposition by the interaction process is estimated at 0.118±0.077 Tg/yr, which is not negligible compared to other deposits (Fig. 4.10b-e). This also greatly decreases the net horizontal transport to the ocean (Fig. 4.10 g). Furthermore, the results show that the amount of plastic storage in reservoirs and estuaries was 0.386±0.103 Tg/yr and 0.218±0.053 Tg/yr, which affects plastic transport to the ocean as well as to lakes and riverbeds (0.110±0.079 Tg/yr and 0.035±0.011 Tg/yr, respectively) (Nakayama, 2024a, 2024b, 2025). Moreover, macroplastics are more susceptible to this effect than microplastics because the inflow of the former is greater than that of the latter, despite their specific gravity and shape.
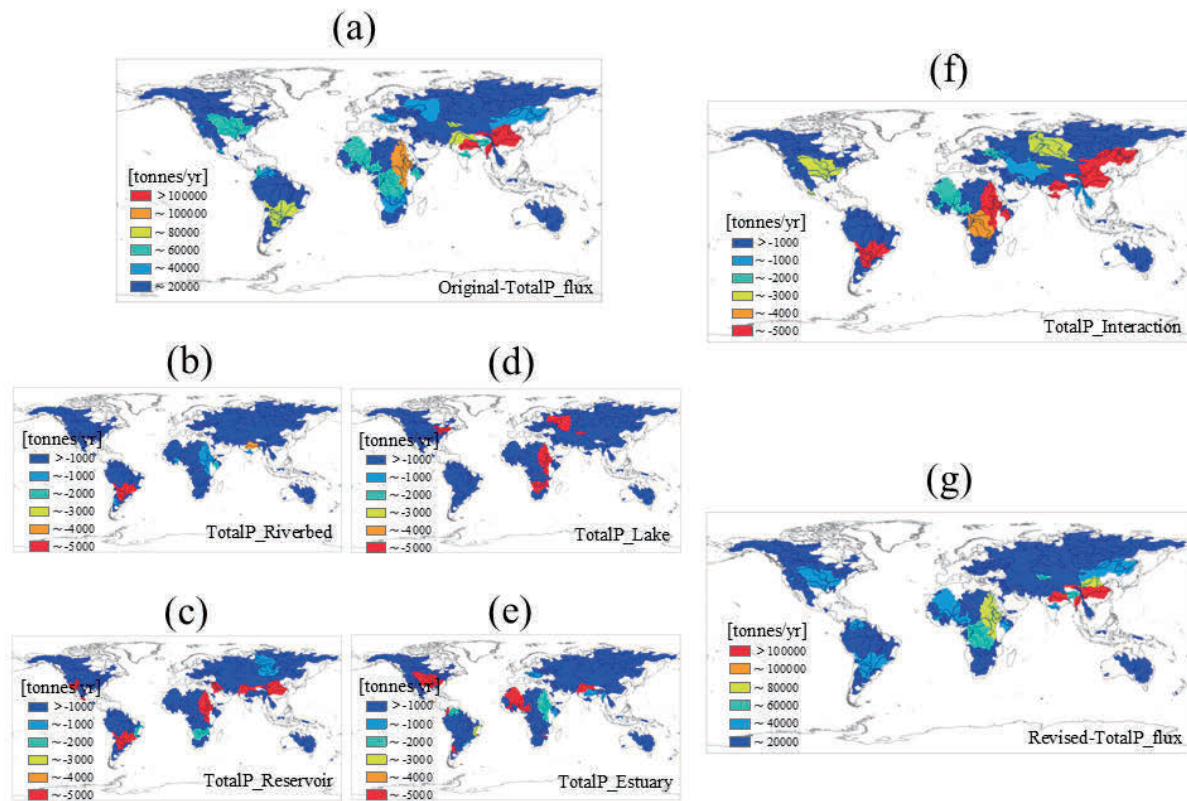
Figure 4.10 Spatial distribution of total plastic transport and deposition in major rivers worldwide. (a) Horizontal transport to the ocean without deposition, (b) riverbed storage, (c) reservoir storage, (d) lake storage, (e) estuarine storage, (f) interaction processes of biofouling and heteroaggregation, and (g) net horizontal transport to the ocean.

Table 4.2 shows the weighted average plastic budget for global major rivers. The simulated result indicates that it is difficult to ignore the sinking of heteroaggregated and biofouled plastics (0.118±0.077 Tg/yr) to riverbeds, reservoirs, and lake beds, and estuarine storage

(Nakayama, 2024a, 2024b, 2025). Moreover, the amount of deposited plastics simulated by the model in this case (0.867 Tg/yr) was smaller than that in the previous case (3.1 Tg/yr) (OECD, 2022). Although the sinking of heteroaggregated and biofouled plastics at the lower limits was not very large, it should be noted that this amount of sedimentation was negligible depending on the river (Fig. 4.7). This result implies that the input flux of microplastics from rivers to the ocean might be reduced if freshwater sediments could retain more microplastics (Nizzetto et al., 2016) (Fig. 4.7). The riverine plastic transport to the ocean revised in the present study is 0.882±0.404 Tg/yr, with macroplastic flux at 0.657±0.309 Tg/yr and microplastic flux at 0.225±0.261 Tg/yr, which are within the range of previous values, i.e. 0.41–4.0 Tg/yr (Meijer et al., 2021).

Table 4.2 Weighted average of the plastic budget in global major rivers (153 basins/watersheds, 325 river channels), including 130 tidal estuaries. The range is also added for each averaged value. The error in simulated value means the standard deviation for the major rivers worldwide; + and - indicate increases and decreases of fluxes (horizontal transport and vertical flux from water to bottom sediment) from the averaged values, respectively. Storage by interaction processes of heteroaggregated and biofouled plastics is newly estimated in the present study.

River	Macro P flux (Tg/yr)	Micro P flux (Tg/yr)	Total P flux (Tg/yr)
Riverine Transport to Ocean *	1.056±0.294	0.693±0.227	1.749±0.371
Reservoir Storage **	0.206±0.065	0.180±0.080	0.386±0.103
Lake Storage **	0.035±0.049	0.075±0.061	0.110±0.079
Estuarine Storage ***	0.135±0.048	0.083±0.022	0.218±0.053
Riverbed Storage ****	0.022±0.010	0.013±0.004	0.035±0.011
Storage by Interaction Processes	-	0.118±0.077	0.118±0.077
Net Transport to Ocean	0.657±0.309	0.225±0.261	0.882±0.404
* Nakayama & Osako (2023b)			
** Nakayama (2024a)			
*** Nakayama (2024b)			
**** Nakayama (2025)			

4.5 Conclusion

In this chapter, the NICE-BGC process-based model was newly extended to incorporate the effect of the interaction processes of heteroaggregation and biofouling on plastic dynamics on a global scale. The model results show how different grid resolutions change the hydrologic and carbon cycle in major global rivers. The results showed that the effects of spatial resolution and mutual interaction should be explicitly included in the global carbon and plastic cycle model to minimize the range of uncertainty. The new model can also simulate different speciation states of microplastics (pristine, heteroaggregated, biofouled, and biofouled & heteroaggregated) to indicate the impact of heteroaggregation and biofouling on plastic dynamics in inland water. The model also estimated the attached algal growth as a function of the encounter kernel rate in the extension of the rate constant for biofouling in the previous studies. The results showed that microplastics may quickly aggregate with suspended particulate matter to form heteroaggregates in rivers with large amounts of microplastics, with

this dominance of heteroaggregates related to the higher concentrations of both suspended particles and TOC. Moreover, algal growth affects the diurnal and seasonal fluctuations of different speciation states of microplastics in some rivers, and the proportion of biofouled plastics increases in waters where the flow is slower and the retention time is longer. Finally, the plastic budgets of global major rivers were estimated by including the storage in reservoirs, lakes, riverbeds, estuaries, and interaction processes. This improvement in the present study helps to ensure that the questions addressed by the model are meaningful, tangible, and specific, and reveals the importance of identifying key decision points within the system from a holistic perspective towards enhancing and scaling up the practice of accurate modelling. The present study represents an important step not only for qualifying the various processes but also for identifying the driver hierarchy in a range of river catchments.

References

Alder, J. (2003) Putting the coast in the "Sea Around Us". The Sea Around Us Newsletter, 15, 1–2. http://data.unep-wcmc.org/datasets/23

Aufdenkampe, A.K., Mayorga, E., Raymond, P.A., Melack, J.M., Doney, S.C., Alin, S.R., Aalto, R.E., Yoo, K. (2011) Riverine coupling of biogeochemical cycles between land, oceans, and atmosphere. Frontiers in Ecology and the Environment, 9(1), 53–60. doi:10.1890/100014

Balmer, M.B., Downing, J.A. (2011) Carbon dioxide concentrations in eutrophic lakes: undersaturation implies atmospheric uptake. Inland Waters, 1, 125–132. doi:10.5268/IW-1.2.366

Battin, T.J., Luyssaert, S., Kaplan, L.A., Aufdenkampe, A.K., Richter, A., Tranvik, L.J. (2009) The boundless carbon cycle. Nature Geoscience, 2, 598–600

Chang, S., Zhou, A., Hua, Z., Meng, H., Zhu, H., Li, S., He, H. (2024) Microplastics alter soil carbon cycling: Effects on carbon storage, CO_2 and CH_4 emission and microbial community. Cambridge Prisms: Plastics, 2, e5, 1–12. doi:10.1017/plc.2024.5

Climatic Research Unit (CRU). (2017) CRU TS3.24 of High Resolution Gridded Data of Month-by-month Variation in Climate. http://catalogue.ceda.ac.uk/

Cohen, J.H., Internicola, A.M., Mason, R.A., et al. (2019) Observations and simulations for microplastic debris in a tide, wind, and freshwater-driven estuarine environment: the Delaware Bay. Environmental Science & Technology, 53, 14204–14211. doi:10.1021/acs.est.9b04814

Cole, J.J., Prairie, Y.T., Caraco, N.F., McDowell, W.H., Tranvik, L.J., Striegl, R.G., Duarte, C.M., Kortelainen, P., Downing, J.A., Middelburg, J.J., Melack, J. (2007) Plumbing the global carbon cycle: integrating inland waters into the terrestrial carbon budget. Ecosystems, 10, 171–184. doi:10.1007/s10021-006-9013-8

D'Avignon, G., Gregory-Eaves, I., Ricciardi, A. (2022) Microplastics in lakes and rivers: an issue of emerging significance to limnology. Environmental Review, 30, 228–244, doi:10.1139/er-2021-0048

Domercq, P., Praetorius, A., MacLeod, M. (2022) The Full Multi: An open-source framework for modelling the transport and fate of nano- and microplastics in aquatic systems. Environmental Modelling and Software, 148, 105291. doi:10.1016/j.envsoft.2021.105291

Drake, T.W., Raymond, P.A., Spencer, R.G.M. (2018) Terrestrial carbon inputs to inland waters: A current synthesis of estimates and uncertainty. Limnology and Oceanography Letters, 3, 132–142. doi:10.1002/lol2.10055

Drummond, J.D., Aquino, T., Davies-Colley, R.J., Krause, S. (2022) Modeling contaminant microbes in rivers during both baseflow and stormflow. Geophysical Research Letters, 49, e2021GL096514. doi:10.1029/2021GL096514

Dürr, H.H., Laruelle, G.G., van Kempen, C.M., et al. (2011) Worldwide typology of nearshore coastal systems: Defining the estuarine filter of river inputs to the oceans. Estuaries and Coasts, 34(3), 441–458, doi:10.1007/s12237-011-9381-y

Elagami, H., Ahmadi, P., Fleckenstein, J.H., et al. (2022) Measurement of microplastic settling velocities and implications for residence times in thermally stratified lakes. Limnology and Oceanography, 67, 934–945, doi:10.1002/lno.12046

Elser, J.J., Bracken, M.E.S., Cleland, E.E., et al. (2007) Global analysis of nitrogen and phosphorus limitation of primary producers in freshwater, marine and terrestrial ecosystems. Ecology Letters, 10, 1135–1142. doi:10.1111/j.1461-0248.2007.01113.x

ESRI. (2019) Overlay Layers. Portal for ArcGIS. https://gislab.depaul.edu/portal/portalhelp/en/portal/latest/use/geoanalytics-overlay-layers.htm

European Centre for Medium-Range Weather Forecasts (ECMWF). (2019) ERA-Interium. https://www.ecmwf.int/en/forecasts/datasets/reanalysis-datasets/era-interim/

European Commission. (2012) Harmonized World Soil Database. http://eusoils.jrc.ec.europa.eu/ESDB_Archive/soil_data/global.htm

European Commission. (2015) Global Land Cover 2000. https://forobs.jrc.ec.europa.eu/products/glc2000/glc2000.php

Food and Agriculture Organization of the United Nations (FAO). (2016) Global Map of Irrigation Areas (GMIA). http://www.fao.org/nr/water/aquastat/irrigationmap/index.stm

Gao, B., Chen, Y., Xu, D., et al. (2023) Substantial burial of terrestrial microplastics in the Three Gorges Reservoir, China. Communications Earth & Environment, 4, 32, doi:10.1038/s43247-023-00701-z

Green, M.B., Finlay, J.C. (2010) Patterns of hydrologic control over stream water total nitrogen to total phosphorus ratios. Biogeochemistry, 99, 15–30. doi:10.1007/s10533-009-9394-9

Guo, Z., Boeing, W., Xu, Y., et al. (2021) Global meta-analysis of microplastic contamination in reservoirs with a novel framework. Water Research, 207, 117828. doi:10.1016/j.watres.2021.117828

Guo, M., Noori, R., Abolfathi, S. (2024) Microplastics in freshwater systems: Dynamic behaviour and transport processes. Resources, Conservation & Recycling, 205, 107578. doi:10.1016/j.resconrec.2024.107578

Hartmann, J., Moosdorf, N. (2012) The new global lithological map database GLiM: A representation of rock properties at the Earth surface. Geochemistry, Geophysics, Geosystems, 13, Q12004, doi:10.1029/2012GC004370

He, B., Smith, M., Egodawatta, P., et al. (2021) Dispersal and transport of microplastics in river sediments. Environmental Pollution, 279, 116884. doi:10.1016/j.envpol.2021.116884

Heathcote, A.J., Downing, J.A. (2012) Impacts of eutrophication on carbon burial in freshwater lakes in an intensively agricultural landscape. Ecosystems, 15, 60–70. doi:10.1007/s10021-011-9488-9

Hurley, E., Woodward, J., Rothwell, J.J. (2018) Microplastic contamination of river beds significantly reduced by catchment-wide flooding. Nature Geoscience, 11, 251–257, doi:10.1038/s41561-018-0080-1

Jakeman, A.J., Elsawah, S., Wang, H.-H., et al. (2024) Towards normalizing good practice across the whole modelling cycle: Its instrumentation and future research topics. Socio-Environmental Systems Modelling, 6, 18755. doi:10.18174/sesmo.18755

Jambeck, J.R., Geyer, R., Wilcox, C., et al. (2015) Plastic waste inputs from land into the ocean. Science, 347, 768–771, doi:10.1126/science.1260352

Jones, E.R., van Vliet, M.T.H., Qadir, M., Bierkens, M.F.P. (2021) Country-level and gridded estimates of wastewater production, collection, treatment and reuse. Earth System Science Data, 13, 237–254, doi:10.5194/essd-13-237-2021

Kaiser, D., Kowalski, N., Waniek, J.J. (2017) Effects of biofouling on the sinking behavior of microplastics. Environmental Research Letters, 12, 124003. doi:10.1088/1748-9326/aa8e8b

Kaandorp, M.L.A., Lobelle, D., Kehl, C., et al. (2023) Global mass of buoyant marine plastics dominated by large long-lived debris. Nature Geoscience, 16, 189–694. doi:10.1038/s41561-023-01216-0

Kooi, M., van Nes, E.H., Scheffer, M., Koelmans, A.A. (2017) Ups and downs in the ocean: Effects of biofouling on vertical transport of microplastics. Environmental Science & Technology, 51, 7963–7971, doi:10.1021/acs.est.6b04702

Kooi, M., Besseling, E., Kroeze, C., et al. (2018) Modelling the fate and transport of plastic decries in freshwaters: review and guidance. In: Wagner, M., Lambert, S. [Eds] Freshwater Microplastics. The Handbook of Environmental Chemistry 58, Springer, pp.125–152

Kooi, M., Koelmans, A.A. (2019) Simplifying microplastic via continuous probability distributions for size, shape, and density. Environmental Science & Technology Letters, 6, 551–557, doi:10.1021/acs.est.9b00379

Koutnik, V.S., Leonard, J., Alkidim, S., et al. (2021) Distribution of microplastics in soil and freshwater environments: global analysis and framework for transport modelling. Environmental Pollution, 224, 116552, doi:10.1016/j.envpol.2021.116552

Laruelle, G. G., Dürr, H. H., Lauerwald, R., Hartmann, J., Slomp, C. P., Goossens, N., & Regnier, P. A. G. (2013) Global multi-scale segmentation of continental and coastal waters from the watersheds to the continental margins. Hydrology and Earth System Sciences, 17, 2029–2051, doi:10.5194/hess-17-2029-2013

Leach, J.A., Larsson, A., Wallin, M.B., et al. (2016) Twelve year interannual and seasonal variability of stream carbon export from a boreal peatland catchment. Journal of Geophysical Research: Biogeosciences, 121, 1851–1866. doi:10.1002/2016JG003357

Lebreton, L, van der Zwet, J., Damsteeg, J.-W., et al. (2017) River plastic emissions to the world's oceans. Nature Communications, 8, 15611, doi:10.1038/ncomms15611

Lebreton, L., Andrady, A. (2019) Future scenarios of global plastic waste generation and disposal. Palgrave Communications, 5, 6, doi:10.1057/s41599-018-0212-7

Lee, K., Tong, L.T., Millero, F.J., et al. (2006) Global relationships of total alkalinity with salinity and temperature in surface waters of the world's oceans. Geophysical Research Letters, 33, L19605. doi:10.1029/2006GL027207

Lehner, B., Döll, P. (2004) Development and validation of a global database of lakes, reservoirs and wetlands. Journal of Hydrology, 296, 1–22, doi:10.1016/j.jhydrol.2004.03.028

Lehner, B., Reidy Liermann, C., Revenga, C., et al. (2011) High-resolution mapping of the world's reservoirs and dams for sustainable river-flow management. Frontiers in Ecology and the Environment, 9, 494–502, doi:10.1890/100125

Leiser, R., Wu, G.-M., Neu T.R., Wendt-Potthoff, K. (2020) Biofouling, metal sorption and aggregation are related to sinking of microplastics in a stratified reservoir. Water Research, 176, 115748, doi:10.1016/j.watres.2020.115748

Li, Y., Tao, L., Wang, Q., et al. (2023) Potential health impact of microplastics: A review of environmental distribution, human exposure, and toxic effects. Environment & Health, 1, 249–257. doi:10.1021/envhealth.3c00052

Liu, Y., You, J., Li, Y., et al. (2021) Insights into the horizontal and vertical profiles of microplastics in a river emptying into the sea affected by intensive anthropogenic activities in Northern China. Science of the Total Environment, 779, 146589, doi:10.1016/j.scitotenv.2021.146589

Meijer, L.J.J., van Emmerik, T., van der Ent, R., et al. (2021) More than 1000 rivers account for 80% of global riverine plastic emissions into the ocean. Science Advances, 7, eaaz5803, doi:10.1126/sciadv.aaz5803

Mendrik, F., Fernandez, R., Hackney, C.R., et al. (2023) Non-buoyant microplastic settling velocity varies with biofilm growth and ambient water salinity. Communications Earth & Environment, 4, 30. doi:10.1038/s43247-023-00690-z

Mueller, N.D., Gerber, J.S., Johnston, M., et al. (2012) Closing yield gaps through nutrient and water management. Nature, 490, 254–257. doi:10.1038/nature11420

Nakayama, T. (2022) Impact of anthropogenic disturbances on carbon cycle changes in terrestrial-aquatic-estuarine continuum by using an advanced process-based model. Hydrological Processes, 36(2), e14471, doi:10.1002/hyp.14471

Nakayama, T., Osako, M. (2023a) Development of a process-based eco-hydrology model for evaluating the spatio-temporal dynamics of macro- and micro-plastics for the whole of Japan. Ecological Modelling, 476, 110243, doi:10.1016/j.ecolmodel.2022.110243

Nakayama, T., Osako, M. (2023b) The flux and fate of plastic in the world's major rivers: Modeling spatial and temporal variability. Global and Planetary Change, 221, 104037, doi:10.1016/j.gloplacha.2023.104037

Nakayama, T. (2024a) Impact of global major reservoirs and lakes on plastic dynamics by using a process-based eco-hydrology model. Lakes & Reservoirs: Science, Policy and Management for Sustainable Use, 29, e12463. doi:10.1111/lre.12463

Nakayama, T. (2024b) Evaluation of flux and fate of plastic in terrestrial-aquatic-estuarine continuum by using an advanced process-based model. Ecohydrology, 17(6), e2678. doi:10.1002/eco.2678

Nakayama, T. (2025) Impact of settling and resuspension on plastic dynamics during extreme flow and their seasonality in global major rivers. Hydrological Processes, 39(2), e70072. doi:10.1002/hyp.70072

NASA. (2013) GLDAS vegetation class. http://ldas.gsfc.nasa.gov/gldas/GLDASvegetation.php

NASA. (2018) Gridded Population of the World, Version 4 (GPWv4). https://sedac.ciesin.columbia.edu/data/set/gpw-v4-population-count-adjusted-to-2015-unwpp-country-totals-rev11

National Oceanic and Atmospheric Administration (NOAA). (2013) World Ocean Atlas 2013 ver.2. https://www.nodc.noaa.gov/OC5/woa13/

Nizzetto, L., Bussi, G., Futter, M.N., et al. (2016) A theoretical assessment of microplastic transport in river catchments and their retention by soils and river sediments. Environmental Science: Processes & Impacts, 18, 1050–1059, doi:10.1039/c6em00206d

Nyberg, B., Harris, P.T., Kane, I., Maes, T. (2023) Leaving a plastic legacy: Current and future scenarios for mismanaged plastic waste in rivers. Science of the Total Environment, 869, 161821. doi:10.1016/j.scitotenv.2023.161821

OECD. (2022) Global Plastics Outlook: Economic Drivers, Environmental Impacts and Policy Options, OECD Publishing, Paris. https://doi.org/10.1787/de747aef-en

Pacheco, F.S., Roland, F., Downing, J.A. (2013) Eutrophication reverses whole-lake carbon budgets. Inland Waters, 4, 41–48. doi:10.5268/IW-4.1.614

Portmann, F.T., Siebert, S., Döll, P. (2010) MIRCA2000 – Global monthly irrigated and rainfed crop areas around the year 2000: A new high-resolution data set for agricultural and hydrological modelling. Global Biogeochemical Cycles, 24, GB 1011, doi:10.1029/2008GB003435

Praetorius, A., Scheringer, M., Hungerbühler, K. (2012) Development of environmental fate models for engineered nanoparticles - A case study of TiO2 nanoparticles in the Rhine River. Environmental Science & Technology, 46, 6705–6713, doi:10.1021/es204530n

Raymond, P.A., Hartmann, J., Lauerwald, R., et al. (2013) Global carbon dioxide emissions from inland waters. Nature, 503, 355–359. doi:10.1038/nature12760

Regnier, P., Friedlingstein, P., Ciais, P., et al. (2013) Anthropogenic perturbation of the carbon fluxes from land to ocean. Nature Geoscience, 6, 597?607. doi:10.1038/ngeo1830

Reichstein, M., Bahn, M., Ciais, P., et al. (2013) Climate extremes and the carbon cycle. Nature, 500, 287–295. doi:10.1038/nature12350

Roebroek, C.T.J., Harrigan, S., van Emmerik, T.H.M., et al. (2021) Plastic in global rivers: are floods making it worse? Environmental Research Letters, 16, 025003. doi:10.1088/1748-9326/abd5df

Schmidt, C., Krauth, T., Wagner, S. (2017) Export of plastic debris by rivers into the sea. Environmental Science & Technology, 51, 12246–12253, doi:10.1021/acs.est.7b02368

Schreyers, L.D.M., van Emmerik, T.H.M., Bui, K., et al. (2024) River plastic transport affected by tidal dynamics. Hydrology and Earth System Sciences, 28, 589–610. doi:10.5194/egusphere-2022-1495

Shams, M., Alam, I., Chowdhury, I. (2020) Aggregation and stability of nanoscale plastics in aquatic environment. Water Research, 171, 115401. doi:10.1016/j.watres.2019.115401

Shen, J., Gu, X., Liu, R., et al. (2023) Damming has changed the migration process of microplastics and increased the pollution risk in the reservoirs in the Shaying River Basin. Journal of Hazardous Materials, 443, 130067, doi:10.1016/j.jhazmat.2022.130067

Siebert, S., Döll, P. (2010) Quantifying blue and green virtual water contents in global crop production as well as potential production losses without irrigation. Journal of Hydrology, 384, 198–217, doi:10.1016/j.jhydrol.2009.07.031

Siegfried, M., Koelmans, A.A., Besseling, E., Kroeze, C. (2017) Export of microplastics from land to sea. A modelling approach. Water Research, 127, 249–257, doi:10.1016/j.watres.2017.10.011

Strokal, M., Bai, Z., Franssen, W., et al. (2021) Urbanization: an increasing source of multiple pollutants to rivers in the 21st century. Urban Sustainability, 1, 24, doi:10.1038/s42949-021-00026-w

Su, X., Yang, L., Yang, K., et al. (2022) Estuarine plastisphere as an overlooked source of N2O production. Nature Communications, 13, 3884. doi:10.1038/s41467-022-31584-x

Thompson, R.C., Olsen, Y., Mitchell, R.P., et al. (2004) Lost at sea: Where is all the Plastic? Science, 304, 838, doi:10.1126/science.1094559

Tian, H., Yang, J., Lu, C., et al. (2018) The global N2O model intercomparison project. Bulletin of the American Meteorological Society, 99(6), 1231–1251, doi:10.1175/bams-d-17-0212.1

Tranvik, L.J., Downing, J.A., Cotner, J.B., et al. (2009) Lakes and reservoirs as regulators of carbon cycling and climate. Limnology and Oceanography, 54(6), 2298–2314

Turner, R.E., Rabalais, N.N., Justice, D., Dortch, Q. (2003) Global patterns of dissolved N, P and Si in large rivers. Biogeochemistry, 64, 297-317. doi:10.1023/A:1024960007569

U. S. Department of Agriculture (USDA), (2022) Global Reservoirs and Lakes Monitor (G-REALM). https://ipad.fas.usda.gov/cropexplorer/global_reservoir/

U.S. Geological Survey (USGS). (1996a) Global 30 Arc-Second Elevation (GTOPO30). USGS. https://doi.org/10.5066/F7DF6PQS

U.S. Geological Survey (USGS). (1996b) HYDRO1K. USGS. https://doi.org/10.5066/F77P8WN0

van Emmerik, T., Strady, E., Kieu-Le, T.-C., Nguyen, L., Gratiot, N. (2019) Seasonality of riverine macroplastic transport. Scientific Reports, 9, 13549, doi:10.1038/s41598-019-50096-1

van Wijnen, J., Ragas, A.M.J., Kroeze, C. (2019) Modelling global river export of microplastics to the marine environment: Sources and future trends. Science of the Total Environment, 673, 392–401, doi:10.1016/j.scitotenv.2019.04.078

Wang, T., Zhao, S., Zhu, L., et al. (2022) Accumulation, transformation and transport of microplastics in estuarine fronts. Nature Reviews Earth & Environment, 3(11), 795–805. doi:10.1038/s43017-022-00349-x

Wehrli, B. (2013) Conduits of the carbon cycle. Nature, 503, 346-347. doi:10.1038/503346a

Windsor, F.M., Durance, I., Horton, A.A., et al. (2019) A catchment-scale perspective of plastic pollution. Global Change Biology, 25, 1207–1221. doi:10.1111/gcb.14572

Xia, F., Liu, H., Zhang, J., Wang, D. (2022) Mitigation characteristics of microplastics based on source-sink investigation in a typical urban wetland. Water Research, 213, 118154. doi:10.1016/j.watres.2022.118154

Yuan, B., Gan, W., Sun, J. et al. (2023) Depth profiles of microplastics in sediments from inland water to coast and their influential factors. Science of the Total Environment, 903, 166151. doi:10.1016/j.scitotenv.2023.166151

Zhang, B., Tian, H., Lu, C., et al. (2017) Global manure nitrogen production and application in cropland during 1860–2014; a 5 arcmin gridded global dataset for Earth system modelling. Earth System Science Data, 9, 667–678, doi:10.5194/essd-9-667-2017

Chapter 5

Improvement in Understanding the Plastic Cycle in Japanese Urban Regions

Abstract

Plastic contamination has received considerable attention in recent decades. In the present study, the process-based National Integrated Catchment-based Eco-hydrology-BioGeochemical Cycle (NICE-BGC) eco-hydrology model was extended and combined with the plastic debris model and applied to all 109 first-class (class A) river basins throughout Japan. The combined model includes advection, dispersion, diffusion, settling, dissolution, and deterioration due to light and temperature, interactions with suspended matter (heteroaggregation), resuspension, and biofouling. These processes may facilitate evaluations of the effect of mismanaged plastic waste (MPW) and point sources (tires, personal care products, dust, and laundry) on the spatiotemporal dynamics of macro- and microplastics. The results showed that models with a finer spatial resolution promoted greater settlement during the runoff process and slightly decreased the flux of macroplastics, particularly in urban regions. The model also revealed that the amount of microplastic flux calculated by accumulating point information at sewage treatment plants could be replaced by analyzing grid data categorized for treatment methods (sewage, septic tank, and untreated) in each grid instead of global data on per capita emissions and treatment rates. The results also clarified that the plastic cycle, particularly micro-plastics, in rivers flowing through urban areas has been significantly altered. Finally, the method was evaluated to improve the plastic cycle in urban regions and understand the urban plastic cycle using less inventory data. These results help to quantify the impacts of plastic waste on the biosphere in urban systems and may aid in the development of solutions and measures to reduce plastic input to the ocean.

Keywords: Eco-hydrology model; flux; mismanaged plastic waste; sewage treatment; urban plastic cycle

5.1 Introduction

Plastic pollution is a main environmental problem, and such pollutants in streams, rivers, and oceans pose potential risks to human health and the environment (Siegfried et al., 2017). In particular, plastic accumulation on riverbanks, deltas, coastlines, and ocean surfaces is rapidly increasing, with 60% of all manufactured plastics estimated to have been discarded in landfills or the natural environment (Meijer et al., 2021). Previous studies on the origin and fate of plastic waste in freshwater systems have suggested that land-derived plastics are among the main sources of marine plastic pollution (Thompson et al., 2004) caused by either direct emissions from coastal areas (Jambeck et al., 2015) or transport via rivers (Lebreton et al., 2017; Schmidt et al., 2017). However, only a few studies have evaluated the concentrations and riverine fluxes of plastics on a regional scale, particularly in Japan (Kataoka et al., 2019; Nihei et al., 2020). Such an assessment of the fate and transport of plastics is necessary to realize the "Osaka Blue Ocean Vision" shared at the G20 Osaka Summit in 2019 (Ministry of Foreign Affairs of Japan, 2019).

Over the last decade, significant progress has been made in modelling the fate and transport of plastics (Praetorius et al., 2012; Quik et al., 2015; Nizzetto et al., 2016; Besseling et al., 2017; Siegfried et al., 2017; Kooi et al., 2018; van Wijnen et al., 2019; Whitehead et al., 2021). However, the fate of microplastics depends on their size, density, shape, and polymer type, which were not included in these previous global analyses of generic materials (Jambeck et al., 2015; Lebreton et al., 2017; Schmidt et al., 2017; Meijer et al., 2021). The accuracy of regional emissions estimated using a probabilistic approach (Meijer et al., 2021) should be improved by using a spatially explicit model (Unice et al., 2019). In contrast, transport of microplastics in river ecosystems is either driven by gravity (vertical transport) or settling (horizontal transport) (Kumar et al., 2021). The vertical profiles of low-density plastics, such as polyethylene (PE), polypropylene (PP), and polystyrene (PS), under the predominance of wind shear differ considerably from the original Rouse profile of natural sediments (Liu et al., 2021). Particle size generally appears to be a more sensitive parameter that influences microplastic transport and retention efficiency because of its wide range across several orders of magnitude, although an obvious sharp change in parameter sensitivity occurs when the density approaches that of water (Nizzetto et al., 2016). These factors must be considered when identifying hotspots and sinks of plastic pollution and resolving the source-flux-sink nexus within river basins (Windsor et al., 2019).

In this chapter, the process-based National Integrated Catchment-based Eco-hydrology-BioGeochemical Cycle (NICE-BGC) model was extended and combined with a plastic debris model for freshwater systems and applied to all 109 first-class (class A) river basins throughout Japan (Fig. 5.1a). This model includes advection, dispersion, diffusion, settling, dissolution, and deterioration due to light and temperature, interactions with suspended matter (heteroaggregation), resuspension, and biofouling (Nakayama and Osako, 2023a, 2023b, 2024; Nakayama, 2025). Based on this background, three basic issues were addressed: (i) How do different grid resolutions affect the macroplastic flux? (ii) How do different levels of data accumulation affect the microplastic flux? (iii) How can the plastics cycle be improved in urban areas? As the contribution to the runoff fluxes of urban regions to rivers is the largest, it is important to improve the accuracy of flux estimates in urban regions. To clarify these issues, NICE-BGC simulated how diffuse sources of mismanaged plastic waste (MPW) (Meijer et al., 2021) and point sources of tires, personal care products (PCPs), dust, and laundry (van Wijnen et al., 2019) throughout the country are transported from land to rivers and finally to the ocean. This research differs from previous studies based on its focus on increasing the spatial

resolution of models for macroplastics and developing a new method to reflect point source information on the grid for microplastics. These results help quantify the impacts of plastic waste on terrestrial and aquatic ecosystems and may be useful for devising solutions and measures to reduce plastic inputs to the ocean.
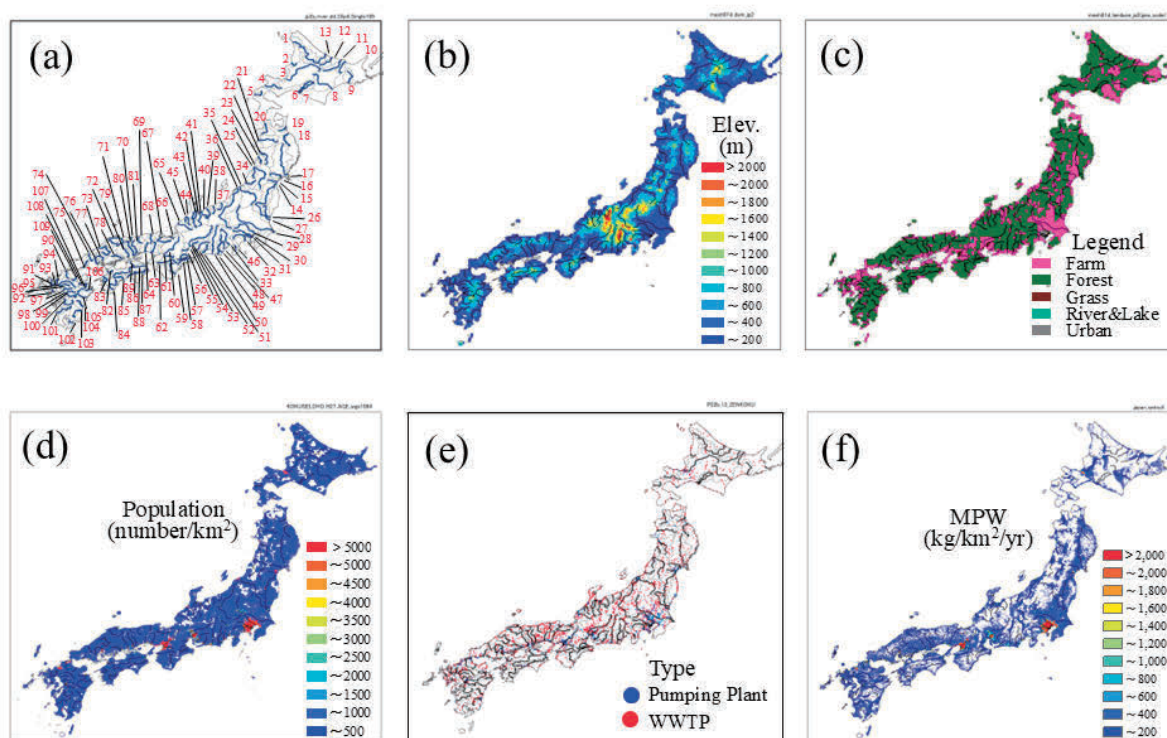
Figure 5.1 Location and characteristics of the study areas throughout Japan: (a) 109 first-class river basins, (b) elevation, (c) land cover, (d) population density, (e) pumping and wastewater treatment plant (WWTPs), and (f) mismanaged plastic waste (MPW), respectively. In the figure, only the main stream of each basin is shown. In panel a, numbers in red show river channel numbers of all 109 first-class river basins. In panels a and e, the grey line indicates the basin boundary of each river.

5.2 Methods

5.2.1 Simulating the Fate and Transport of Macro- and Microplastics in Urban Regions

The original National Integrated Catchment-based Eco-hydrology (NICE) coupled with various biogeochemical cycle models (NICE-BGC) consists of complex sub-compartments, such as the surface hydrology of hillslopes and stream flows, a land-surface model that includes urban and crop processes, a groundwater model, a regional atmospheric model, a sediment, nutrient, and carbon cycle model, and a vegetation succession model (Nakayama and Watanabe,

2004; Nakayama, 2017a, 2017b). In this study, NICE-BGC was extended to model the fate and transport of macro- and microplastics on land and in water. The transport of plastic on a hillslope assumes that the heterogeneous distribution of settled and deposited plastic on hillslopes is negligible in comparison to discharged plastic and that resuspension is zero on hillslopes (Waldschlager and Schüttrumpf, 2019). After simulating plastic transport on a hillslope, the authors used the estimated rate of conversion of macroplastics to microplastics (3%/yr) in the same way as van Wijnen et al. (2019), with an extension of the conversion rate employed by Jambeck et al. (2015). NICE-BGC simulated the transport of plastics in a river channel by extending QUAL2Kw (Pelletier et al., 2006). Macro- and microplastics are buried through settling, dissolution, and deterioration due to light and temperature, and are affected by advection, dispersion, and diffusion. The author assumed that deterioration due to light can be modelled as a first-order temperature-dependent decay and that the deterioration rate due to light is based on the Beer-Lambert law. The model includes advection, dispersion, diffusion, settling, dissolution, deterioration due to light and temperature, interactions with suspended matter (heteroaggregation) (Praetorius et al., 2012), resuspension (Waldschlager and Schüttrumpf, 2019), and biofouling (Kooi et al., 2017).

5.2.2 Model Input Data including Plastic Sources

The input data at various spatial resolutions were prepared and arranged to calculate spatially averaged 0.1° x 0.1° grids (approximately 9–11 km resolution) and 0.05° x 0.05° grids (approximately 4.5–5.5 km resolution) using the Spatial Analyst Tools in ArcGIS v10.8 to simulate the entirety of Japan (Fig. 5.1 and Table 5.1). Elevation, land cover, soil texture, vegetation type, river networks, lakes and wetlands, reservoirs and dams, geological structures, crop types, irrigation types, irrigation water use, fertilizer use, and manure use were categorized on the basis of the global and Japanese datasets. The optimal river width of 513 river channels was calculated by visually reading the width of each river channel from Google Earth images and calculating the average value from the downstream of each river channel up to 1/3 of the way upstream in the existing high-resolution flow direction dataset (Yamazaki, 2022) (Fig. 5.2). Sewage treatment areas were digitized and expanded to 109 basins through a comparison with scanned images of 17 basins and the use of a population density threshold greater than 1000 (number/km^2) (Fig. 5.3). For septic tanks and agricultural village drainage areas, calculations were made by setting a threshold for population density that would be closest to the statistical values for the treated population and coverage rate for the whole of Japan (greater than 200 number/km^2) (Ministry of Land, Infrastructure, Transport, and Tourism, 2021a). The coverage rate and population of sewage and septic tank treatments calculated using the above method were in relatively good agreement with statistical values from previous studies. To reasonably create grid data from point, polyline, and polygon data for different sources with different spatial resolutions, an overlay analysis was conducted using GIS tools (intersect, union, and identity) (ESRI, 2019).

Table 5.1 List of input datasets for the NICE and NICE-BGC simulations.

Data set	Original resolution	Year	Source and reference
Climatology	1.0 °	1998-2015	ERA-interim; ECMWF (2019)
Elevation	1.0 km	around 1996	GTOPO30; U.S. Geological Survey (1996)
Land cover	1.0 km	around 2000	GLC2000; European Commission (2015)
Soil texture	1.0 km	around 1970-2000	HWSD; European Commission (2012)
Vegetation type	0.25 °	around 2000	GLDAS Vegetation Class; NASA (2013)
River networks	line	around 2000	MLIT (2012)
River width	point	around 2000	J-FlwDir; Yamazaki (2022)
Lakes and wetlands	0.5 min	around 1990-2000	GLWD; Lehner and Döll (2004)
Geological structures	0.5 °	around 1970-2000	GLiM; Hartmann and Moosdorf (2012)
Crop type	5 min	around 2000	MIRCA2000; Portmann et al. (2010)
Irrigation type	5 min	2000-2008	GMIA; FAO (2016)
Irrigation water use	5 min	1998-2002	GCWM; Siebert and Döll (2010)
Basin boundary	50 m	around 2010	MLIT (2011)
Reservoirs and dams	point	2014	MLIT (2016)
Fertilizer use	5 min	around 2000	Earth Stat; Mueller et al. (2012)
Manure use	5 min	1998-2014	Zhang et al. (2017)
Population	250 m	2015	Japanese Government Statistics (2021)
Wastewater treatment plants	point	2010	MLIT (2013)
Mismanaged plastic waste	1.0 km	2015	Lebreton and Andrady (2019)
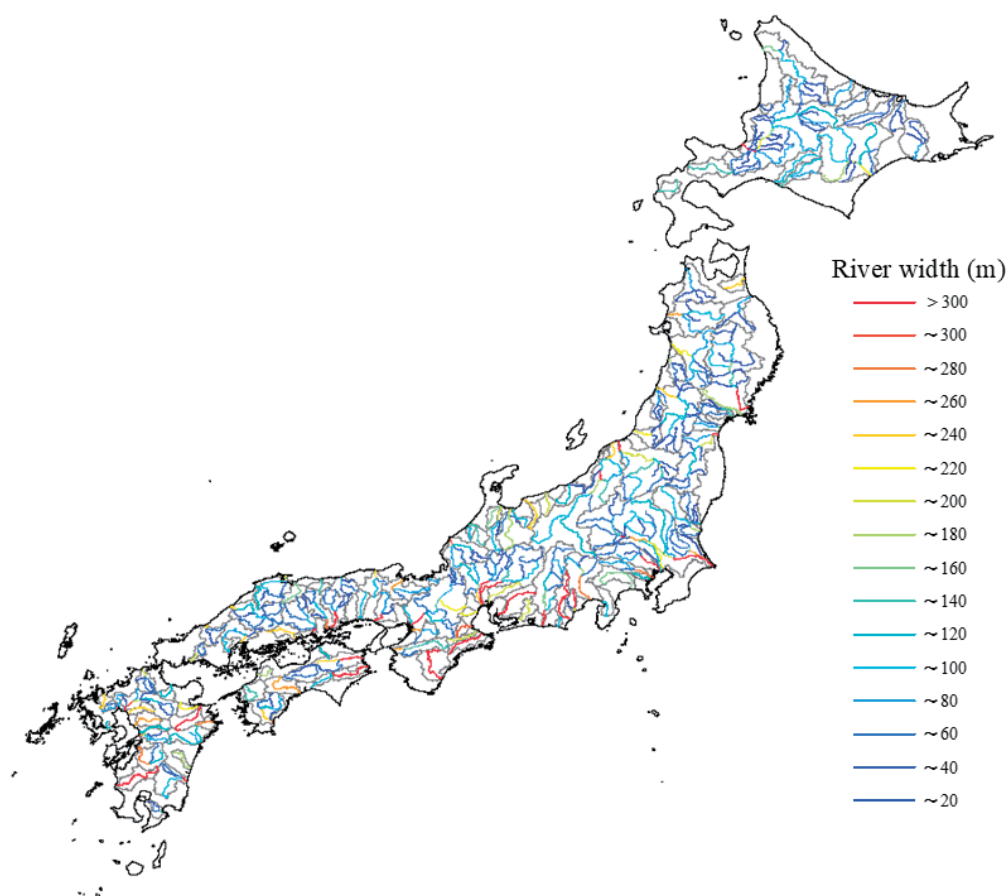
Figure 5.2 Optimal river width of 513 river channels estimated using datasets obtained from previous studies.
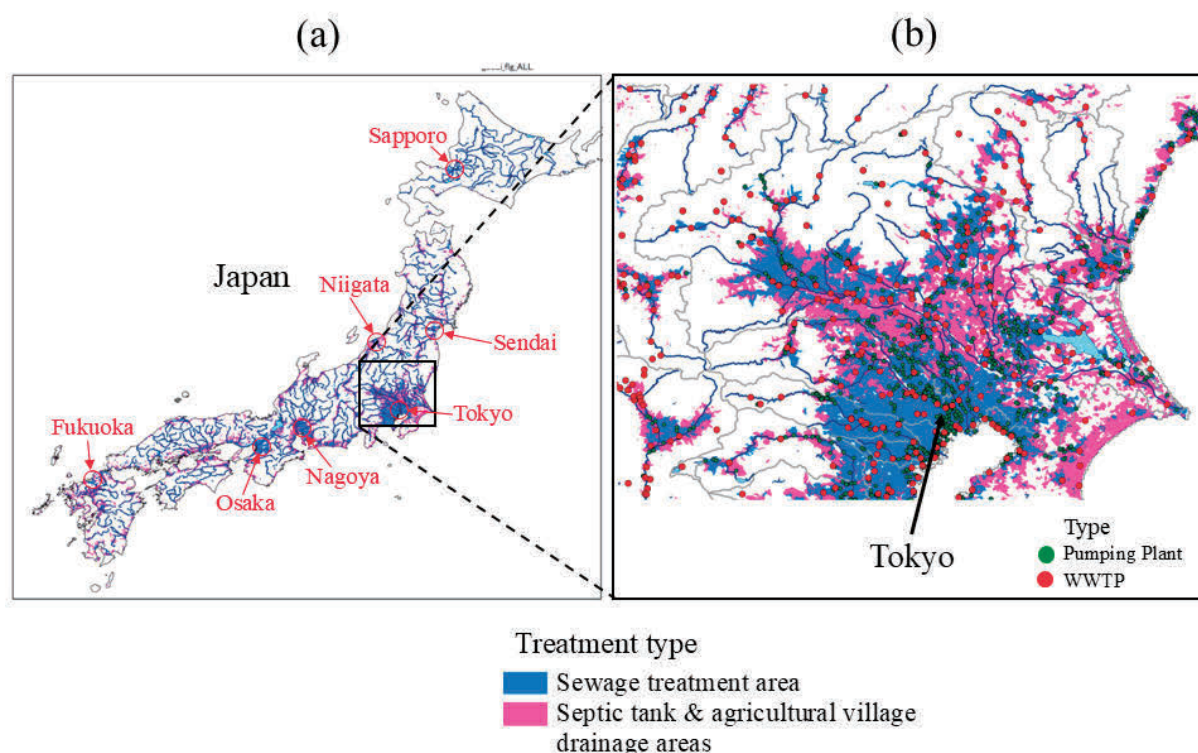
Figure 5.3 Spatial distribution of treatment type. Sewage treatment, septic tank, and agricultural village drainage areas (a) throughout Japan and (b) in the Kanto region, including the Tokyo Metropolitan area. Blue and pink polygons indicate the treatment areas of sewerage and septic tanks estimated by the present study. Black and grey lines mean the river channels and their basin boundaries. Red circles show major metropolitan areas in Japan.

For plastic data, the authors used previous data (Ministry of Land, Infrastructure, Transport and Tourism, 2013) for per capita emissions of microplastics into rivers (personal care products (PCPs), dust, laundry, and tires) and removal efficiency of wastewater treatment plant (WWTPs) (Siegfried et al., 2017) as a point source (Table 5.2). The model also simulated the outflow of macroplastics originating from MPW (Lebreton and Andrady, 2019) as a diffuse source (Fig. 5.1f). Table 5.2 summarizes the per capita emissions of macroplastics and microplastics into rivers, as determined in previous studies (Siegfried et al., 2017; van Wijnen et al., 2019; Boucher et al., 2020; Strokal et al., 2021). Generally, microplastics at point sources originate from PCPs, laundry fibers, car tire wear, and macroplastic fragmentation. The authors estimated the fluxes of microplastics by multiplying these per capita emissions and their population distribution for each catchment flowing into WWTPs (Table 5.1). The total flux throughout the entire country was determined based on the removal efficiency of microplastics in WWTPs (99%, 97%, and 95%) (higher removal efficiency was observed for almost all secondary and tertiary treatments in Japan) (Ministry of Land, Infrastructure, Transport and Tourism, 2021a) (Fig. 5.3) and the density of the plastic (1010.0, 1001.0, and 1000.5 kg/m^3) (lower-density plastics PE, PP, and PS are overwhelmingly present in Japanese rivers) in Japan

(Kataoka et al., 2019; Nihei et al., 2020) and other developed countries (Siegfried et al., 2017; van Wijnen et al., 2019; Strokal et al., 2021).

Table 5.2 Per capita emission of macroplastics and microplastics into rivers in previous materials.

Plastic sources	Quantitative estimate (kg/capita/year)	OECD Countries	Africa	Middle East & North Africa	East Asia & Pacific (incl. Japan)	Eastern & Central Asia	Latin America	South Asia	Reference
Personal care products (PCPs)	0.0071								Siegfried et al.(2017)
Household dust (HD)	0.08								
Laundry inputs or fibres (LD)	0.12								
Tyre wear (TRWP)	0.18								
Personal care products (PCPs)	0.0071								Strokal et al.(2021)
Household dust (HD)	0.08								
Laundry inputs or fibres (LD)	0.12								
Tyre wear (TRWP); HDI<0.785	0.018								
Tyre wear (TRWP); HDI>0.785	0.18								
Macroplastics (non-point sources)	17.3	8.8	27	16	23	15	23	8.5	van Wijnen et al.(2019)
Personal care products (PCPs)	0.0028	0.0055	0.0007	0.0007	0.0049	0.0049	0.0025	0.0007	
Laundry inputs or fibres (LD)	0.0451	0.11	0.007	0.047	0.041	0.047	0.028	0.036	
Tyre wear (TRWP)	0.0662	0.18	0.0072	0.068	0.018	0.077	0.041	0.072	
Personal care products (PCPs)	0.005								Boucher et al.(2020)
Laundry inputs or fibres (LD)	0.015								
Tyres (car)	0.43								
Tyres (truck)	0.43								
Tyres (plane)	0.01								
Plastic production (pellet loss)	0.005								

5.2.3 Running the Simulation and Verification

The simulation area for all 109 first-class river basins throughout Japan was 26.0° wide (longitude) by 22.0° long (latitude) (Fig. 5.1). The NICE simulation of hillslope runoff was performed at 0.1° × 0.1° and 0.05° × 0.05° resolutions in vertical 20 layers with a time step of $\Delta t = 1$ h during 2014–2015 after a 6-month warm-up period until time-varying equilibrium was reached. Then, the simulation for aquatic ecosystems was conducted by inputting the simulated results for land to a stream network model with a time step of $\Delta t = 0.70$ min to ensure the stability of the model. The results yielded quantitative measures of model performance in terms of reproducing the seasonality and interannual variability in nutrient, carbon, and plastic fluxes (Ministry of Land, Infrastructure, Transport, and Tourism, 2021b; Nakayama, 2020, 2022, 2025; Nakayama and Osako, 2023a, 2024).

5.3 Results and Discussion

5.3.1 Comparison of the Macroplastic Cycle as a Diffuse Source between Different Grid Resolutions

The author evaluated the hydrological cycles of first-class river basins in Japan. Fig. 5.4 shows a comparison of the annually averaged water flux from terrestrial to aquatic ecosystems simulated by NICE-BGC with different grid resolutions. Although the amount of runoff in the same basin was the same, the heterogeneous distribution of the water flow became clear when the resolution of the model was increased (0.05° × 0.05°) (Fig. 5.4d-f). In particular, the spatial distribution of the flow in the mountainous areas in the central part of the archipelago (Fig. 5.1b) became clearer with the finer mesh (0.05° × 0.05°), and areas of high flow that were not visible with a coarse mesh (0.1° × 0.1°) became visible in the plains of the river mouth.
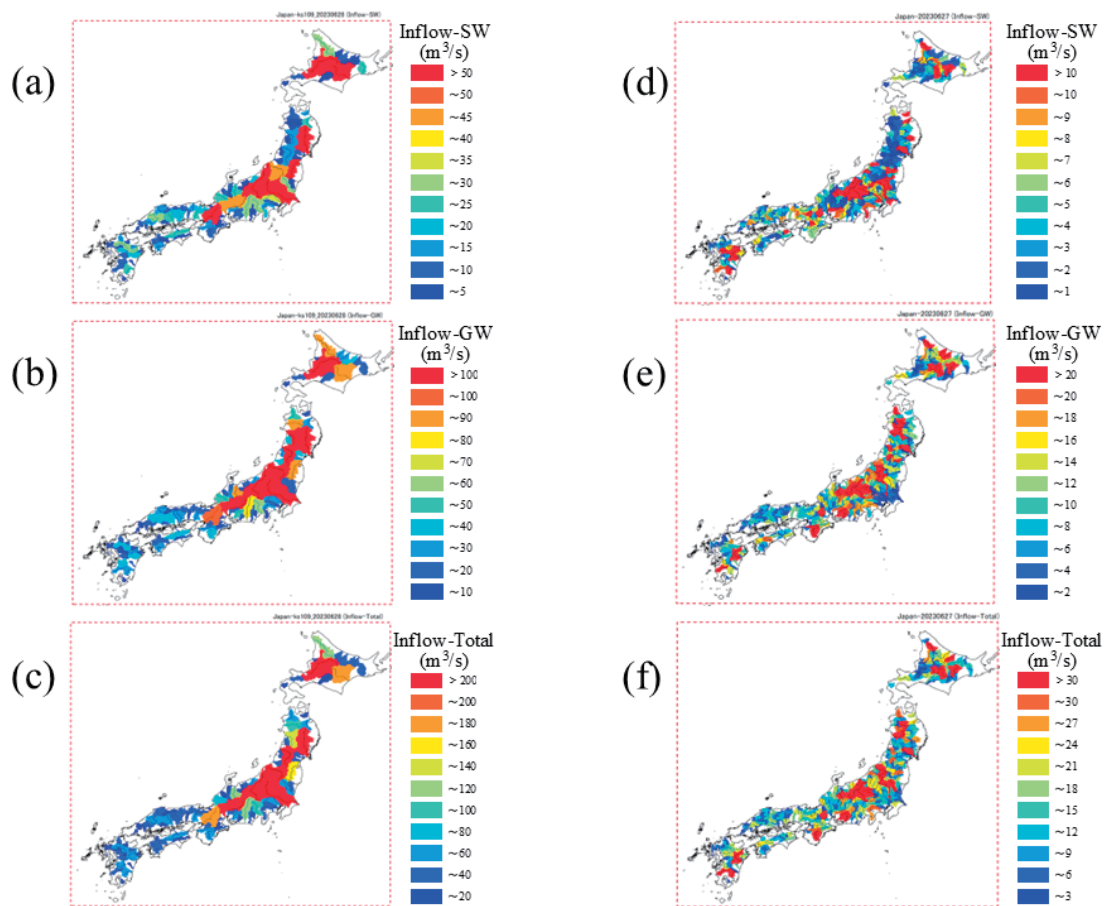
Figure 5.4 Comparison of annual-averaged water flux from terrestrial into aquatic ecosystems simulated by the NICE-BGC model with different grid resolutions. (a)-(c) Surface water, groundwater, and total inflow (= surface water + groundwater) in 109 river channels (at 0.1° × 0.1° resolution), and (d)-(f) surface water, groundwater, and total inflow in 513 river channels (at 0.05° × 0.05° resolution).

The model also simulated the macroplastic flux at different grid resolutions in all the 109 first-class river basins (a plastic density of 1001.0 kg/m^3 was assumed) (Fig. 5.5). Using a finer model resolution (0.05° × 0.05°) improved the calculation of macroplastic fluxes in smaller rivers in comparison to the coarser resolution (0.1° × 0.1°) and slightly decreased the flux of macroplastics, particularly in the urban regions (1170.0 ton/yr) (Fig. 5.5a). This suggests that some of the macroplastics do not settle during the runoff process and flow downstream with a coarser mesh (0.1° × 0.1°), whereas a finer mesh can reproduce the runoff process in more detail (0.05° × 0.05°). Fig. 5.5b shows the simulated riverine macroplastic flux to the ocean, which has a larger value in major metropolitan areas (Fig. 5.3). The results also indicated that the flux was amplified and relatively larger than the flux from the hill slope in small- and medium-sized rivers. In addition, the flux value calculated by multiplying the flow rate based on the existing concentration value (Nihei et al., 2024) was underestimated compared to the simulated value because the existing data only included mesoplastics (5–25 mm) and did not include larger macroplastics. Although the amount of MPW in the Ara River was by far the largest among all first-class rivers (Nakayama and Osako, 2023a), the macroplastic runoff in the hillslope (Fig. 5.5a) and in the river (Fig. 5.5b) was not very high because the elevation in the urban region downstream of the Ara River is very low and the topographical slope is very

small (Fig. 5.3), which prevents macroplastics from flowing downhill into the river, despite the relatively small slope roughness in cities.
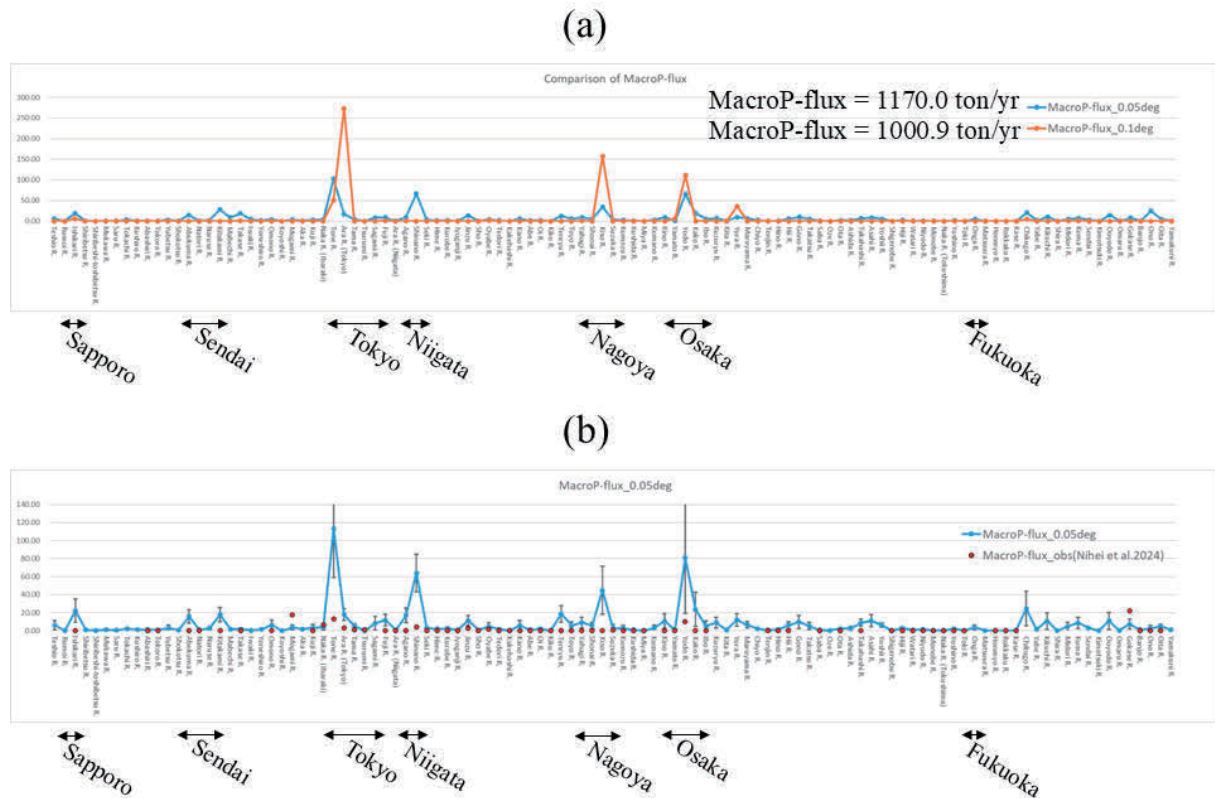
Figure 5.5 Estimation of macroplastic flux in all 109 first-class river basins (plastic density was assumed to be 1001.0 kg/m^3). (a) Comparison of different grid resolutions and (b) simulated riverine macroplastic flux to the ocean. In panel b, the red circle means mesoplastic flux calculated by multiplying the flow rate based on the existing concentration value, and the error bar means the standard deviation of annual-averaged values simulated by the model. The arrow on the horizontal axis of the figure shows the major metropolitan areas displayed in Fig. 5.3.

5.3.2 Verification of Microplastic Cycle as a Point Source through Data Accumulation

The microplastic flux in all 109 first-class river basins was estimated (Fig. 5.6). The results show that the amount of microplastic flux calculated by accumulating point information at sewage treatment plants (Fig. 5.1e) could be replaced by analyzing grid data categorized for treatment methods (sewage, septic tank, untreated) in each grid (SANIHUB, 2024) (Fig. 5.3) instead of grid data of per capita emission (Table 5.2) and treatment rates (Jones et al., 2021) obtained from global data (1314.4 ton/yr) (Fig. 5.6a). These methodologies are effective for extrapolating microplastic flux to a broader scale (Nakayama and Osako, 2023b, 2024). Fig. 5.6b shows the simulated riverine microplastic flux to the ocean (using grid data of various treatments). Compared with the macroplastic flux, the microplastic flux from the river was attenuated and relatively smaller than the flux from the hill slope in small- and medium-sized rivers (Fig. 5.5b). Consequently, the flux was more concentrated in rivers that flow through

major cities. In addition, the results show that the standard deviation of annually averaged values simulated by the model was much smaller than that in the macroplastic flux (Fig. 5.5b) because the calculated amount of microplastics drained from the sewage and septic tank was assumed to be proportional to the runoff discharge (plastic concentrations were assumed to be constant at a point source).
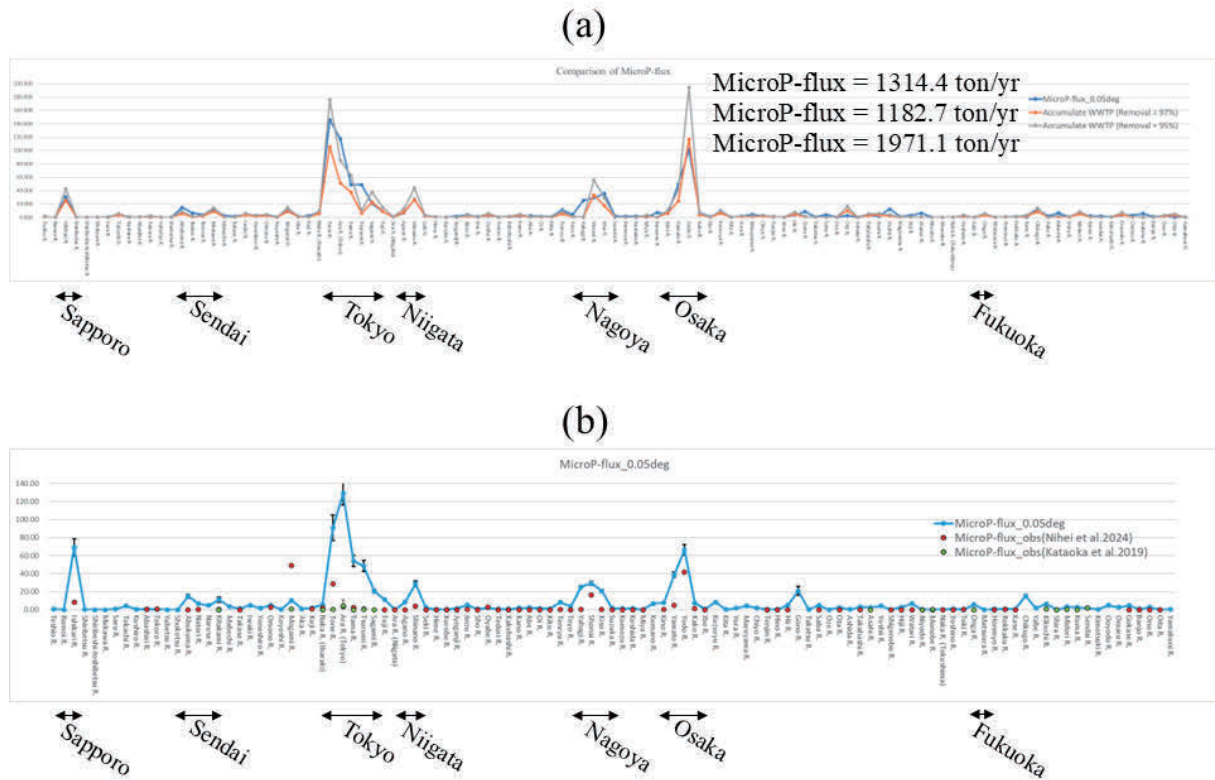
Figure 5.6 Estimation of microplastic flux in all 109 first-class river basins. (a) Comparison between accumulating point information at sewage treatment plants (orange and grey lines) and analyzing grid data categorized for treatment methods (sewage, septic tank, and untreated) in each grid (Fig. 5.3) and (b) simulated riverine microplastic flux to the ocean (using grid data of various treatments). In panel b, the red circle means microplastic flux calculated by multiplying the flow rate based on the existing concentration value, the green circle means microplastic flux in the previous study, and the error bar means the standard deviation of annual-averaged values simulated by the model. The arrow on the horizontal axis of the figure shows the major metropolitan areas displayed in Fig. 5.3.

5.3.3 Improvement of the Plastic Cycle in Urban Regions

The model compared the gridded data of the treatment type between the maximum area of each treatment type and the maximum user population within the grid (Fig. 5.7). The sewerage utilization areas expanded to the surrounding areas of cities in the latter method (Fig. 5.7). This corresponds to grids in which most of the area is a septic tank area with a small population, whereas the sewerage areas are highly concentrated in a limited area. Fig. 5.8 shows the effect

of sewage treatment on the hydrologic cycle in the basins. The results show that the ratio of the sewage treatment population to the total population was positively related to the urban ratio (Fig. 5.8a). Similarly, the ratio of the sewage treatment area to the total area was higher in the urban areas and lower in the surrounding and rural areas because of the expansion of septic tanks and agricultural village drainage (Fig. 5.8b). In addition, by comparing the microplastic flux with artificial discharge from the treatment plant and with discharge along the terrain in 109 river basins, more microplastics flowed through sewage treatment areas than naturally along the topography in some urban rivers (Yodo, Shonai, Ishikari, and Tsurumi Rivers), although the distribution of flux was almost similar for each river (Fig. 5.8c). This is also related to the simulated result showing that more than 80% of the discharged microplastics originated from sewage. This implies that the microplastic flux flowing through urban areas has been significantly altered from the natural terrain.
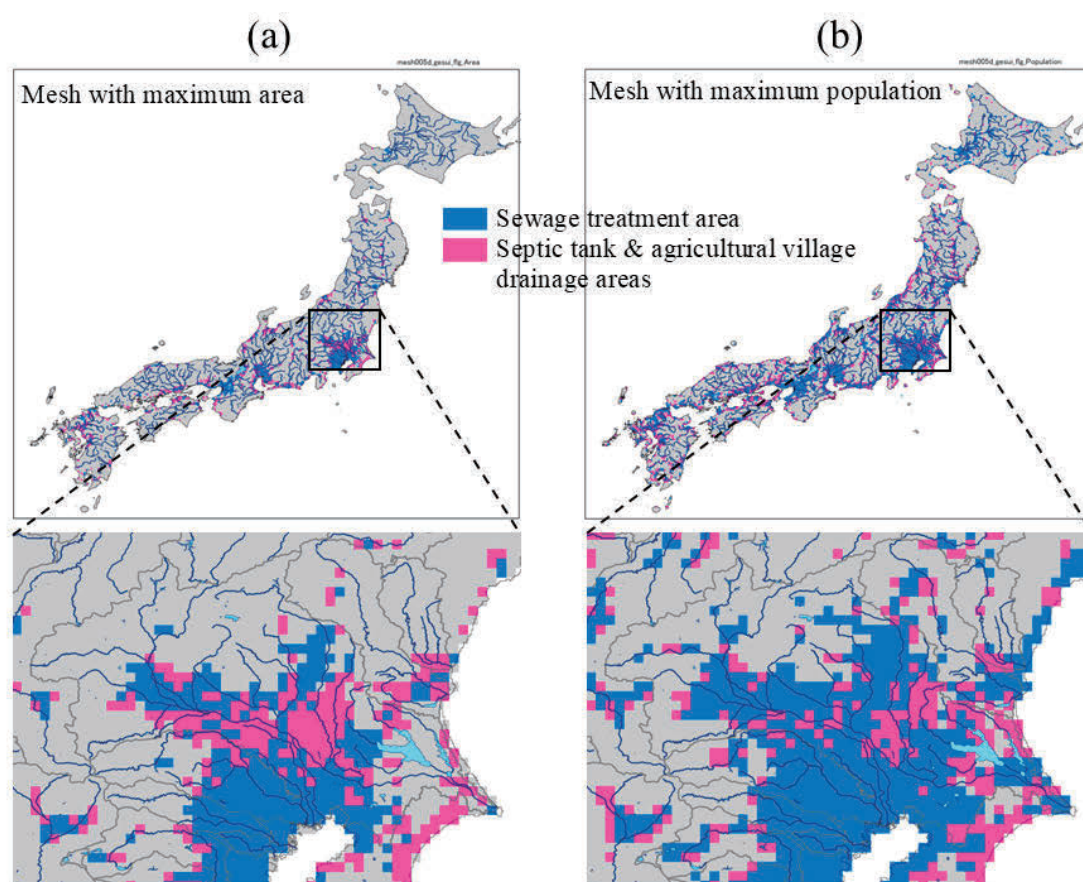
Figure 5.7 Gridded data of treatment type: sewage treatment, septic tank, and agricultural village drainage areas throughout Japan and in the Kanto region. (a) Maximum area of each treatment type and (b) maximum user population within the grid.
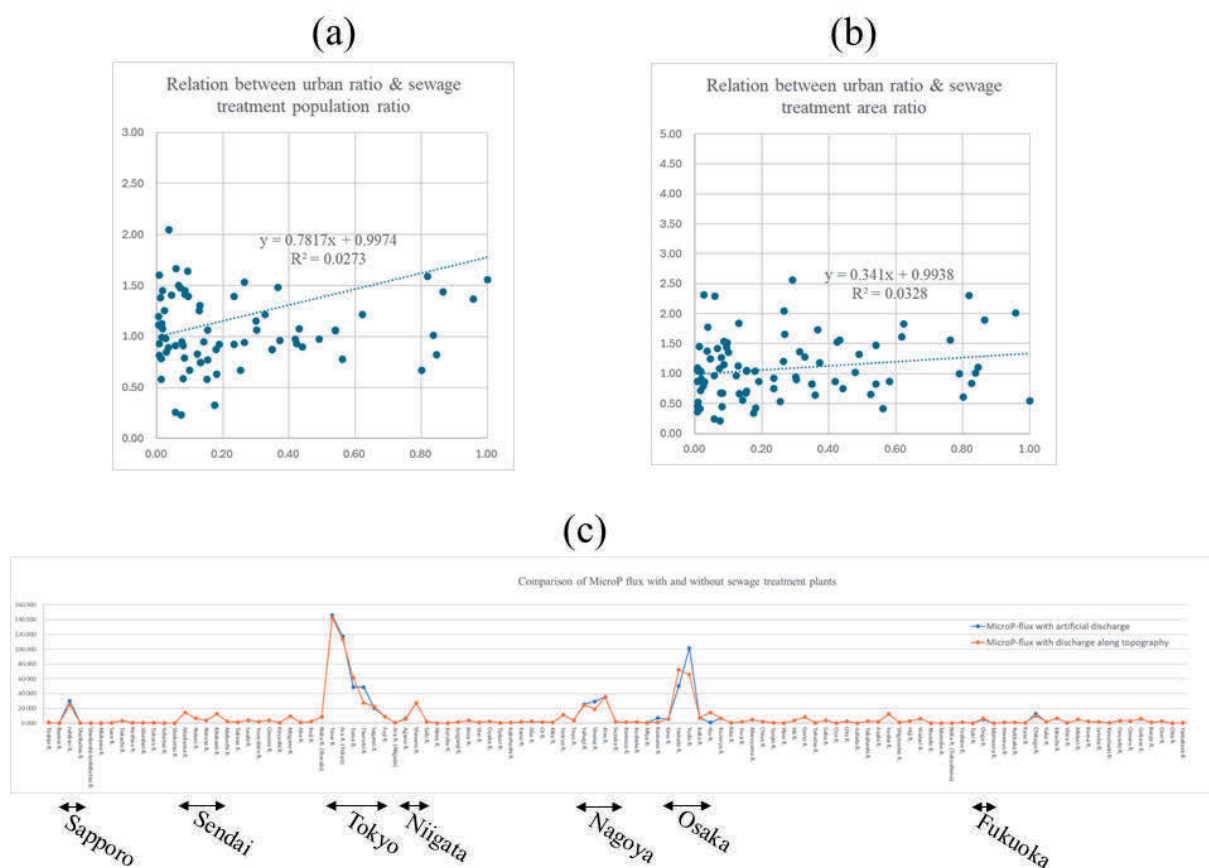
Figure 5.8 Effect of sewage treatment on the hydrologic cycle in basins. (a) Relation between urban ratio and ratio of sewage treatment population to total population, (b) relation between urban ratio and ratio of sewage treatment area to total area in each treatment plant, and (c) comparison of microplastic flux with artificial discharge from the treatment plant and with discharge along the topography in 109 river basins. In panel c, the arrow on the horizontal axis shows the major metropolitan areas displayed in Fig. 5.3.

5.4 Conclusion

In this chapter, the process-based NICE-BGC was extended and coupled with the plastic debris model for freshwater systems and then applied to all first-class (class A) river basins in Japan (109 river basins). The model was constructed to include various processes, such as advection, dispersion, diffusion, settling, dissolution, and deterioration due to light and temperature, interactions with suspended matter (heteroaggregation), resuspension, and biofouling. NICE-BGC simulated how the diffuse source of MPW and point sources of tires, PCPs, dust, and laundry throughout the country are transported from land to rivers and finally to the ocean. The results clarified that increasing the spatial resolution of the model reduced the macroplastic fluxes in urban areas owing to more settlement during the runoff process. The model also revealed that the amount of microplastic flux calculated by accumulating point information at sewage treatment plants could be replaced by analyzing grid data categorized for the treatment method (sewage, septic tank, and untreated) in each grid instead of global data of per capita emissions and treatment rates. The results also clarified that the plastic cycle,

particularly microplastics, in rivers flowing through urban areas was significantly altered. Finally, methods of improving the plastic cycle in urban regions were evaluated to determine whether the urban plastic cycle could be modeled using less inventory data. These results will help quantify the impacts of plastic waste on terrestrial and aquatic ecosystems and identify solutions and measures to reduce plastic input to the ocean.

References

Besseling, E., Quik, J.T.K., Sun, M., Koelmans, A.A. (2017) Fate and nano- and microplastic in freshwater systems: A modelling study. Environmental Pollution, 220, 540–548. doi:10.1016/j.envpol.2016.10.001

Boucher, J., Billard, G., Simeone, E., Sousa, J. (2020) The marine plastic footprint. Global Marine and Polar Programme. IUCN. Switzerland. 69 pp. doi:10.2305/IUCN.CH.2020.01.en

De Carvalho, A.R., Garcia, F., Riem-Galliano, L., et al. (2021) Urbanization and hydrological conditions drive the spatial and temporal variability of microplastic pollution in the Garonne River. Science of the Total Environment, 769, 144479. doi:10.1016/j.scitotenv.2020.144479

ESRI. (2019) Overlay Layers. Portal for ArcGIS. https://gislab.depaul.edu/portal/portalhelp/en/portal/latest/use/geoanalytics-overlay-layers.htm

European Centre for Medium-Range Weather Forecasts (ECMWF). (2019) ERA-Interim. http://data-portal.ecmwf.int/data/d/interim_daily/

European Commission. (2012) Harmonized World Soil Database. http://eusoils.jrc.ec.europa.eu/ESDB_Archive/soil_data/global.htm

European Commission. (2015) Global Land Cover 2000. https://forobs.jrc.ec.europa.eu/products/glc2000/glc2000.php

Food and Agriculture Organization of the United Nations (FAO). (2016) Global Map of Irrigation Areas (GMIA). http://www.fao.org/nr/water/aquastat/irrigationmap/index.stm

Guo, Y., Ayeri, T., van Puijenbroek, P., Strokal, M. (2024) Microplastics in global rivers: sustainable practices. Sustainable Development, 1–24. doi:10.1002/sd.3279

Hartmann, J., Moosdorf, N. (2012) The new global lithological map database GLiM: A representation of rock properties at the Earth surface. Geochemistry, Geophysics, Geosystems, 13, Q12004, doi:10.1029/2012GC004370

Holmes, C.M., Dyer, S.D., Vamshi, R., et al. (2020) A national-scale framework for visualizing riverine concentrations of microplastics released from municipal wastewater treatment incorporating generalized instream losses. Environmental Toxicology and Chemistry, 39(1), 210–219. doi:1002/etc.4610

Hurley, E., Woodward, J., Rothwell, J.J. (2018) Microplastic contamination of river beds significantly reduced by catchment-wide flooding. Nature Geoscience, 11, 251–257, Doi:10.1038/s41561-018-0080-1

Jambeck, J.R., Geyer, R., Wilcox, C., et al. (2015) Plastic waste inputs from land into the ocean. Science, 347, 768–771, doi:10.1126/science.1260352

Japanese Government Statistics. (2021) E-Stat: Statistics of Japan. https://www.e-stat.go.jp/en

Jones, E.R., van Vliet, M.T.H., Qadir, M., Bierkens, M.F.P. (2021) Country-level and gridded estimates of wastewater production, collection, treatment and reuse. Earth System Science Data, 13, 237–254, doi:10.5194/essd-13-237-2021

Kataoka, T., Nihei, Y., Kudou, K., Hinata, H. (2019) Assessment of the sources and inflow processes of microplastics in the river environments of Japan. Environmental Pollution, 244, 958?965. doi:10.1016/j.envpol.2018.10.111

Kooi, M., van Nes, E.H., Scheffer, M., Koelmans, A.A. (2017) Ups and downs in the ocean: Effects of biofouling on vertical transport of microplastics. Environmental Science & Technology, 51, 7963–7971, doi:10.1021/acs.est.6b04702

Kooi, M., Besseling, E., Kroeze, C., et al. (2018) Modelling the fate and transport of plastic decries in freshwaters: review and guidance. In: Wagner, M., Lambert, S. [Eds] Freshwater Microplastics. The Handbook of Environmental Chemistry 58, Springer, pp.125–152

Kumar, R., Sharma, P., Verma, A., et al. (2021) Effect of physical characteristics and hydrodynamic conditions on transport and deposition of microplastics in riverine ecosystem. Water, 13, 2710. doi:10.3390/w13192710

Lebreton, L., Andrady, A. 2019. Future scenarios of global plastic waste generation and disposal. Palgrave Communications, 5, 6, doi:10.1057/s41599-018-0212-7

Lebreton, L, van der Zwet, J., Damsteeg, J.-W., et al. (2017) River plastic emissions to the world's oceans. Nature Communications, 8, 15611, doi:10.1038/ncomms15611

Lehner, B., Döll, P. (2004) Development and validation of a global database of lakes, reservoirs and wetlands. Journal of Hydrology, 296, 1–22, doi:10.1016/j.jhydrol.2004.03.028

Liu, Y., You, J., Li, Y., et al. (2021) Insights into the horizontal and vertical profiles of microplastics in a river emptying into the sea affected by intensive anthropogenic activities in Northern China. Science of the Total Environment, 779, 146589, doi:10.1016/j.scitotenv.2021.146589

MacAfee, E.A., Lohr, A.J. (2023) Multi-scalar interactions between mismanaged plastic waste and urban flooding in an era of climate change and rapid urbanization. WIREs Water. E1708. doi:10.1002/wat2.1708

Meijer, L.J.J., van Emmerik, T., van der Ent, R., et al. (2021) More than 1000 rivers account for 80% of global riverine plastic emissions into the ocean. Science Advances, 7, eaaz5803, doi:10.1126/sciadv.aaz5803

Ministry of Foreign Affairs of Japan. (2019) G20 Osaka Leader's Declaration. https://www.mofa.go.jp/policy/economy/g20_summit/osaka19/en/documents/final_g20_osaka_leaders_declaration.html

Ministry of Land, Infrastructure, Transport and Tourism (MLIT). (2011) Digital national land information: Basin boundary ver.2.1. https://nlftp.mlit.go.jp/ksj/gml/datalist/KsjTmplt-W07.html

Ministry of Land, Infrastructure, Transport and Tourism (MLIT). (2012) Digital national land information: River networks ver.3.1. https://nlftp.mlit.go.jp/ksj/gml/datalist/KsjTmplt-W05.html

Ministry of Land, Infrastructure, Transport and Tourism (MLIT). (2013) Digital national land information: Sewerage system related facility ver.1.1. https://nlftp.mlit.go.jp/ksj/gml/datalist/KsjTmplt-P22.html

Ministry of Land, Infrastructure, Transport and Tourism (MLIT). (2016) Digital national land information: Reservoirs and dams ver.3.0. https://nlftp.mlit.go.jp/ksj/gml/datalist/KsjTmplt-W01.html

Ministry of Land, Infrastructure, Transport and Tourism (MLIT). (2021a) Latest situation of the spread of sewage treatment population in Japan. Press Release. https://www.mlit.go.jp/report/press/content/001421074.pdf (in Japanese)

Ministry of Land, Infrastructure, Transport and Tourism (MLIT). (2021b) Water information system. http://www1.river.go.jp/

Mueller, N.D., Gerber, J.S., Johnston, M., et al. (2012) Closing yield gaps through nutrient and water management. Nature, 490, 254–257, doi:10.1038/nature11420

Murphy, F., Ewins, C., Carbonnier, F., Quinn, B. (2016) Wastewater Treatment Works (WwTW) as a source of microplastics in the aquatic environment. Environmental Science & Technology, 50, 5800–5808. doi:10.1021/acs.est.5b05416

Nakayama, T., Watanabe, M. (2004) Simulation of drying phenomena associated with vegetation change caused by invasion of alder (Alnus japonica) in Kushiro Mire. Water Resources Research, 40(8), W08402. doi:10.1029/2004WR003174

Nakayama, T., Watanabe, M., Tanji, K., Morioka, T. (2007) Effect of underground urban structures on eutrophic coastal environment. Science of the Total Environment, 373(1), 270–288. doi:10.1016/j.scitotenv.2006.11.033

Nakayama, T. (2017a) Development of an advanced eco-hydrologic and biogeochemical coupling model aimed at clarifying the missing role of inland water in the global biogeochemical cycle. Journal of Geophysical Research: Biogeosciences, 122, 966–988, doi:10.1002/2016JG003743

Nakayama, T. (2017b) Scaled-dependence and seasonal variations of carbon cycle through development of an advanced eco-hydrologic and biogeochemical coupling model. Ecological Modelling, 356, 151–161, doi:10.1016/j.ecolmodel.2017.04.014

Nakayama, T. (2020) Inter-annual simulation of global carbon cycle variations in a terrestrial-aquatic continuum. Hydrological Processes, 34(3), 662–678. doi:10.1002/hyp.13616

Nakayama, T. (2022) Impact of anthropogenic disturbances on carbon cycle changes in terrestrial-aquatic-estuarine continuum by using an advanced process-based model. Hydrological Processes, 36(2), e14471, doi:10.1002/hyp.14471

Nakayama, T., Osako, M. (2023a) Development of a process-based eco-hydrology model for evaluating the spatio-temporal dynamics of macro- and micro-plastics for the whole of Japan. Ecological Modelling, 476, 110243, doi:10.1016/j.ecolmodel.2022.110243

Nakayama, T., Osako, M. (2023b) The flux and fate of plastic in the world's major rivers: Modeling spatial and temporal variability. Global and Planetary Change, 221, 104037, doi:10.1016/j.gloplacha.2023.104037

Nakayama, T., Osako, M. (2024) Plastic trade-off: Impact of export and import of waste plastic on plastic dynamics in Asian region. Ecological Modelling, 489, 110624, doi:10.1016/j.ecolmodel.2024.110624

Nakayama, T. (2025) Impact of settling and resuspension on plastic dynamics during extreme flow and their seasonality in global major rivers. Hydrological Processes, 39(2), e70072. doi:10.1002/hyp.70072

NASA. (2013) GLDAS vegetation class. http://ldas.gsfc.nasa.gov/gldas/GLDASvegetation.php

Nihei, Y., Yoshida, T., Kataoka, T., Ogata, R. (2020) High-resolution mapping of Japanese microplastic and microplastic emissions from the land into the sea. Water, 12, 951. doi:10.3390/w12040951

Nihei, Y., Ota, H., Tanaka, M., Kataoka, T., Kashiwada, J. (2024) Comparison of concentration, shape, and polymer composition between microplastics and mesoplastics in Japanese river waters. Water Research, 249, 120979. doi:10.1016/j.watres.2023.120979

Nizzetto, L., Bussi, G., Futter, M.N., et al. (2016) A theoretical assessment of microplastic transport in river catchments and their retention by soils and river sediments. Environmental Science: Processes & Impacts, 18, 1050–1059, doi:10.1039/c6em00206d

Pelletier, G.J., Chapra, S.C., Tao, H. (2006) QUAL2Kw ? A framework for modeling water quality in streams and rivers using a genetic algorithm for calibration. Environmental Modelling and Software, 21, 419–425. doi:10.1016/j.envsoft.2005.07.002

Portmann, F.T., Siebert, S., Döll, P. (2010) MIRCA2000 – Global monthly irrigated and rainfed crop areas around the year 2000: A new high-resolution data set for agricultural and hydrological modelling. Global Biogeochemical Cycles, 24, GB 1011, Doi:10.1029/2008GB003435

Praetorius, A., Scheringer, M., Hungerbühler, K. (2012) Development of environmental fate models for engineered nanoparticles - A case study of TiO2 nanoparticles in the Rhine River. Environmental Science & Technology, 46, 6705–6713, doi:10.1021/es204530n

Quik, J.T.K., de Klein, J.J.M., Koelmans, A.A. (2015) Spatially explicit fate modelling of nanomaterials in natural waters. Water Research, 80, 200–208. doi:10.1016/ j.watres.2015.05.025

SANIHUB (2024) Septik tank - Humanitarian sanitation hub. https://sanihub.info/topic/septic-tank/

Schmidt, C., Krauth, T., Wagner, S. (2017) Export of plastic debris by rivers into the sea. Environmental Science & Technology, 51, 12246–12253, doi:10.1021/acs.est.7b02368

Siebert, S., Döll, P. (2010) Quantifying blue and green virtual water contents in global crop production as well as potential production losses without irrigation. Journal of Hydrology, 384, 198–217

Siegfried, M., Koelmans, A.A., Besseling, E., Kroeze, C. (2017) Export of microplastics from land to sea. A modelling approach. Water Research, 127, 249–257, doi:10.1016/j.watres.2017.10.011

Strokal, M., Bai, Z., Franssen, W., et al. (2021) Urbanization: an increasing source of multiple pollutants to rivers in the 21st century. Urban Sustainability, 1, 24, doi:10.1038/s42949-021-00026-w

Tasseron, P.F., van Emmerik, T.H.M., de Winter, W., et al. (2024) Riverbank plastic distributions and how to sample them. Microplastics and Nanoplastics, 4, 22. doi:10.1186/s43591-024-00100-x

Thompson, R.C., Olsen, Y., Mitchell, R.P., et al. (2004) Lost at sea: Where is all the Plastic? Science, 304, 838, doi:10.1126/science.1094559

Unice, K.M., Weeber, M.P., Abramson, M.M., et al. (2019) Characterizing export of land-based microplastics to the estuary - part I: Application of integrated geospatial microplastic transport models to assess tire and road wear particles in the Seine watershed. Science of the total Environmental, 646, 1639–1649. doi:10.1016/j.scitotenv.2018.07.368

U.S. Geological Survey (USGS). (1996) GTOPO30 Global 30 Arc Second Elevation Data Set. USGS. http://www1.gsi.go.jp/geowww/globalmap-gsi/gtopo30/gtopo30.html

van Wijnen, J., Ragas, A.M.J., Kroeze, C. (2019) Modelling global river export of microplastics to the marine environment: Sources and future trends. Science of the Total Environment, 673, 392–401, doi:10.1016/j.scitotenv.2019.04.078

Wagner, S., Klöckner, P., Stier, B., Römer, M., Seiwert, B., Reemtsma, T., Schmidt, C. (2019) Relationship between discharge and river plastic concentrations in a rural and an urban catchment. Environmental Science & Technology, 53, 10082–10091, doi:10.1021/acs.est.9b03048

Waldschläger, K., Schüttrumpf, H. (2019) Erosion behavior of different microplastic particles in comparison to natural sediments. Environmental Science & Technology, 53, 13219–13227, doi:10.1021/acs.est.9b05394

Whitehead, P.G., Bussi, G., Hughes, J.M.R., et al. (2021) Modelling microplastics in the River Thames: sources, sinks and policy implications. Water, 13, 861. doi:10.3390/w13060861

Windsor, F.M., Durance, I., Horton, A.A., et al. (2019) A catchment-scale perspective of plastic pollution. Global Change Biology, 25, 1207–1221. doi:10.1111/gcb.14572

Woodward, J., Li, J., Rothwell, J., Hurley, R. (2021) Acute riverine microplastic contamination due to avoidable releases of untreated wastewater. Nature Sustainability, 4, 793–802. doi:10.1038/s41893-021-00718-2

Yamazaki, D. (2022) J-FlwDir: Japan Flow Direction Map. http://hydro.iis.u-tokyo.ac.jp/~yamadai/JapanDir/index.html

Zhang, B., Tian, H., Lu, C., et al. (2017) Global manure nitrogen production and application in cropland during 1860–2014; a 5 arcmin gridded global dataset for Earth system modelling. Earth System Science Data, 9, 667–678, doi:10.5194/essd-9-667-2017

Zhu, X., Hoffman, M.J., Rochman, C.M. (2024) A city-wide emissions inventory of plastic pollution. Environmental Science & Technology, 58, 3375–3385. doi:10.1021/acs.est.3c04348

Chapter 6

Final Conclusions and Future Work

6.1 Final Conclusions

In a previous study, the National Integrated Catchment-based Eco-hydrology (NICE) model, which includes surface–groundwater interactions and assimilates land-surface processes, was developed to describe phenological variations based on satellite data (Nakayama, 2008a-c, 2009, 2010, 2011a–d, 2012a–d, 2013, 2014a,b, 2015, 2016, 2017a–c, 2018, 2019, 2020, 2022, 2023a,b; 2024a–c; 2025a–d; Nakayama and Fujita, 2010; Nakayama and Hashimoto, 2011; Nakayama and Maksyutov, 2018; Nakayama and Osako, 2023a,b, 2024; Nakayama and Pelletier, 2018; Nakayama and Shankman, 2013a,b; Nakayama and Watanabe, 2004, 2005, 2006a,b, 2008a–c; Nakayama et al., 2006, 2007, 2010, 2012, 2021a,b, 2023) (Fig. 1.1). NICE has been applied to various basins/catchments at local and regional scales, such as the Tokyo Metropolitan Area in Japan, Kushiro Wetland (the largest wetland in Japan), Lake Kasumigaura catchment (a highly eutrophic lake in Japan), and all of Japan, and to continental and global scales, such as the Changjiang and Yellow Rivers in China, Ob River in West Siberia, Mekong River in Southeast Asia, and Mongolia. The results of these studies have been summarized in previous monograph series, namely, the 11th (Part I), 14th (Part II), 18th (Part III), 20th (Part IV), 26th (Part V), 29th (Part VI), and 30th publications (Part VII) (Fig. 1.2).

In this monograph (Part VIII), NICE coupled with the plastic debris model was further extended to incorporate resuspension, bedload transport, estuarine dynamics, heteroaggregation, and biofouling to quantify plastic dynamics along the terrestrial-aquatic-estuarine continuum and devise solutions and measures for reducing plastic inputs to the ocean as an extension of the 30th publication (Part VII) (Nakayama, 2024c) (Fig. 1.4). The model also improved the accuracy of simulating the plastic cycle in urban regions and clarified that the plastic cycle, particularly microplastic cycle, in rivers flowing through urban areas has been significantly altered.

Chapter 2 reports on the extension of the NICE-BGC model to incorporate resuspension and bedload transport in the world's major rivers (325 rivers) by extending the author's previously published work. Although small-sized microplastics are suspended in the water and large-sized microplastics settle on the riverbed under normal flow, floods completely disturb this equilibrium and resuspend large-sized microplastics into the water (Nakayama, 2025a).

Chapter 3 reports the extension of the NICE-BGC to incorporate plastic dynamics in major global rivers, including 130 tidal estuaries, by extending previous studies. The model showed that plastics with smaller particle sizes accumulated more in estuarine waters than rivers, and plastics with larger particle sizes accumulated more on riverbeds. The simulated results also showed that estuaries trap more plastic than lakes and riverbeds (0.218 ± 0.053 Tg/yr), although not as much as reservoirs (0.386 ± 0.103 Tg/yr) (Nakayama, 2024b).

Chapter 4 reports the extension of the NICE-BGC to evaluate biogeochemical cycles and their relationship with plastic dynamics in the terrestrial-aquatic continuum on a global scale. The model could simulate different speciation states of microplastics to indicate the impact of the interaction processes of heteroaggregation and biofouling on plastic dynamics. The model could also estimate attached algal growth as a function of the encounter kernel rate (Nakayama, 2025c).

Chapter 5 reports the extension of the NICE-BGC to downscale to the entirety of Japan. A finer resolution promoted more settlement during the runoff process and slightly decreased the macroplastic flux, particularly in urban regions. The model also revealed that microplastic flux calculated by accumulating point information at sewage treatment plants can be replaced by grid data categorized by treatment methods instead of global data. The results clarified that the plastic cycle in urban rivers has been significantly altered (Nakayama, 2025b).

Thus, the new model improved the accuracy of the plastic budget (Table 4.2) and the spatial distribution of plastic transport and deposition (Fig. 4.10) in global major rivers. The model includes transport processes (advection, diffusion, settling, resuspension, bedload, and burial), transformation processes (fragmentation, dissolution, and degradation), and interaction processes (heteroaggregation, breakup, biofouling, and defouling) (Fig. 1.4), which represents a significant improvement over previous studies. The results showed that the process-based model is sufficiently powerful to quantify the detailed processes of the plastic cycle, which were frequently simulated as black boxes in previous models. In contrast, more spatiotemporal input data for MPW in various sectors are required. However, this new model is useful for evaluating the spatiotemporal dynamics of plastic cycles at the basin scale. The use of more ground data, GPS tracking, drone images, and aerial photographs, and the application of learning algorithms, such as random forest, to improve census data downscaling (Nicolas et al., 2016), are necessary to improve the accuracy of the heterogeneous distribution of plastic dynamics and their seasonal variations in various basins.

The new model also showed that a finer resolution promoted more settlement during runoff process, which slightly decreased the flux of macroplastics, particularly in urban regions (Fig. 5.5). In addition, the results clarified that the plastic cycle, particularly the microplastic cycle, in rivers flowing through urban areas was significantly altered (Fig. 5.8). In this way, the model helped to provide a better understanding of the plastic cycle in urban regions based on limited inventory data. Plastic pollution has recently been considered a serious environmental problem, and pollutants transported from land to rivers and finally to oceans severely affect human health and the environment (Siegfried et al., 2017). Plastic pollution hotspots and sinks, and resolve the source–flux–sink nexus within river basins (Windsor et al., 2019). From another perspective, developing a framework to reverse the degradation of global water resources, particularly plastic pollution, is crucial for achieving Sustainable Development Goals (SDGs) (UNESCO, 2022). The recent G20 Osaka Summit in 2019 shared the "Osaka Blue Ocean Vision" (Ministry of Foreign Affairs of Japan, 2019), which is positioned alongside the Conference of the Parties (COP) as a global warming countermeasure.

The NICE model is a useful tool for predicting and resolving future problems related to plastic pollution in various basins. This methodology is also useful for evaluating spatiotemporal variations in plastic dynamics using limited inventory data, particularly in developing countries. Furthermore, it is valuable to combine NICE with social system methods, such as material flow analysis, to assess the loss and emissions of plastics into the aquatic environment (OECD, 2022) instead of inputting the given value of MPW (Fig. 1.4). However, the effects of extensive plastic disposal in the future have not yet been clarified. It is necessary to quantify the plastic budget and develop solutions and measures to reduce plastic input to the ocean. A quantitative assessment of plastic fate and transport is necessary to realize this vision because countries worldwide have decided on concrete future measures for dealing with plastics based on scientific results.

6.2 Future Work

This monograph (Part VIII) describes the new development of a process-based NICE model coupled with a plastic debris model and its application to various basins from regional to global scales for quantifying the fate and transport of plastic dynamics. Although the plastic cycle is connected to the water cycle, the water cycle is also related to the dynamics of ecosystem

changes, including vegetation. This implies that the plastic cycle not only depends on the complexity of the plastic inventory but is also closely related to the complexity of the ecosystem.

　　To address the above plastic-related issues, the model was further extended to include another process capable of integrating various datasets and improving the accuracy of the simulated results on both regional and global scales.

(i) Most previous models ignored the different characteristics of the interaction processes of biofouling and heteroaggregation between natural lakes and man-made reservoirs (Nakayama, 2023a, 2024a). Because the hydraulic and hydrological conditions of lakes and reservoirs are significantly different, a model that can evaluate plastic circulation with greater accuracy is required (Nakayama, under review) (Fig. 6.1).

(ii) Recent research indicates that vegetation, including water hyacinth plants, wood jams, and debris rafts, effectively accumulates plastic pollution in and around rivers (van Emmerik et al., 2019). In particular, wetlands have an important influence on the hydrological cycle and play an important role in biogeochemical processes. Therefore, it is important to quantitatively clarify and reproduce the causal relationships between the water cycle and changes in marsh vegetation (Nakayama, 2008a, 2008b; Nakayama, under review) (Fig. 6.2), which will also help enhance the accuracy of the plastic cycle.

(iii) Ecosystem resilience is greatly dependent on the hydrological cycle and vegetation status, which have major impacts on plastic dynamics at the basin scale. (Nakayama, 2008a, 2008b; Nakayama, 2025d). To achieve sustainable development, it is necessary to strengthen ecosystem resilience against human activities (Fig. 6.3).

　　Ongoing studies (i)–(iii) are expected to be reported in the next monograph (Part IX) in the future.
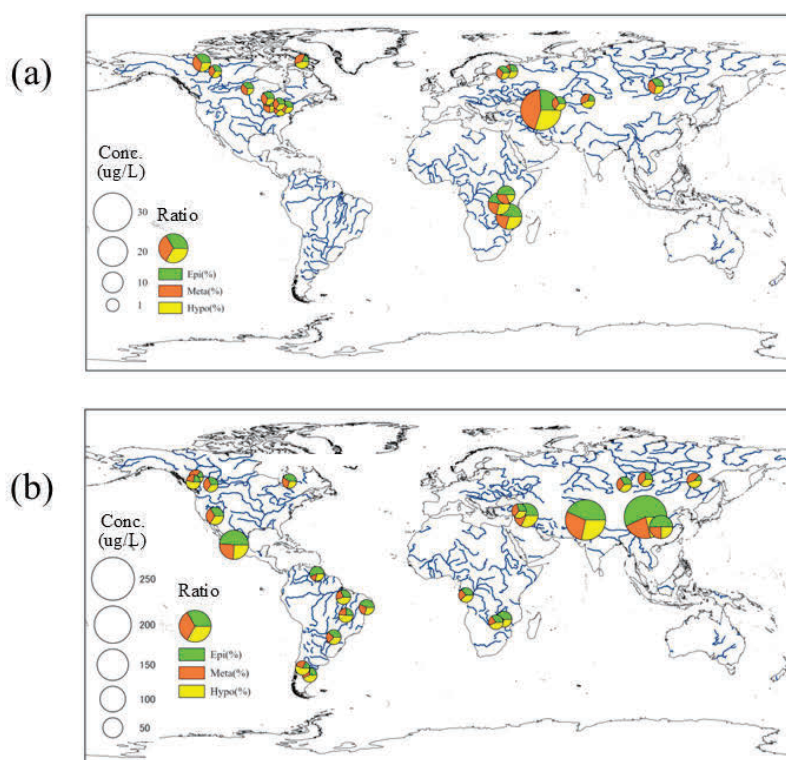
Figure 6.1 Difference of microplastic concentration in (a) lakes and (b) reservoirs as simulated by

NICE. The circle size indicates the microplastic concentration, and each pie chart shows the proportion of the microplastic concentrations in three vertical layers (epilimnion, metalimnion, and hypolimnion).
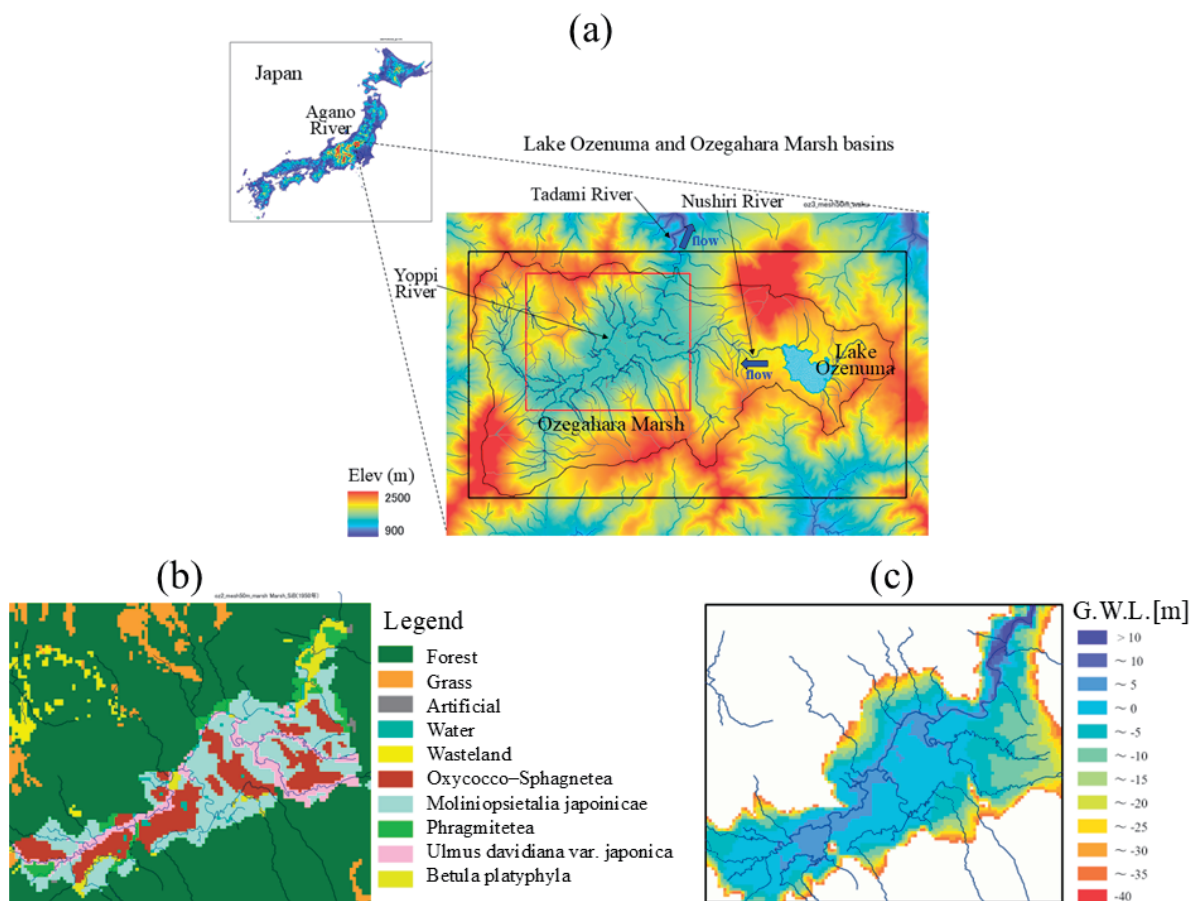
Figure 6.2 Ozegahara Marsh in Japan: (a) location and elevation, and relation between the spatial distribution of (b) vegetation (Biodiversity Center of Japan, 2025) and (c) groundwater level simulated by NICE in the 2000s.
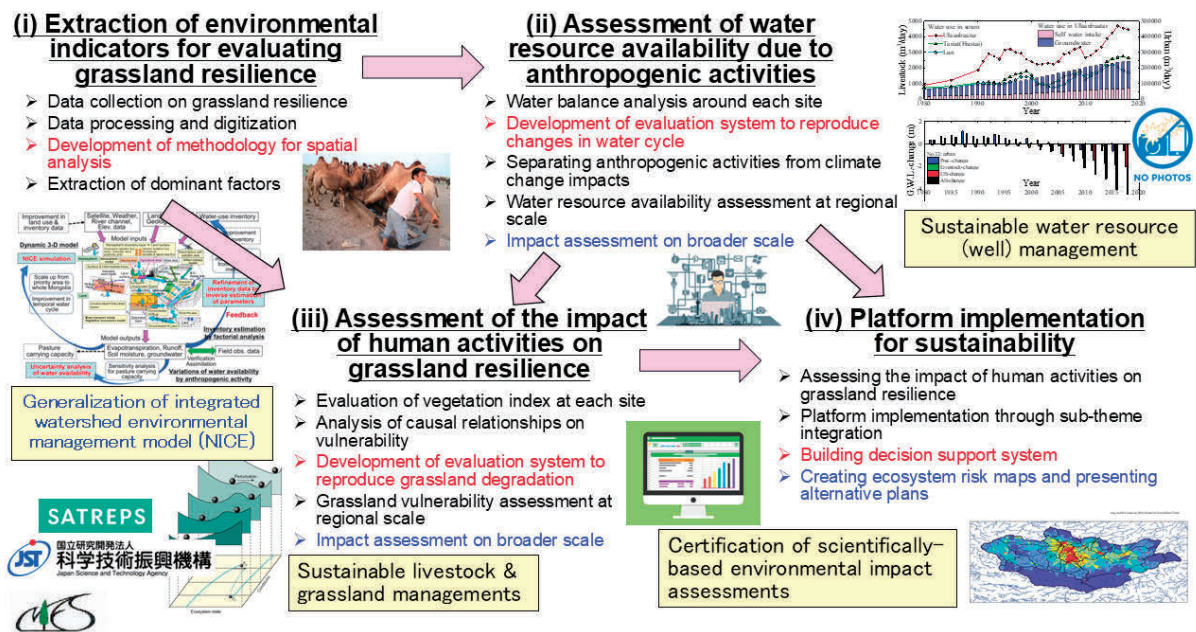
Figure 6.3 Implementation of ecosystem resilience for human activities in a new project (SATREPS).

References

Biodiversity Center of Japan. (2025) Vegetation Map of Japan 1:25,000, ver3.2, Ministry of Environment. http://gis.biodic.go.jp/webgis/sc-043.html

Ministry of Foreign Affairs of Japan. (2019) G20 Osaka Leader's declaration. https://www.mofa.go.jp/policy/economy/g20_summit/osaka19/en/documents/final_g20_osaka_leaders_declaration.html

Nakayama, T., Watanabe, M. (2004) Simulation of drying phenomena associated with vegetation change caused by invasion of alder (*Alnus japonica*) in Kushiro Mire. Water Resources Research, 40, W08402. doi:10.1029/2004WR003174

Nakayama, T., Watanabe, M. (2005) Re-evaluation of groundwater dynamics about water and nutrient budgets in Lake Kasumigaura, Annual. Journal of Hydroscience and Hydraulic Engineering, 49, 1231–1236 (Abst. in English)

Nakayama, T., Watanabe, M. (2006a) Simulation of spring snowmelt runoff by considering micro-topography and phase changes in soil layer. Hydrology and Earth System Sciences Discussions, 3, 2101–2144

Nakayama, T., Watanabe, M. (2006b) Development of process-based NICE model and simulation of ecosystem dynamics in the catchment of East Asia (Part I). CGER's supercomputer monograph report, 11. NIES, 100 p. http://www.cger.nies.go.jp/publications/report/i063/I063e

Nakayama, T., Yang, Y., Watanabe, M., Zhang, X. (2006) Simulation of groundwater dynamics in the North China Plain by coupled hydrology and agricultural models. Hydrological Processes, 20, 3441–3466, doi:10.1002/hyp.6142

Nakayama, T., Watanabe, M., Tanji, K., Morioka, T. (2007) Effect of underground urban structures on eutrophic coastal environment. Science of the Total Environment, 373, 270–288. doi:10.1016/j.scitotenv.2006.11.033

Nakayama, T. (2008a) Factors controlling vegetation succession in Kushiro Mire. Ecological Modelling, 215, 225–236. doi:10.1016/j.ecolmodel.2008.02.017

Nakayama, T. (2008b) Shrinkage of shrub forest and recovery of mire ecosystem by river restoration in northern Japan. Forest Ecology and Management, 256, 1927–1938. doi:10.1016/j.foreco.2008.07.017

Nakayama, T. (2008c) Development of process-based NICE model and simulation of ecosystem dynamics in the catchment of East Asia (Part II). CGER's supercomputer monograph report, 14. NIES, 91 p. http://www.cger.nies.go.jp/publications/report/i083/i083e

Nakayama, T., Watanabe, M. (2008a) Missing role of groundwater in water and nutrient cycles in the shallow eutrophic Lake Kasumigaura, Japan. Hydrological Processes, 22, 1150–1172. doi:10.1002/hyp.6684

Nakayama, T., Watanabe, M. (2008b) Role of flood storage ability of lakes in the Changjiang River catchment. Global and Planetary Change, 63, 9–22. doi:10.1016/j.gloplacha.2008.04.002

Nakayama, T., Watanabe, M. (2008c) Modelling the hydrologic cycle in a shallow eutrophic lake. SIL Proceedings, 1922-2010 (International Association of Theoretical and Applied Limnology), 30, 345–348

Nakayama, T. (2009) Simulation of ecosystem degradation and its application for effective policy-making in regional scale. In: Gallo, M. N. M., Ferrari, H. (Eds) River Pollution Research Progress (Chapter 1), Nova Science Pub., Inc., New York, pp. 1–89

Nakayama, T. (2010) Simulation of hydrologic and geomorphic changes affecting a shrinking mire. River Research and Applications, 26, 305–321. doi:10.1002/rra.1253

Nakayama, T., Fujita, T. (2010) Cooling effect of water-holding pavements made of new materials on water and heat budgets in urban areas. Landscape and Urban Planning, 96, 57–67. doi:10.1016/j.landurbplan.2010.02.003

Nakayama, T., Sun, Y., Geng, Y. (2010) Simulation of water resource and its relation to urban activity in Dalian City, Northern China. Global and Planetary Change, 73, 172–185. doi:10.1016/j.gloplacha.2010.06.001

Nakayama, T. (2011a) Simulation of complicated and diverse water system accompanied by human intervention in the North China Plain. Hydrological Processes, 25, 2679–2693. doi:10.1002/hyp.8009

Nakayama, T. (2011b) Simulation of the effect of irrigation on the hydrologic cycle in the highly cultivated Yellow River Basin. Agricultural and Forest Meteorology, 151, 314–327. doi:10.1016/j.agrformet.2010.11.006

Nakayama, T. (2011c) Feedback mechanism and complexity in ecosystem–development of integrated assessment system towards eco-conscious society-, Chemical Engineering of Japan, 75, 789–791 (in Japanese)

Nakayama, T. (2011d) Construction of integrated assessment system for win-win solution of hydrothermal degradations in urban area towards eco-conscious society, Chemical Information and Computer Sciences, 29, 63–65 (in Japanese)

Nakayama, T., Hashimoto, S. (2011) Analysis of the ability of water resources to reduce the urban heat island in the Tokyo megalopolis. Environmental Pollution, 159, 2164–2173. doi:10.1016/j.envpol.2010.11.016

Nakayama, T. (2012a) Visualization of the missing role of hydrothermal interactions in a Japanese megalopolis for a win-win solution. Water Science and Technology, 66, 409–414. doi:10.2166/wst.2012.205

Nakayama, T. (2012b) Feedback and regime shift of mire ecosystem in northern Japan. Hydrological Processes, 26, 2455–2469. doi:10.1002/hyp.9347

Nakayama, T. (2012c) Impact of anthropogenic activity on eco-hydrological process in continental scales. Procedia Environmental Sciences, 13, 87–94. doi:10.1016/j.proenv.2012.01.008

Nakayama, T. (2012d) Development of process-based NICE model and simulation of ecosystem dynamics in the catchment of East Asia (Part III). CGER's supercomputer monograph report, 18. NIES, 98 p. http://www.cger.nies.go.jp/publications/report/i103/en/

Nakayama, T., Hashimoto, S., Hamano, H. (2012) Multiscaled analysis of hydrothermal dynamics in Japanese megalopolis by using integrated approach. Hydrological Processes, 26, 2431–2444. doi:10.1002/hyp.9290

Nakayama, T. (2013) For improvement in understanding eco-hydrological processes in mire. Ecohydrology and Hydrobiology, 13, 62–72. doi:10.1016/j.ecohyd.2013.03.004

Nakayama, T., Shankman, D. (2013a) Impact of the Three-Gorges Dam and water transfer project on Changjiang floods. Global and Planetary Change, 100, 38–50. doi:10.1016/j.gloplacha.2012.10.004

Nakayama, T., Shankman, D. (2013b) Evaluation of uneven water resource and relation between anthropogenic water withdrawal and ecosystem degradation in Changjiang and Yellow River Basins. Hydrological Processes, 27(23), 3350–3362. doi:10.1002/hyp.9835

Nakayama, T. (2014a) Hydrology–ecology interactions. In: Eslamian, S. (Ed.) Handbook of Engineering Hydrology, 1: Fundamentals and Applications (Chapter 16), Taylor & Francis, pp. 329–344

Nakayama, T. (2014b) Development of process-based NICE model and simulation of ecosystem dynamics in the catchment of East Asia (Part IV). CGER's supercomputer monograph report, 20. NIES, 102 p. http://www.cger.nies.go.jp/publications/report/i114/en/

Nakayama, T. (2014) Integrated assessment system using process-based eco-hydrology model for adaptation strategy and effective water resources management. In: Lakshmi, V. (Ed.) Remote Sensing of the Terrestrial Water Cycle (Geophysical Monograph Series 206) (Chapter 33), AGU, pp. 521–535. doi:10.1002/9781118872086.ch33

Nakayama, T. (2016) New perspective for eco-hydrology model to constrain missing role of inland waters on boundless biogeochemical cycle in terrestrial-aquatic continuum. Ecohydrology and Hydrobiology, 16, 138–148, doi:10.1016/j.ecohyd.2016.07.002

Nakayama, T. (2017a) Development of an advanced eco-hydrologic and biogeochemical coupling model aimed at clarifying the missing role of inland water in the global biogeochemical cycle. Journal of Geophysical Research: Biogeosciences, 122, 966–988. doi:10.1002/2016JG003743

Nakayama, T. (2017b) Scaled-dependence and seasonal variations of carbon cycle through development of an advanced eco-hydrologic and biogeochemical coupling model. Ecological Modelling, 356, 151–161. doi:10.1016/j.ecolmodel.2017.04.014

Nakayama, T. (2017c) Biogeochemical contrast between different latitudes and the effect of human activity on spatiotemporal carbon cycle change in Asian river systems. Biogeosciences Discussions, doi:10.5194/bg-2017-447

Nakayama, T. (2018) Interaction between surface water and groundwater and its effect on ecosystem and biogeochemical cycle. Journal of Groundwater Hydrology, 60, 143–156. doi:10.5917/jagh.60.143 (in Japanese)

Nakayama, T., Maksyutov, S. (2018) Application of process-based eco-hydrological model to broader northern Eurasia wetlands through coordinate transformation. Ecohydrology and Hydrobiology, 18, 269–277. doi:10.1016/j.ecohyd.2017.11.002

Nakayama, T., Pelletier, G.J. (2018) Impact of global major reservoirs on carbon cycle changes by using an advanced eco-hydrologic and biogeochemical coupling model. Ecological Modelling, 387, 172–186. doi:10.1016/j.ecolmodel.2018.09.007

Nakayama, T. (2019) Development of process-based NICE model and simulation of ecosystem dynamics in the catchment of East Asia (Part V). CGER's supercomputer monograph report, 26. NIES, 122 p. http://www.cger.nies.go.jp/publications/report/i148/en/

Nakayama, T. (2020) Inter-annual simulation of global carbon cycle variations in a terrestrial-aquatic continuum. Hydrological Processes, 34, 662–678. doi:10.1002/hyp.13616

Nakayama, T., Wang, Q., Okadera, T. (2021a) Evaluation of spatio-temporal variations in water availability using a process-based eco-hydrology model in arid and semi-arid regions of Mongolia. Ecological Modelling, 440, 109404. doi:10.1016/j.ecolmodel.2020.109404

Nakayama, T., Wang, Q., Okadera, T. (2021b) Sensitivity analysis and parameter estimation of anthropogenic water uses for quantifying relation between groundwater overuse and water stress in Mongolia. Ecohydrology and Hydrobiology, 21, 490–500. doi:10.1016/j.ecohyd.2021.07.006

Nakayama, T. (2022) Impact of anthropogenic disturbances on carbon cycle changes in terrestrial-aquatic-estuarine continuum by using an advanced process-based model. Hydrological Processes, 36, e14471. doi:10.1002/hyp.14471

Nakayama, T. (2023a) Evaluation of global biogeochemical cycle in lotic and lentic waters by developing an advanced eco-hydrologic and biogeochemical coupling model. Ecohydrology, 17(4), e2555. doi:10.1002/eco.2555

Nakayama, T. (2023b) Development of process-based NICE model and simulation of ecosystem dynamics in the catchment of East Asia (Part VI). CGER's supercomputer monograph report, 29. NIES, 95 p. http://www.cger.nies.go.jp/publications/report/i164/en/

Nakayama, T., Okadera, T., Wang, Q. (2023) Impact of various anthropogenic disturbances on water availability in the entire Mongolian basins towards effective utilization of water resources. Ecohydrology and Hydrobiology, 23(4). doi:10.1016/j.ecohyd.2023.04.006

Nakayama, T., Osako, M. (2023a) Development of a process-based eco-hydrology model for evaluating the spatio-temporal dynamics of macro- and micro-plastics for the whole of Japan. Ecological Modelling, 476, 110243. doi:10.1016/j.ecolmodel.2022.110243

Nakayama, T., Osako, M. (2023b) The flux and fate of plastic in the world's major rivers: Modelling spatial and temporal variability. Global and Planetary Change, 221, 104037. doi:10.1016/j.gloplacha.2023.104037

Nakayama, T. (2024a) Impact of global major reservoirs and lakes on plastic dynamics by using a process-based eco-hydrology model. Lakes and Reservoirs: Research and Management, 29, e12463, doi:10.1111/lre.12463

Nakayama, T. (2024b) Evaluation of flux and fate of plastic in terrestrial-aquatic-estuarine continuum by using an advanced process-based model. Ecohydrology, 17(6), e2678. doi:10.1002/eco.2678

Nakayama, T. (2024c) Development of process-based NICE model and simulation of ecosystem dynamics in the catchment of East Asia (Part VII). CGER's Supercomputer Monograph Report, 30, NIES, 111 p. http://www.cger.nies.go.jp/publications/report/i169/en/

Nakayama, T., Osako, M. (2024) Plastic trade-off: Impact of export and import of waste plastic on plastic dynamics in Asian region. Ecological Modelling, 489, 110624. doi:10.1016/j.ecolmodel.2024.110624

Nakayama, T. (2025a) Impact of settling and resuspension on plastic dynamics during extreme flow and their seasonality in global major rivers. Hydrological Processes, 39(2), e70072. doi:10.1002/hyp.70072

Nakayama, T. (2025b) Improvement in understanding of plastic cycle in Japanese urban regions. Hydrological Processes, 39(6), e70168. doi:10.1002/hyp.70168

Nakayama, T. (2025c) Improvement to simulate plastic dynamics and their relation to biogeochemical cycles in global rivers by considering effect of interaction processes of biofouling and heteroaggregation. Global and Planetary Change, 253, 104917. doi:10.1016/j.gloplacha.2025.104917

Nakayama, T. (2025d) Grazing impacts on Mongolian grasslands assessed by an eco-hydrology model. Environmental Science Pollution Research, 32, 13626-13637. doi:10.1007/s11356-025-36083-2

Nakayama, T. (under review) Different characteristics of interaction processes of biofouling and heteroaggregation between natural lakes and man-made reservoirs. Ecological Modelling

Nakayama, T. (under review) Impact of water diversion on hydrologic cycle and vegetation changes in downstream wetland. Hydrological Processes

Nicolas, G., Robinson, T.P., Wint, G.R., et al. (2016) Using random forest to improve the downscaling of global livestock census data. PLOS ONE, 11, e0150424. doi:10.1371/journal.pone.0150424

OECD. (2022) Global Plastics Outlook: Economic Drivers, Environmental Impacts and Policy Options, OECD Publishing, Paris. https://doi.org/10.1787/de747aef-en

Siegfried, M., Koelmans, A.A., Besseling, E., Kroeze, C. (2017) Export of microplastics from land to sea. A modelling approach. Water Research, 127, 249–257. doi:10.1016/j.watres.2017.10.011

UNESCO (2022) IHP-IX: Strategic Plan of the intergovernmental hydrological programme: Science for a water secure world in a changing environment, ninth phase 2022–2029. https://unesdoc.unesco.org/ark:/48223/pf0000381318.locale=en

van Emmerik, T., Strady, E., Kieu-Le, T.-C., Nguyen, L., Gratiot, N. (2019) Seasonality of riverine macroplastic transport. Scientific Reports, 9, 13549. doi:10.1038/s41598-019-50096-1

Windsor, F.M., Durance, I., Horton, A.A., et al. (2019) A catchment-scale perspective of plastic pollution. Global Change Biology, 25, 1207–1221. doi:10.1111/gcb.14572

Appendix

Publications and Presentations

Publications and Presentations

Original Papers and Reviews Related to This Monograph:

Nakayama, T. (2024a) Impact of global major reservoirs and lakes on plastic dynamics by using a process-based eco-hydrology model. Lakes and Reservoirs: Research and Management, 29, e12463, doi:10.1111/lre.12463

Nakayama, T. (2024b) Evaluation of flux and fate of plastic in terrestrial-aquatic-estuarine continuum by using an advanced process-based model. Ecohydrology, 17(6), e2678, doi:10.1002/eco.2678

Nakayama, T. (2025a) Impact of settling and resuspension on plastic dynamics during extreme flow and their seasonality in global major rivers. Hydrological Processes, 39(2), e70072, doi:10.1002/hyp.70072

Nakayama, T. (2025b) Improvement in understanding of plastic cycle in Japanese urban regions. Hydrological Processes, 39(6), e70168, doi:10.1002/hyp.70168

Nakayama, T. (2025c) Improvement to simulate plastic dynamics and their relation to biogeochemical cycles in global rivers by considering effect of interaction processes of biofouling and heteroaggregation. Global and Planetary Change, 253, 104917, doi:10.1016/j.gloplacha.2025.104917

Nakayama, T. (2025d) Grazing impacts on Mongolian grasslands assessed by an eco-hydrology model. Environ. Sci. Pollut. Res. 32, 13626–13637, doi:10.1007/s11356-025-36083-2

Nakayama, T. (under review) Different characteristics of interaction processes of biofouling and heteroaggregation between natural lakes and man-made reservoirs. Ecological Modelling

Nakayama, T. (under review) Impact of water diversion on hydrologic cycle and vegetation changes in downstream wetland. Hydrological Processes

Conference Reports Related to This Monograph:

Nakayama, T., Osako, M. (2023) Seasonal variations of plastic transport in global major rivers. session number 12dO1, Goldschmidt2023, Lyon, France (Virtual Conference), 9–14 July (Website)

Nakayama, T. (2023) Impact of extreme flow and seasonality on plastic dynamics in global river basins. paper number H52F-06, AGU23, San Francisco, USA (Virtual Conference), 11–15 December (Website)

Nakayama, T. (2024) Evaluation of biogeochemical cycles and their relation to plastic dynamics in terrestrial-aquatic-estuarine continuum by using an advanced process-based model. paper number OP31F-07, Ocean Sciences Meeting 2024, New Orleans, USA (Virtual Conference), 18–23 February (Website)

Nakayama, T. (2024) Towards improvement to understand plastic dynamics in global rivers. paper number EGU24-3263, EGU General Assembly 2024, Vienna, Austria (Virtual Conference), 14–19 April (Website), doi:10.5194/egusphere-egu24-3263

Nakayama, T. (2024) Modeling of global plastic dynamics and their relation to biogeochemical cycles in terrestrial-aquatic-estuarine continuum. session number 10dP1, Goldschmidt2024, Chicago (Virtual Conference), 18–24 August (Website), doi:10.46427/gold2024.22295

Nakayama, T. (2024) Impact of biofouling and heteroaggregation on plastic budget in global major rivers. paper number H02-07, AGU24, Washington, D.C., USA (Virtual Conference), 9–13 December (Website)

Nakayama, T. (2025) Towards improving the accuracy of plastic cycle in urban regions. paper number EGU25-7481, EGU General Assembly 2025 Vienna, Austria (Virtual Conference), 27 April–2 May (Website), doi:10.5194/egusphere-egu25-7481

Nakayama, T., Wang, Q., Okadera, T., Nagai, M., Kinugasa, T. (2025) Towards comprehensive evaluation of ecosystem dynamics in arid and semi-arid regions of Mongolia by a process-based eco-hydrology model. Session 1, EST2025, Ulaanbaatar, 18–19 June

Nakayama, T. (2025) Impact of interaction processes on plastic dynamics in global major rivers. session number 11R, Goldschmidt2025, Prague (Virtual Conference), 6–11 July (Website)

Nakayama, T. (2025) Comprehensive assessment of plastic dynamics in global river basins by developing a new process-based model. Session number O01.3, ISEM2025, Kashiwa, 19–23 October (Website)

Nakayama, T., Okadera, T., Wang, Q. (2025) Developing a new eco-hydrology model to fill the gap between socio-economic transition and ecosystem degradation in Mongolia. Session number O05.3, ISEM2025, Kashiwa, 19–23 October (Website)

Nakayama, T., Murata, T., Nohara, S. (2025) Impact of water diversion in upstream water source on hydrologic cycle and its resultant vegetation changes in downstream wetland. paper number H21Q-VR8931, AGU25, New Orleans, USA (Virtual Conference), 15–19 December (Website)

NICE Series in CGER's Supercomputer Monograph Report (Part I - VII):

Nakayama, T., Watanabe, M. (2006) Development of process-based NICE model and simulation of ecosystem dynamics in the catchment of East Asia (Part I). CGER's Supercomputer Monograph Report, 11, NIES, 100 p., http://www.cger.nies.go.jp/publications/report/i063/I063e

Nakayama, T. (2008) Development of process-based NICE model and simulation of ecosystem dynamics in the catchment of East Asia (Part II). CGER's Supercomputer Monograph Report, 14, NIES, 91 p., http://www.cger.nies.go.jp/publications/report/i083/i083_e

Nakayama, T. (2012) Development of process-based NICE model and simulation of ecosystem dynamics in the catchment of East Asia (Part III). CGER's Supercomputer Monograph Report, 18, NIES, 98 p., http://www.cger.nies.go.jp/publications/report/i103/en/

Nakayama, T. (2014) Development of process-based NICE model and simulation of ecosystem dynamics in the catchment of East Asia (Part IV). CGER's Supercomputer Monograph Report, 20, NIES, 102 p., http://www.cger.nies.go.jp/publications/report/i114/en/

Nakayama, T. (2019) Development of process-based NICE model and simulation of ecosystem dynamics in the catchment of East Asia (Part V). CGER's Supercomputer Monograph Report, 26, NIES, 122 p., http://www.cger.nies.go.jp/publications/report/i148/en/

Nakayama, T. (2023) Development of process-based NICE model and simulation of ecosystem dynamics in the catchment of East Asia (Part VI). CGER's Supercomputer Monograph Report, 29, NIES, 95 p., http://www.cger.nies.go.jp/publications/report/i167/en/

Nakayama, T. (2024) Development of process-based NICE model and simulation of ecosystem dynamics in the catchment of East Asia (Part VII). CGER's Supercomputer Monograph Report, 30, NIES, 111 p., http://www.cger.nies.go.jp/publications/report/i169/en/

Contact Person

Tadanobu Nakayama

Regional Environment Conservation Division
National Institute for Environmental Studies (NIES)
16-2 Onogawa, Tsukuba, Ibaraki 305-8506, Japan
Phone: +81-29-850-2564
E-mail: nakat@nies.go.jp

Profile: https://www.nies.go.jp/researchers-e/100190.html
ORCID: https://orcid.org/0000-0002-8233-034X
Web of Science: https://www.webofscience.com/wos/author/record/938567
ResearchGate: https://www.researchgate.net/profile/Tadanobu_Nakayama

CGER'S SUPERCOMPUTER ACTIVITY REPORT
(Out of stock)

Vol. 1-1992 (CGER-I010-1994)   Vol. 8-1999 (CGER-I043-2000)
Vol. 2-1993 (CGER-I016-1994)   Vol. 9-2000 (CGER-I050-2002)
Vol. 3-1994 (CGER-I020-1995)   Vol.10-2001 (CGER-I054-2002)
Vol. 4-1995 (CGER-I024-1996)   Vol.11-2002 (CGER-I058-2004)
Vol. 5-1996 (CGER-I030-1997)   Vol.12-2003 (CGER-I061-2005)
Vol. 6-1997 (CGER-I034-1999)   Vol.13-2004 (CGER-I064-2006)
Vol. 7-1998 (CGER-I039-2000)   Vol.14-2005 (CGER-I070-2007)

....

国立環境研究所スーパーコンピュータ利用研究年報
NIES Supercomputer Annual Report

平成 18 年度 2006 (CGER-I078-2008) Out of stock
平成 19 年度 2007 (CGER-I086-2008) Out of stock
平成 20 年度 2008 (CGER-I090-2009) Out of stock
平成 21 年度 2009 (CGER-I095-2010) Out of stock
平成 22 年度 2010 (CGER-I099-2011) Out of stock
平成 23 年度 2011 (CGER-I106-2012) Out of stock
平成 24 年度 2012 (CGER-I113-2013) Out of stock
平成 25 年度 2013 (CGER-I119-2014) Out of stock
平成 26 年度 2014 (CGER-I125-2015)
平成 27 年度 2015 (CGER-I130-2016)
平成 28 年度 2016 (CGER-I136-2017)
平成 29 年度 2017 (CGER-I141-2018)
平成 30 年度 2018 (CGER-I146-2019)
令和元年度 2019 (CGER-I151-2020)
令和 2 年度 2020 (CGER-I156-2021)
令和 3 年度 2021 (CGER-I161-2022)
令和 4 年度 2022 (CGER-I168-2024)
令和 5 年度 2023 (CGER-I173-2024)
令和 6 年度 2024 (CGER-I176-2025)

....

CGER'S SUPERCOMPUTER MONOGRAPH REPORT

Vol. 1   CGER-I021-'96 (Out of stock)
KOMORI S.: Turbulence Structure and CO_2 Transfer at the Air-Sea Interface and Turbulent Diffusion in Thermally-Stratified Flows

Vol. 2   CGER-I022-'96 (Out of stock)
TOKIOKA T., NODA A., KITOH A., NIKAIDOU Y., NAKAGAWA S., MOTOI T., YUKIMOTO S., TAKATA K.: A Transient CO_2 Experiment with the MRI CGCM -Annual Mean Response-

Vol. 3   CGER-I025-'97 (Out of stock)
NUMAGUTI A., SUGATA S., TAKAHASHI M., NAKAJIMA T., SUMI A.: Study on the Climate System and Mass Transport by a Climate Model

Vol. 4   CGER-I028-'97 (Out of stock)
AKIYOSHI H.: Development of a Global 1-D Chemically Radiatively Coupled Model and an

Introduction to the Development of a Chemically Coupled General Circulation Model

Vol. 5   CGER-I035-'99 (Out of stock)
Watanabe M., Amano K., Kohata K.: Three-Dimensional Circulation Model Driven by Wind, Density, and Tidal Force for Ecosystem Analysis of Coastal Seas

Vol. 6   CGER-I040-2000 (Out of stock)
Hayashi Y.Y., Toyoda E., Hosaka M., Takehiro S., Nakajima K., Ishiwatari M.: Tropical Precipitation Patterns in Response to a Local Warm SST Area Placed at the Equator of an Aqua Planet

Vol. 7   CGER-I045-2001 (Out of stock)
Noda A., Yukimoto S., Maeda S., Uchiyama T., Shibata K., Yamaki S.: A New Meteorological Research Institute Coupled GCM (MRI-CGCM2) -Transient Response to Greenhouse Gas and Aerosol Scenarios-

Vol. 8   CGER-I055-2003 (Out of stock)
Nozawa T., Emori S., Numaguti A., Tsushima Y., Takemura T., Nakajima T., Abe-Ouchi A., Kimoto M.: Transient Climate Change Simulations in the 21st Century with the CCSR/NIES CGCM under a New Set of IPCC Scenarios

Vol. 9   CGER-I057-2004 (Out of stock)
Miyazaki T., Fujishima S., Yamamoto M., Wei Q., Hanazaki H.: Vortices, Waves and Turbulence in a Rotating Stratified Fluid

Vol. 10   CGER-I060-2005 (Out of stock)
Hayashi S., Murakami S., Xu K., Watanabe M.: Modeling of Daily Runoff in the Changjiang (Yangtze) River Basin and Its Application to Evaluating the Flood Control Effect of the Three Gorges Project

Vol. 11   CGER-I063-2006 (Out of stock)
Nakayama T., Watanabe M.: Development of Process-based NICE Model and Simulation of Ecosystem Dynamics in the Catchment of East Asia (Part I)

Vol. 12   CGER-I073-2007 (Out of stock)
Nozawa T., Nagashima T., Ogura T., Yokohata T., Okada N., Shiogama H.: Climate Change Simulations with a Coupled Ocean-Atmosphere GCM Called the Model for Interdisciplinary Research on Climate: MIROC

Vol. 13   CGER-I080-2008 (Out of stock)
Shibata K., Deushi M.: Simulations of the Stratospheric Circulation and Ozone during the Recent Past (1980-2004) with the MRI Chemistry-Climate Model

Vol. 14   CGER-I083-2008 (Out of stock)
Nakayama T.: Development of Process-based NICE Model and Simulation of Ecosystem Dynamics in the Catchment of East Asia (Part II)

Vol. 15   CGER-I092-2010 (Out of stock)
Maksyutov, S., Nakatsuka Y., Valsala V., Saito M., Kadygrov N., Aoki T., Eguchi N., Hirata R., Ikeda M., Inoue G., Nakazawa T., Onishi R., Patra P.K., Richardson A.D., Saeki T., Yokota T.: Algorithms for Carbon Flux Estimation Using GOSAT Observational Data

Vol. 16   CGER-I097-2011 (Out of stock)
Nakajima K.: Idealized Numerical Experiments on the Space-time Structure of Cumulus Convection Using a Large-domain Two-dimensional Cumulus-Resolving Model

Vol. 17   CGER-I098-2011 (Out of stock)
Ueda H.: Atmospheric Motion and Air Quality in East Asia

Vol. 18   CGER-I103-2012 (Out of stock)
Nakayama T.: Development of Process-based NICE Model and Simulation of Ecosystem Dynamics in the Catchment of East Asia (Part III)

Vol. 19   CGER-I108-2013 (Out of stock)

KOMORI S.: Numerical Simulations of Turbulence Structure and Scalar Transfer across the Air-Water Interfaces

Vol. 20   CGER-I114-2014 (Out of stock)
NAKAYAMA T.: Development of Process-based NICE Model and Simulation of Ecosystem Dynamics in the Catchment of East Asia (Part IV)

Vol. 21   CGER-I120-2015
SHIOGAMA H.: Influence of Anthropogenic Aerosol Emissions on Pattern Scaling Projections

Vol. 22   CGER-I127-2016
SATOH M., ROH, W., HASHINO, T.: Evaluations of Clouds and Precipitations in NICAM Using the Joint Simulator for Satellite Sensors

Vol. 23   CGER-I132-2017
GOTO D., SCHUTGENS, N.A.J., OIKAWA, E., TAKEMURA, T., NAKAJIMA, T.: Improvement of a global aerosol transport model through validation and implementation of a data assimilation system

Vol. 24   CGER-I138-2018
TAKEMURA T., AND SPRINTARS DEVELOPER TEAM : Development of a global aerosol climate model SPRINTARS

Vol. 25   CGER-I143-2019
MAKSYUTOV, S., ODA, T., SAITO, M., TAKAGI, H., BELIKOV, D., VALSALA, V.: Transport modeling algorithms for application of the GOSAT observations to the global carbon cycle modeling

Vol. 26   CGER-I148-2019
NAKAYAMA T.: Development of Process-based NICE Model and Simulation of Ecosystem Dynamics in the Catchment of East Asia (Part V)

Vol. 27   CGER-I153-2021
ISHIWATARI M., NAKAJIMA K., TAKEHIRO, S., KAWAI Y., TAKAHASHI Y. O., HASHIMOTO G. L., SASAKI Y., and HAYASHI Y.-Y.: Numerical studies on the variety of climates of exoplanets using idealistic configurations

Vol. 28   CGER-I158-2022
YOKOHATA T.: Development of an integrated land surface model with ecosystems, human water management, crop growth, and land-use change: MIROC-INTEG-LAND

Vol. 29   CGER-I167-2023
NAKAYAMA T.: Development of Process-based NICE Model and Simulation of Ecosystem Dynamics in the Catchment of East Asia (Part VI)

Vol. 30   CGER-I169-2024
NAKAYAMA T.: Development of Process-based NICE Model and Simulation of Ecosystem Dynamics in the Catchment of East Asia (Part VII)

Vol. 31   CGER-I178-2025
NAKAYAMA T.: Development of Process-based NICE Model and Simulation of Ecosystem Dynamics in the Catchment of East Asia (Part VIII)